



---

# THE 12TH WORKSHOP ON VISUAL ANALYTICS IN HEALTHCARE

---

VAHC 2021



OCTOBER 24, 2021  
VIRTUAL MEETING  
IEEE VIS 2021

# VAHC 2021 (11th workshop on Visual Analytics in Healthcare)

## Session 1 – Best Paper

### Best Paper: A Multi-scale Visual Analytics Approach for Exploring Biomedical Knowledge

Fahd Husain<sup>1</sup>, Rosa Romero-Gómez<sup>1</sup>, Emily Kuang<sup>1</sup>, Dario Segura<sup>1</sup>, Adamo Carolli Carolly<sup>1</sup>, Lai Chung Liu<sup>1</sup>, Manfred Cheung<sup>1</sup>, Yohann Paris<sup>1</sup>

<sup>1</sup>Uncharted Software, Toronto, Ontario, Canada

**Abstract:** This paper describes an ongoing multi-scale visual analytics approach for exploring and analyzing biomedical knowledge at scale. We utilize global and local views, hierarchical and flow-based graph layouts, multi-faceted search, neighborhood recommendations, and document visualizations to help researchers interactively explore, query, and analyze biological graphs against the backdrop of biomedical knowledge. The generality of our approach - insofar as it requires only knowledge graphs linked to documents - means it can support a range of therapeutic use cases across different domains, from disease propagation to drug discovery. Early interactions with domain experts support our approach for use cases with graphs with over 40,000 nodes and 350,000 edges.

**Keywords:** Human-centered computing—Visualization—Visualization techniques—Treemaps; Human-centered computing—Visualization—Visualization design and evaluation methods

## Session 2 – Clinical and Medical Decision Making

### Paper 1: Towards a Comprehensive Cohort Visualization of Patients with Inflammatory Bowel Disease

Salmah Ahmad<sup>1</sup>, David Sessler<sup>1</sup>, Jörn Kohlhammer<sup>2</sup>

<sup>1</sup>Fraunhofer IGD, Darmstadt, Hessen, Germany; <sup>2</sup>Fraunhofer IGD, Darmstadt, Germany GRIS, TU Darmstadt, Darmstadt, Germany

**Abstract:** This paper reports on a joint project with medical experts on inflammatory bowel disease (IBD). Patients suffering from IBD, e.g. Crohn's disease or ulcerative colitis, do not have a reduced life expectancy and disease progressions easily span several decades. We designed a visualization to highlight information that is vital for comparing patients and progressions, especially with respect to the treatments administered over the years. Medical experts can interactively determine the amount of information displayed and can synchronize the progressions to the beginning of certain treatments and medications. While the visualization was designed in close collaboration with IBD experts, we additionally evaluated our approach with 35 participants to ensure good usability and accessibility. The paper also highlights the future work on similarity definition and additional visual features in this on-going project.

**Keywords:** Cohort Visualization; Visual Cohort Analysis; Inflammatory Bowel Disease

### Paper 2: Phoenix Virtual Heart: A Hybrid VR-Desktop Visualization System for Cardiac Surgery Planning and Education

Jinbin Huang<sup>1</sup>, Jonathan Douglas Plasencia<sup>2</sup>, Dianna M.E. Bardo<sup>3</sup>, Nicholas C. Rubert<sup>3</sup>, Erik G. Ellsworth<sup>4</sup>, Steven D. Zangwill<sup>4</sup>, Chris Bryan<sup>1</sup>

<sup>1</sup>CIDSE, Arizona State University, Tempe, Arizona, United States; <sup>2</sup>Cardiology, Phoenix Children's Hospital, Phoenix, Arizona, United States 4D CAVA Lab, Phoenix Children's Hospital, Phoenix, Arizona, United States; <sup>3</sup>Radiology, Phoenix Children's Hospital, Phoenix, Arizona, United States; <sup>4</sup>Cardiology, Phoenix Children's Hospital, Phoenix, Arizona, United States

**Abstract:** Physicians diagnosing and treating complex, structural congenital heart disease (CHD), i.e., heart defects present at birth, often rely on visualization software that scrolls through a volume stack of two-dimensional (2D) medical images. Due to limited display dimensions, conventional desktop-based applications have difficulties facilitating physicians converting 2D images to 3D intelligence. Recently, 3D printing of anatomical models has

# VAHC 2021 (11th workshop on Visual Analytics in Healthcare)

*emerged as a technique to analyze CHD, but current workflows are tedious. To this end, we introduce and describe our ongoing work developing the Phoenix Virtual Heart (PVH), a hybrid VR-desktop software to aid in CHD surgical planning and family consultation. PVH is currently being integrated into a 3D printing workflow at a children's hospital as a way to increase physician efficiency and confidence, allowing physicians to analyze virtual anatomical models for surgical planning and family consultation.*

*We describe the iterative design process that led to PVH, discuss how it fits into a 3D printing workflow, and present formative feedback from clinicians that are beginning to use the application.*

**Keywords:** Human-computer Interaction, Immersive Visualization, Virtual Reality, Interactive Data Analytics; Radiology, Surgical Planning, Medical Education, Medical Imaging

## Paper 3: Communicating Performance of Regression Models Using Visualization in Pharmacovigilance

Ashley Suh<sup>1</sup>, Gabriel Appleby<sup>1</sup>, Erik W Anderson<sup>2</sup>, Luca Finelli<sup>3</sup>, Dylan Cashman<sup>4</sup>

<sup>1</sup>Tufts University, Medford, Massachusetts, United States; <sup>2</sup>Novartis, Inc., Medford, Massachusetts, United States;

<sup>3</sup>Novartis, Inc., Basel, Switzerland; <sup>4</sup>Novartis, Inc., Cambridge, Massachusetts, United States

**Abstract:** Statistical regression methods can help pharmaceutical organizations improve the quality of their pharmacovigilance by predicting the expected quantity of adverse events during a trial. However, the use of statistical techniques also changes the risk profile of any downstream tasks, due to bias and noise in the model's predictions. That risk profile must be clearly understood, documented, and communicated across many different stakeholders in a highly regulated environment. Aggregated performance metrics such as explained variance or mean average error fail to tell the whole story, making it difficult for subject matter experts to feel confident in deciding to use a model. In this work, we describe guidelines for communicating regression model performance for models deployed in predicting adverse events. First, we describe an interview study in which both data scientists and subject matter experts within a pharmaceutical organization describe their challenges in communicating and understanding regression performance. Based on the responses in this study, we develop guidelines for which visualizations to use to communicate performance, and use a publicly available trial safety database to demonstrate their use.

**Keywords:** Visual Communication, Regression Models, Pharmacovigilance

## Paper 4: Interactive Cohort Analysis and Hypothesis Discovery by Exploring Temporal Patterns in Population-Level Health Records

Tianyi Zhang<sup>1</sup>, Thomas H. McCoy<sup>2</sup>, Roy H. Perlis<sup>2</sup>, Finale Doshi-Velez<sup>3</sup>, Prof. Elena L. Glassman<sup>3</sup>

<sup>1</sup>Computer Science, Purdue University, West Lafayette, Indiana, United States; <sup>2</sup>Center for Quantitative Health, Massachusetts General Hospital, Boston, Massachusetts, United States Harvard Medical School, Boston, Massachusetts, United States; <sup>3</sup>SEAS, Harvard University, Cambridge, Massachusetts, United States

**Abstract:** It is challenging to visualize temporal patterns in electronic health records (EHRs) due to the high volume and high dimensionality of EHRs. In this paper, we conduct a formative study with three clinical researchers to understand their needs of exploring temporal patterns in EHRs. Based on those insights, we develop a new visualization interface that renders medical event trajectories in a holistic timeline view and guides users towards interesting patterns using an information scent based method. We demonstrate how a clinical researcher can use our tool to discover interesting sub-cohorts with unique disease progression and treatment trajectories in a case study.

**Keywords:** Human-centered computing—Visualization—Visualization techniques; Human-centered computing—Visualization—Visualization design and evaluation methods

# VAHC 2021 (11th workshop on Visual Analytics in Healthcare)

## Session 3 – COVID-19 and Public Health

### Paper 5: Enabling Longitudinal Exploratory Analysis of Clinical COVID Data

David Borland<sup>1,2</sup>, Irena Brain<sup>1</sup>, Karamarie Fecho<sup>3,2</sup>, Emily Pfaff<sup>1</sup>, Hao Xu<sup>2</sup>, James Champion<sup>1</sup>, Chris Bizon<sup>2</sup>, David Gotz<sup>1</sup>

<sup>1</sup>University of North Carolina at Chapel Hill, Chapel Hill, North Carolina, United States; <sup>2</sup>RENCI, Chapel Hill, North Carolina, United States; <sup>3</sup>Copperline Professional Solutions, Pittsboro, North Carolina, United States

**Abstract:** As the COVID-19 pandemic continues to impact the world, data is being gathered and analyzed to better understand the disease. Recognizing the potential for visual analytics technologies to support exploratory analysis and hypothesis generation from longitudinal clinical data, a team of collaborators worked to apply existing event sequence visual analytics technologies to a longitudinal clinical data from a cohort of 998 patients with high rates of COVID-19 infection. This paper describes the initial steps toward this goal, including: (1) the data transformation and processing work required to prepare the data for visual analysis, (2) initial findings and observations, and (3) qualitative feedback and lessons learned which highlight key features as well as limitations to address in future work.

**Keywords:** Visual analytics, temporal event sequence visualization, human-computer interaction, medical informatics, COVID-19

### Paper 6: COVID-19 EnsembleVis: Visual Analysis of County-level Ensemble Forecast Models

Sanjana Srabanti<sup>1</sup>, G. Elisabeta Marai<sup>2</sup>, Fabio Miranda<sup>1</sup>

<sup>1</sup>University of Illinois at Chicago, Chicago, Illinois, United States; <sup>2</sup>Electronic Visualization Laboratory, University of Illinois at Chicago, Chicago, Illinois, United States

**Abstract:** The spread of the SARS-CoV-2 virus and its contagious disease COVID-19 has impacted countries to an extent not seen since the 1918 flu pandemic. In the absence of an effective vaccine and as cases surge worldwide, governments were forced to adopt measures to inhibit the spread of the disease. To reduce its impact and to guide policy planning and resource allocation, researchers have been developing models to forecast the infectious disease. Ensemble models, by aggregating forecasts from multiple individual models, have been shown to be a useful forecasting method. However, these models can still provide less-than-adequate forecasts at higher spatial resolutions. In this paper, we built COVID-19 EnsembleVis, a web-based interactive visual interface that allows the assessment of the errors of ensembles and individual models by enabling users to effortlessly navigate through and compare the outputs of models considering their space and time dimensions. COVID-19 EnsembleVis enables a more detailed understanding of uncertainty and the range of forecasts generated by individual models.

**Keywords:** Human-centered computing—Visualization—Visualization application domains—Visual analytics

### Paper 7: Visual Analytics for Decision-Makers and Public Audiences within the United States National COVID-19 Response

Elisha Peterson<sup>1</sup>, Philip B Graff<sup>1</sup>, Peter Gu<sup>1</sup>, Max Robinson<sup>1</sup>

<sup>1</sup>Applied Physics Laboratory, Johns Hopkins University, Laurel, Maryland, United States

**Abstract:** The COVID-19 pandemic launched a worldwide effort to collect, process, and communicate public health data at unprecedented scales, and a host of visualization capabilities have been launched and maintained to meet the need for presenting data in ways that the general public can understand. This paper presents a selection of visualizations developed in support of the United States National COVID-19 Response, describes the unique set of constraints and challenges of operational visualization in this context, and reflects on ways the visualization community might be able to support public health operations moving forward.

**Keywords:** Human-centered computing—Visualization—Empirical studies in visualization; Applied computing—Life and medical sciences—Health informatics

# VAHC 2021 (11th workshop on Visual Analytics in Healthcare)

## Paper 8: Communicating Area-level Social Determinants of Health Information: The Ohio Children's Opportunity Index Dashboards

Pallavi Jonnalagadda<sup>1</sup>, Christine M Swoboda<sup>1</sup>, Priti Singh<sup>1</sup>, Harish Gureddygari<sup>1</sup>, Seth Scarborough<sup>1</sup>, Ian Dunn<sup>2</sup>, Nathan Doogan<sup>2</sup>, Naleef Fareed<sup>3</sup>

<sup>1</sup>Center for the Advancement of Team Science, Analytics, and Systems Thinking in Health Services and Implementation Science Research, The Ohio State University, Columbus, Ohio, United States; <sup>2</sup>The Ohio Colleges of Medicine Government Resource Center, The Ohio State University, Columbus, Ohio, United States; <sup>3</sup>Biomedical Informatics, Ohio State University, Columbus, Ohio, United States

**Abstract:** Social determinants of health (SDoH) can be measured at the geographic level to convey information about neighborhood deprivation. The Ohio Children's Opportunity Index (OCOI) is a multi-dimensional area-level opportunity index comprised of eight health dimensions. Our research team has documented the design, development, and use cases of dashboard solutions to visualize OCOI. The OCOI is a multi-dimensional index spanning the following eight domains or dimensions: family stability, infant health, children's health, access, education, housing, environment, and criminal justice. Information on these eight domains is derived from the American Community Survey and other administrative datasets maintained by the state of Ohio. Our team used the Tableau Desktop visualization software and applied a user-centered design approach to developing the two OCOI dashboards—main OCOI dashboard and OCOI-race dashboard. We also performed convergence analysis to visualize the census tracts, where different health indicators simultaneously exist at their worst levels. The OCOI dashboards have multiple, interactive components: a choropleth map of Ohio displaying OCOI scores for a specific census tract, graphs presenting OCOI or domain scores to compare relative positions for tracts, and a sortable table to visualize scores for specific county and census tracts. Stakeholders provided iterative feedback on dashboard design in regard to functionality, content, and aesthetics. A case study using the two dashboards for convergence analysis revealed census tracts in neighborhoods with low infant health scores and a high proportion of minority population. The OCOI dashboards could assist end-users in making decisions that tailor health care delivery and policy decision-making regarding children's health particularly in areas where multiple health indicators exist at their worst levels.

**Keywords:** Data visualization, social determinants of health, geographical information system, area level deprivation, opportunity index

# A Multi-scale Visual Analytics Approach for Exploring Biomedical Knowledge

Fahd Husain\*

Rosa Romero-Gómez  
Lai Chung Liu

Emily Kuang  
Manfred Cheung

Dario Segura  
Yohann Paris

Adamo Carolli

Uncharted Software Inc.

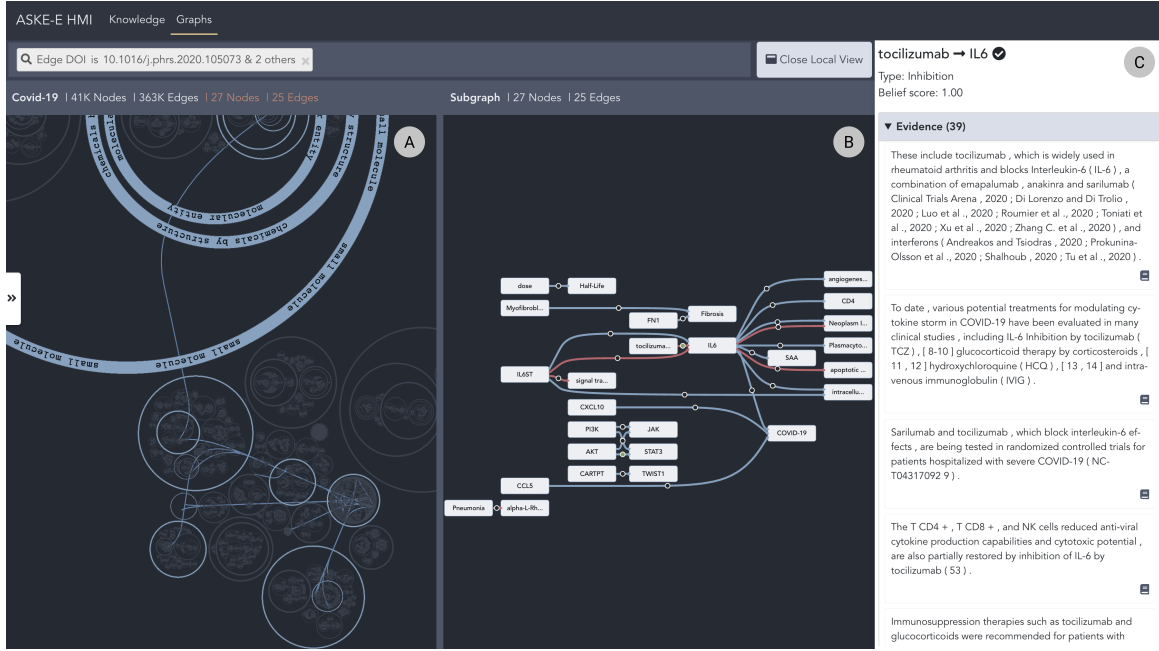


Figure 1: A biomedical researcher uses our system prototype to investigate potential drug treatments for SARS-CoV-2 using the COVID-19 biological graph that was automatically derived from literature. **A. The Global View** provides an overview of the biological graph with bundled edges and nodes organized hierarchically in a biomedical ontology. The results of searching for links from several articles using DOIs are highlighted. **B. The Local View** shows the highlighted results extracted as a node-link flow graph for further analysis. **C. The Drill-down Panel** displays the underlying evidence extracted from scientific articles for the inhibition relationship between *tocilizumab* and *IL6*.

## ABSTRACT

This paper describes an ongoing multi-scale visual analytics approach for exploring and analyzing biomedical knowledge at scale. We utilize global and local views, hierarchical and flow-based graph layouts, multi-faceted search, neighborhood recommendations, and document visualizations to help researchers interactively explore, query, and analyze biological graphs against the backdrop of biomedical knowledge. The generality of our approach - insofar as it requires only knowledge graphs linked to documents - means it can support a range of therapeutic use cases across different domains, from disease propagation to drug discovery. Early interactions with domain experts support our approach for use cases with graphs with over 40,000 nodes and 350,000 edges.

**Index Terms:** Human-centered computing—Visualization—Visualization techniques—Treemaps; Human-centered computing—

\*e-mail: [fhusain, rgomez, ekuang, dsegura, acarolli, nliu, mcheung, yparis]@uncharted.software

## Visualization—Visualization design and evaluation methods

### 1 INTRODUCTION

With over 1.5 million publications a year and more than 50 million peer-reviewed articles in existence, the rate and volume of novel scientific research remains overwhelming, having long surpassed our ability to fully understand and utilize what is known [19]. Crises like the COVID-19 pandemic only exacerbate this situation, with critical information dispersed across the papers published each day [15]. To stay up-to-date, scientists must manually review publications to internalize new knowledge. Therefore, their coverage of the field remains small, and at this scale and pace, contextualization of new knowledge and synthesis with prior knowledge is often impractical, biased, and error-prone. While all disciplines are subject to the effects of rapidly-changing knowledge, the cost in medical research can be measured in human lives.

In the field of biomedicine, it is already difficult and time-consuming to develop and validate hypotheses. Against the backdrop of all scientific knowledge, biomedical researchers start with a certain question, and turn to their prior domain knowledge and the mental models from their specific experiences [17]. As many biological processes are inherently network phenomena, they are well suited for graph analysis [37]. For example, when analyzing the

effects of a drug on a disease, biomedical researchers must assemble (or update) biological graphs from literature, analyze their causal structure, extract relevant subgraphs, highlight novel or alternative pathways that could aid in drug discovery, flag potential viral mutations should new pathways appear, and distill all this analysis into a list of drug candidates for downstream trials. Similar graph analytic workflows are required across a range of biomedical use cases. However, the sheer size and dense connectivity of such graphs makes them hard to visualize and analyze in real-time.

The primary research contribution of this paper is a multi-scale visual analytics approach that enables the investigation of biological graphs to facilitate a variety of use cases such as drug discovery, disease analysis, and identification of side-effects. This research is part of our ongoing effort for DARPA’s Automating Scientific Knowledge (ASKE) program [7]. Utilizing data from our ASKE collaborators [14, 29], we developed a web-based prototype that visualizes 16 biological graphs against a corpus of 176,000 documents. We then conducted an expert evaluation in order to better understand how the system helps biomedical researchers in identifying drug-target interactions. Domain experts believe our approach to have unique value for knowledge exploration, and our initial iteration with users underscored that the prototype was easy to interact with and useful for navigating and analyzing large graphs against the backdrop of scientific knowledge. More generally, we believe our design approach is flexible enough to be used for knowledge discovery in other graph-based domains.

## 2 RELATED WORK

### 2.1 Biological Graph Visualization

Graph-based visualizations remain key to understanding biological graphs across a range of use cases [10, 30]. Most existing visualization approaches support static overviews of the entire graph [18, 20] and interactive views of focused subgraphs [1, 11, 40]. However, research has shown that the inherent multi-scale nature of biological graphs can only be fully appreciated when the entire range from local to global graph structures can be inspected continuously and interactively [32]. Some tools such as Reactome [35] strike a balance by displaying overviews of biological graphs as well as detailed views of selected subgraphs or pathways. Yet, in the workflow, the overviews are replaced by selected pathways and thus global insight is decreased. By contrast, we propose a novel approach for scalable and performant graph analysis with coordinated and adjustable global and local views so the multi-scale character of biological graphs can be preserved and interrogated with multi-faceted search, interactive navigation, and progressive drill-down on demand.

### 2.2 Large-Scale Scientific Knowledge Exploration

Visualizations of large-scale scientific corpora can be broadly categorized into citation-linked graphs [5, 9] and similarity clusters [23, 38]. Citation-linked graphs represent articles as nodes and edges as citations. Cluster visualizations typically apply dimensionality reduction to produce text embeddings that can be visualized as interactive 2-D scatterplots. For example, Open Knowledge Maps [24] displays clusters of PubMed [8] articles based on textual similarity. More recent approaches visualize biomedical data repositories and scientific articles, using metadata for overview, organization, custom user-feeds and semantic querying [22, 24, 25].

Taking inspiration from the above work, we are building the capability for interactive exploration of hierarchical clusters of scientific knowledge, where nested sub-clusters organize related knowledge at finer resolution. To our knowledge, this visual and interactive approach is not yet present in the field at large.

## 3 DESIGN PROCESS AND GOALS

Our user-centered design process was based on periodic meetings over eight months with domain experts and stakeholders in systems

biology, bioinformatics, and causal reasoning applied to the study of infectious diseases. Based on these interactions, we identified the following high-level design goals (DG):

- **DG1. Provide scalable, interactive, and performant visualizations of biological graphs.** Such graphs range from small ones visualized in standard ways to those with over tens of thousands of nodes and hundreds of thousands of edges. The visualization approach should therefore be scalable with real-time interactivity, and should organize knowledge to be as visually digestible as possible. Leveraging the data and ontology provided by our knowledge assembly collaborators [12, 14], our approach should enable biomedical researchers to query and analyze the high-level structures of biological graphs derived from domain literature, thereby gaining insight on the ontological structure of the extracted causal knowledge.
- **DG2. Provide iterative local analysis coordinated with global context.** While interactive graph overviews are useful to identify high-level structural and ontological patterns, biomedical researchers need to isolate and extract relevant subgraphs for more focused analysis. They also need to iterate on these subgraphs as needed while keeping global context in mind. For example, to judge drug side effects, our approach must enable researchers to identify incoming and outgoing pathways from particular agents, and iteratively expand or truncate the subgraph under analysis in light of all pathways available in the global graph.
- **DG3. Promote scientific knowledge synthesis and discovery.** Researchers should be able to access backing scientific corpora to further contextualize their analysis and explore related knowledge spaces. Using data provided by our collaborators [12, 14, 29], our visualization approach allow researchers to seamlessly navigate back and forth from biological graphs to the scientific corpus at large. In this manner, researchers can trace pathways expressed in graph form to source documents and explore related knowledge to broaden their analysis.

## 4 DATA PROCESSING

Our approach leverages graph and knowledge data from collaborating systems in INDRA and COSMOS. INDRA (the Integrated Network and Dynamical Reasoning Assembler) assembles a network of biological processes from statements extracted from source documents using natural language processing techniques [14]. Extracted mechanistic and causal assertions are standardized and mapped to a biological ontology [13], generating an assembled set of causal statements that constitute a biological graph. We further normalize this statement data into a multidigraph optimized for real-time browser rendering. Here, biological agents are mapped to nodes clustered as per their ontological category and causal statements are mapped to directed edges between agents, with edges bundled into hyper-edges to enable layout generation at each level of the ontology.

COSMOS is a knowledge discovery platform that automates the process of extracting and assimilating heterogeneous artifacts from diverse scientific publications [29]. In addition to enabling search over a large corpus of publications, COSMOS extracts tables, text, images and source code. The corpus provided by COSMOS consists of 176,000 documents, complete with metadata and document artifact extraction. Knowledge search over this corpus is made available in our prototype via API. The corpus is also available as an embedding dataset, with each document cast as a vector embedding [33]. To these embeddings, we apply dimensional reduction via UMAP and hierarchical clustering via HDBSCAN to first project the embeddings into a 2D space and then group semantically proximate documents as nested clusters [27, 28]. Moreover, for each cluster, we compute the alpha shape of its point subspace to establish a polygon cluster boundary [4].

## 5 VISUALIZATION DESIGN

The following two subsections describe the two main spaces of our approach - the Graphs space and the Knowledge space - that were developed in light of the above design goals (DG). While the skeleton and core components of our approach are in place, we continue to refine the visualization, interaction, and analytic design for both spaces with domain experts.

### 5.1 Graphs Space

The Graphs space is composed of two coordinated views (Fig. 1) that seek to simultaneously provide the global and local perspectives needed for multi-scale graph sense-making [31]. As the default view, the *Global View* (Fig. 1. A) provides a visual overview of a biological graph, and has multi-faceted search, real-time navigation, and semantic zoom. The *Local View* (Fig. 1. B) is a sandbox to which search results can be iteratively added as a flow graph for further inspection. Our coordinated approach uses linked filtering and highlighting so changes in one view are reflected in the other. In this way, we look to enable biomedical researchers to engage in local subgraph analysis while contextualizing this analysis within the global context of the large-scale graph.

#### 5.1.1 Global View

The Global View shows an overview of a selected biological graph [DG1] assembled from large sets of biological causal statements. Each causal statement represents regulations between biological agents such as proteins or viruses (e.g. CDC12 phosphorylates MID1). The overview global graph displays nested clusters of biological agents organized in the background biomedical ontology. We use a hierarchical circle-packing graph layout [3] to show high-level relationship structure and the nested concepts of the ontology [DG1]. Each ontological group is rendered as rings (in blue) around their children (in orange). To avoid displaying hundreds of thousands of edges, we also apply edge bundling techniques [16], where edges with multiple nodes grounded to the same ontological category are bundled into hyper-edges. Hyper-edges are also wrapped around ontological rings to avoid edge clutter between groups, and hyper-edge brightness corresponds to the number of bundled statements. Semantic zooming progressively discloses the nested categories of the ontology as the researcher dives deeper into an ontological branch.

This view also allows researchers to interrogate biological graphs by using multi-faceted queries [DG2]. Researchers can chain multiple queries related to node attributes (e.g. node degree), edge attributes (e.g. edge type), and path queries via a search box at the top of the Graphs space (Fig. 1). Query results are displayed on the Global View using contrast-based highlighting, with results foregrounded and the rest of the graph faded out.

#### 5.1.2 Local View

While such global views provide high-level structural information, they face sense-making challenges for multi-scale graphs [16, 21, 31]. To this end, we coordinate the Global View with the Local View (Fig. 1.B), where the latter displays a subgraph containing the subset of causal statements resulting from preceding search queries [DG2].

Edges are visually encoded based on the implied polarity of the regulation type (e.g. activation, inhibition), curation state (human-verified or unexamined), and directionality (directed or not). We use the following scale to encode edge polarity: blue for “positive”, red for “negative”, and gray for “unknown.” We use a filled arrow for directed edges and a filled box arrow for undirected edges. Human-verified statements are shown with a filled circle, and unexamined statements have empty circles (incorrect statements are removed during data pre-processing) (Fig. 1. B). As directionality is critical for understanding causality [41], we use a traditional left-to-right flow layout algorithm [39] with recent extensions [6].

Selecting a node in the Local View opens a Drill-down Panel for the Graphs Space to show node metadata (e.g. agent description) and link suggestions for incoming and outgoing relationships ranked by supporting evidence [DG2]. Neighborhood suggestions are also highlighted in the Global View so researchers can visualize the global connectivity of a given node. Selecting one or more of these relationship suggestions adds them to the subgraph, which helps with neighborhood expansion.

#### 5.1.3 Graphs to Knowledge

To aid trust-building, researchers need to link their graph exploration back to scientific knowledge [DG3]. We build on the links present in the provided data. For example, selecting an edge reveals the underlying evidence extracted by INDRA, where this evidence is surfaced as a short-text fragment (Fig. 1. C). Clicking the text opens a modal dialog displaying associated metadata on both source and neighborhood documents provided by COSMOS. The neighborhood of a given document is taken as the set of semantically similar documents within the corpus [33]. In this manner, researchers can seamlessly trace a graph edge to its underlying textual evidence and then to the backing scientific paper.

## 5.2 Knowledge Space

The Knowledge space displays an interactive overview of the scientific corpus. The corpus data contains all source material from which all biological graphs have been assembled, thus encouraging moving back and forth between graph-centric analysis and the literature at large [DG3]. Two perspectives on the knowledge corpus [DG3] are available via: a *Card-based View* and a *Clusters View*.

#### 5.2.1 Card-based View

The Card-based View has a tabular layout with each document as a card, including a preview image of a document artifact and title. Cards organize information in chunks, which aids in user scannability. As in the Graphs space, the Knowledge space also has rich search capabilities where researchers can perform multiple compound queries on document attributes, including free text, author, publisher, and the presence of artifacts such as tables or figures.

#### 5.2.2 Clusters View

While the Card-based View supports visual scannability, it suffers from visual scalability for large numbers of documents. The Clusters View (Fig. ??) thus provides a more scalable perspective on the scientific corpus using document embeddings. Organized in a 2D topology, a point in this visual space is a document, and spatial distance between points measures semantic similarity. Cluster members have the same color and are enclosed within a bounding alpha shape. Documents designated as “noise” by the clustering algorithm (not in any cluster) are coloured grey with no boundary. To visually encode cluster hierarchy, color hue is preserved across levels with lower opacity being applied to coarsest clustering levels.

#### 5.2.3 Metadata and Knowledge to Graphs

Selecting a document from either a card in the Card-based View or a point in the Clusters View opens a Drill-down Panel in the Knowledge Space with three tabs for deeper interrogation of the document content. The *Preview* tab shows document metadata including title, DOI, authors and publisher-related information, with further drill-down available via a dialog with more detailed information including figures and text excerpts as well as the link back to the source document. This allows the researcher to discover related documents in addition to using spatially proximate documents in the Cluster view. The *Graphs* tab contains links to existing biological graphs in the Graphs space, and fortifies the connection between user analysis and background scientific literature. The *Entities* tab shows related keywords that helps researchers guide subsequent search.

## 6 USAGE SCENARIO

While our approach remains general across various biomedical graph-based use cases, we focus here on a usage scenario relevant to our current era around the exploration of biological mechanisms of COVID-19. A biomedical researcher is investigating potential drug treatments for SARS-CoV-2. Due to prior knowledge, they know that SARS-CoV-2 leads to the release of cytokines like IL6, which is associated with more severe symptoms and higher mortality in COVID-19 patients [2]. They hypothesize that identifying inhibitors of IL6 may provide potential therapeutics for the treatment of SARS-CoV-2.

They start their investigation by selecting the COVID-19 graph from the available list in the Graphs space. Using their prior knowledge of articles related to cytokine release syndrome in severe COVID-19 cases [42] and recommended medications for COVID-19 [26, 34], they do a search query using the DOIs of these papers. Highlighted results in the Global View show the causal relationships extracted from these papers (Fig. 1. A). To further examine these results, they click on the “Open Local View” button, which displays the corresponding subgraph in the Local View (Fig. 1. B). They then select the IL6 node to open the Drill-down Panel with node metadata and neighboring relationships. They explore the incoming relationships for IL6 and identifies a relationship with SARS-CoV-2, and adds this relationship to the subgraph. They then click on the new relationship to read the underlying evidence, which confirms their prior knowledge i.e. that SARS-CoV-2 increases the amount of IL6.

They continue exploring the subgraph in the Local View and notices that the relationship from tocilizumab to IL6 is encoded in red, which indicates that tocilizumab is an inhibitor of IL-6. They start to wonder if treating a COVID-19 patient with tocilizumab alter their chances of survival. To better understand the involved biological mechanisms, they click on the edge to read the pieces of evidence underlying this relationship in the Drill-down Panel (Fig. 1. C). In this panel, they see a check-mark beside the relationship heading, indicating that this relationship has been vetted by domain experts and is also supported by 39 pieces of evidence. In this light, they execute a path query that is chained with their prior queries. The results show a pathway from tocilizumab to IL6 to COVID-19, suggesting that tocilizumab (insofar as it acts upon IL6 and therefore could inhibit the cytokine storm) might be a drug candidate for severe COVID-19. Having formulated a hypothesis around tocilizumab and COVID-19 survival rates, they now want to identify if tocilizumab could have any side effects. To explore this, they inspect the 121 outgoing nodes from tocilizumab and see a relationship to immune responses. After adding this relationship to the subgraph, they find that it is of the inhibition type. By inspecting the underlying evidence, they also learn that tocilizumab may lower the ability of the immune system, increasing the risk of superinfections [36]. Through this quick exploration using our approach, the researcher has been able to quickly identify a potential drug to treat COVID-19 as well as potential side effects. They can continue to expand this line of inquiry to the backing scientific corpus available in the Knowledge space, and look to discover publications and research artifacts related to this drug. They can also choose to explore other biomedical hypotheses across the COVID19 graph, and quickly isolate relevant graph structures and textual support to further analysis.

## 7 EXPERT EVALUATION

For an initial assessment on our approach to inform future iteration, we conducted a two-part evaluation: (i) a focus group with five external researchers for high-level feedback; and (ii) an online questionnaire focused on usability and utility with one biomedical researcher with over ten years of experience. All experts conduct research on systems biology, bioinformatics, and causal reasoning using biological models in their daily work. For the focus group,

we presented a demo of the tool before the experts were asked to give general feedback about system function in a group discussion that lasted around two hours. For the questionnaire, the expert was first asked to complete a task scenario, which was the same as the usage scenario described in Section 6 for investigating potential drug treatments for SARS-CoV-2. After completing the scenario, the expert was encouraged to keep using the tool, then respond to the questionnaire.

The overall opinion of the domain experts was quite positive regarding the ease of interaction, the scale covered and the overall usefulness of the prototype. Specifically, the experts found the coordination between the Global and Local Views very useful for navigating the contained knowledge. The experts felt that this prototype achieves the goal of supporting query formulation while representing biological relationships in a visually organized way. Some critical feedback received regarded a slight delay when conducting large-scale path queries (due to the query’s time-complexity not currently optimized over large graphs), inconsistencies in some path query results (because of path alternatives), and the general need for better notifications. We plan to address all these concerns in the near future. Overall, domain experts agreed that they would like to use the tool frequently as new features, optimizations and improvements continue to be developed.

## 8 CONCLUSION AND FUTURE WORK

In this paper, we introduced a visual analytics approach for scalable exploration of biomedical knowledge that can aid across a range of biomedical use cases, from disease propagation to drug discovery. To demonstrate the feasibility of our approach, we implemented a web-based prototype that displays 16 biological models against a corpus of 176,000 documents. Positive feedback from domain experts underscores the usefulness and usability of our prototype in helping them to explore, formulate and validate hypotheses.

Several promising directions exist in terms of future research. While the Global View is visually scalable for graphs of thousands of nodes and edges, better overviews can be provided to the user via high-level summaries and aggregate graph statistics that surface interactively during graph exploration. Search remains a critical research thread, given the scale and complexity of biological graphs. Highlighting and navigation of search results could be further improved. Search functionality can also better incorporate user context, so more relevant results are returned. Similarly, refinements in the Local View can improve neighborhood suggestions for user-extracted subgraphs. For example, there are almost 2,000 incoming nodes and 1,000 outgoing ones for IL-6 alone in the COVID-19 graph: path ranking based on user context could help prioritize the edge list for the problem at hand. For such global and local improvements, we look to explore graph embedding techniques that convert graph structures into vector representations. Such representations enable various downstream analytic tasks, including similarity search for pathways and subgraphs, path ranking, link prediction and so on. In the Knowledge space, we plan to refine our hierarchical clustering for better visual separation, as well as enrich the view with search capability. We also plan to incorporate citation graphs and add semantic layers such as topics and extracted artifacts to better facilitate exploration across the available corpus.

On the whole, the generality of our approach means it can extend to other workflows that utilize hierarchically organized knowledge graphs that are linked to backing documents. In this way, we believe our approach can be applied to a range of biomedical use-cases and ultimately support knowledge discovery across different scientific domains.

## ACKNOWLEDGMENTS

This work was supported by the Defense Advanced Research Projects Agency (DARPA) under Contract (HR0011199005).

## REFERENCES

- [1] G. Cesareni. SIGNOR 2.0: The signaling network open resource, 2021.
- [2] V. J. Costela-Ruiz, R. Illescas-Montes, J. M. Puerta-Puerta, C. Ruiz, and L. Melguizo-Rodríguez. SARS-CoV-2 infection: The role of cytokines in COVID-19 disease. *Cytokine & Growth Factor Reviews*, 54:62–75, Aug. 2020. doi: 10.1016/j.cytofr.2020.06.001
- [3] d3. d3-hierarchy, July 2021.
- [4] H. Edelsbrunner, D. Kirkpatrick, and R. Seidel. On the shape of a set of points in the plane. *IEEE Transactions on Information Theory*, 29(4):551–559, July 1983. doi: 10.1109/TIT.1983.1056714
- [5] A. T. Eitan, E. Smolyansky, I. K. Harpaz, and S. Perets. Connected Papers | Find and explore academic papers, 2021.
- [6] elk.js. elk.js, 2020.
- [7] J. Elliot. Automating scientific knowledge extraction (aske), 2020.
- [8] N. C. for Biotechnology Information. PubMed, 2021.
- [9] A. J. Gates, Q. Ke, O. Varol, and A.-L. Barabási. Nature’s reach: narrow work has broad impact. *Nature*, 575(7781):32–34, Nov. 2019. doi: 10.1038/d41586-019-03308-7
- [10] N. Gehlenborg, S. I. O’Donoghue, N. S. Baliga, A. Goessmann, M. A. Hibbs, H. Kitano, O. Kohlbacher, H. Neuweiler, R. Schneider, D. Tenenbaum, and A.-C. Gavin. Visualization of omics data for systems biology. *Nature Methods*, 7(3):S56–68, Mar. 2010. doi: 10.1038/nmeth.1436
- [11] B. M. Gyori. Bob with bioagents dialogue system, 2020.
- [12] B. M. Gyori and J. A. Bachman. EMMAA: Ecosystem of Machine-maintained models with Automated Analysis, 2020.
- [13] B. M. Gyori and J. A. Bachman. INDRA BioOntology — INDRA 1.20.0 documentation, 2020.
- [14] B. M. Gyori, J. A. Bachman, K. Subramanian, J. L. Muhlich, L. Galescu, and P. K. Sorger. From word models to executable models of signaling networks using automated assembly. *Molecular Systems Biology*, 13:953, July 2017. doi: 10.1525/msb.20177651
- [15] E. M. Hechenbleikner, D. V. Samarov, and E. Lin. Data explosion during COVID-19: A call for collaboration with the tech industry & data scrutiny. *eClinicalMedicine*, 23, June 2020. doi: 10.1016/j.eclim.2020.100377
- [16] D. Holten. Hierarchical Edge Bundles: Visualization of Adjacency Relations in Hierarchical Data. *IEEE Transactions on Visualization and Computer Graphics*, 12(5):741–748, Sept. 2006. doi: 10.1109/TVCG.2006.147
- [17] K. A. Janes, P. L. Chandran, R. M. Ford, M. J. Lazzara, J. A. Papin, S. M. Peirce, J. J. Saucerman, and D. A. Lauffenburger. An engineering design approach to systems biology. *Integrative biology : quantitative biosciences from nano to macro*, 9(7):574–583, July 2017. doi: 10.1039/c7ib00014f
- [18] L. Jeske, S. Placzek, I. Schomburg, A. Chang, and D. Schomburg. BRENDa in 2019: a European ELIXIR core data resource. *Nucleic Acids Research*, 47(D1):D542–D549, Jan. 2019. doi: 10.1093/nar/gky1048
- [19] A. E. Jinha. Article 50 million: an estimate of the number of scholarly articles in existence. *Learned Publishing*, 23(3):258–263, 2010.
- [20] M. Kanehisa and S. Goto. KEGG: Kyoto Encyclopedia of Genes and Genomes. *Nucleic Acids Research*, 28(1):27–30, Jan. 2000.
- [21] D. A. Keim. Visual exploration of large data sets. *Communications of the ACM*, 44(8):38–44, Aug. 2001. doi: 10.1145/381641.381656
- [22] A. Kerren, K. Kucher, Y.-F. Li, and F. Schreiber. BioVis Explorer: A visual guide for biological data visualization techniques. *PLOS ONE*, 12(11):e0187341, Nov. 2017. doi: 10.1371/journal.pone.0187341
- [23] E. Kibardin. Using topological text analysis for COVID-19 Open Research Challenge, Apr. 2020.
- [24] P. Kraker, C. Kittel, and A. Enkhbayar. Open Knowledge Maps: Creating a Visual Interface to the World’s Scientific Knowledge Based on Natural Language Processing. *027.7 Zeitschrift für Bibliothekskultur*, 4(2):98–103, Nov. 2016. doi: 10.12685/027.7-4-2-157
- [25] F. Lekschas and N. Gehlenborg. SATORI: a system for ontology-guided visual exploration of biomedical data repositories. *Bioinformatics*, 34(7):1200–1207, Apr. 2018. doi: 10.1093/bioinformatics/btx739
- [26] Q. Ma, M. Qiu, H. Zhou, J. Chen, X. Yang, Z. Deng, L. Chen, J. Zhou, Y. Liao, Q. Chen, Q. Zheng, L. Cai, L. Shen, and Z. Yang. The study on the treatment of Xuebijing injection (XBJ) in adults with severe or critical Corona Virus Disease 2019 and the inhibitory effect of XBJ against SARS-CoV-2. *Pharmacological Research*, 160:105073, Oct. 2020. doi: 10.1016/j.phrs.2020.105073
- [27] L. McInnes, J. Healy, and S. Astels. HdbSCAN: Hierarchical density based clustering. *The Journal of Open Source Software*, 2(11), mar 2017. doi: 10.21105/joss.00205
- [28] L. McInnes, J. Healy, and J. Melville. UMAP: Uniform Manifold Approximation and Projection for Dimension Reduction. *arXiv:1802.03426 [cs, stat]*, Sept. 2020.
- [29] U. of Wisconsin Madison. Cosmos: An ai platform for knowledge discovery and scientific model curation, 2021.
- [30] G. A. Pavlopoulos, A.-L. Wegener, and R. Schneider. A survey of visualization tools for biological network analysis. *BioData Mining*, 1(1):12, Dec. 2008. doi: 10.1186/1756-0381-1-12
- [31] R. Pienta, J. Abello, M. Kahng, and D. H. Chau. Scalable graph exploration and visualization: Sensemaking challenges and opportunities. In *2015 International Conference on Big Data and Smart Computing (BIGCOMP)*, pp. 271–278, Feb. 2015. doi: 10.1109/35021BIGCOMP.2015.7072812
- [32] S. Pirch, F. Müller, E. Iofinova, J. Pazmandi, C. V. R. Hüttler, M. Chittini, C. Sin, K. Boztug, I. Podkosova, H. Kaufmann, and J. Menche. The VRNetzer platform enables interactive network analysis in Virtual Reality. *Nature Communications*, 12(1):2432, Apr. 2021. doi: 10.1038/s41467-021-22570-w
- [33] R. Řehůrek and P. Sojka. Software Framework for Topic Modelling with Large Corpora. In *Proceedings of the LREC 2010 Workshop on New Challenges for NLP Frameworks*, pp. 45–50. ELRA, Valletta, Malta, May 2010.
- [34] H. Samaee, M. Mohsenzadegan, S. Ala, S. S. Maroufi, and P. Moradimajd. Tocilizumab for treatment patients with COVID-19: Recommended medication for novel disease. *International Immunopharmacology*, 89(Pt A):107018, Dec. 2020. doi: 10.1016/j.intimp.2020.107018
- [35] K. Sidiropoulos, G. Viteri, C. Sevilla, S. Jupe, M. Webber, M. Orlic-Milacic, B. Jassal, B. May, V. Shamovsky, C. Duenas, K. Rothfels, L. Matthews, H. Song, L. Stein, R. Haw, P. D’Eustachio, P. Ping, H. Hermjakob, and A. Fabregat. Reactome enhanced pathway visualization. *Bioinformatics (Oxford, England)*, 33(21):3461–3467, Nov. 2017. doi: 10.1093/bioinformatics/btx441
- [36] E. C. Somers, G. A. Eschenauer, J. P. Troost, J. L. Golob, T. N. Gandhi, L. Wang, N. Zhou, L. A. Petty, J. H. Baang, N. O. Dillman, D. Frame, K. S. Gregg, D. R. Kaul, J. Nagel, T. S. Patel, S. Zhou, A. S. Lauring, D. A. Hanauer, E. Martin, P. Sharma, C. M. Fung, and J. M. Pogue. Tocilizumab for Treatment of Mechanically Ventilated Patients With COVID-19. *Clinical Infectious Diseases*, (ciaa954), July 2020. doi: 10.1093/cid/ciaa954
- [37] D. N. Sosa, A. Derry, M. Guo, E. Wei, C. Brinton, and R. B. Altman. A Literature-Based Knowledge Graph Embedding Method for Identifying Drug Repurposing Opportunities in Rare Diseases. In *Biocomputing 2020*, pp. 463–474. WORLD SCIENTIFIC, Kohala Coast, Hawaii, USA, Dec. 2019. doi: 10.1142/9789811215636\_0041
- [38] J. Stasko. Jigsaw: Visual Analytics for Exploring and Understanding Document Collections, 2013.
- [39] K. Sugiyama, S. Tagawa, and M. Toda. Methods for visual understanding of hierarchical systems structure. *Systems, Man and Cybernetics, IEEE Transactions on*, 11:109 – 125, 03 1981.
- [40] P. V. Todorov, B. M. Gyori, J. A. Bachman, and P. K. Sorger. INDRA-IPM: interactive pathway modeling using natural language with automated assembly, Nov. 2019. doi: 10.1093/bioinformatics/btz289
- [41] W. T. Wright and T. Kapler. Challenges in visualizing complex causality characteristics. In *IEEE Pacific Visualization Symposium (PacificVis 2018)*, 2018.
- [42] C. Zhang, Z. Wu, J.-W. Li, H. Zhao, and G.-Q. Wang. Cytokine release syndrome in severe COVID-19: interleukin-6 receptor antagonist tocilizumab may be the key to reduce mortality. *International Journal of Antimicrobial Agents*, 55(5):105954, May 2020. doi: 10.1016/j.ijantimicag.2020.105954

## A APPENDIX



# Towards a Comprehensive Cohort Visualization of Patients with Inflammatory Bowel Disease

Salmah Ahmad\*  
Fraunhofer IGD

David Sessler†  
Fraunhofer IGD

Jörn Kohlhammer‡  
Fraunhofer IGD  
TU Darmstadt

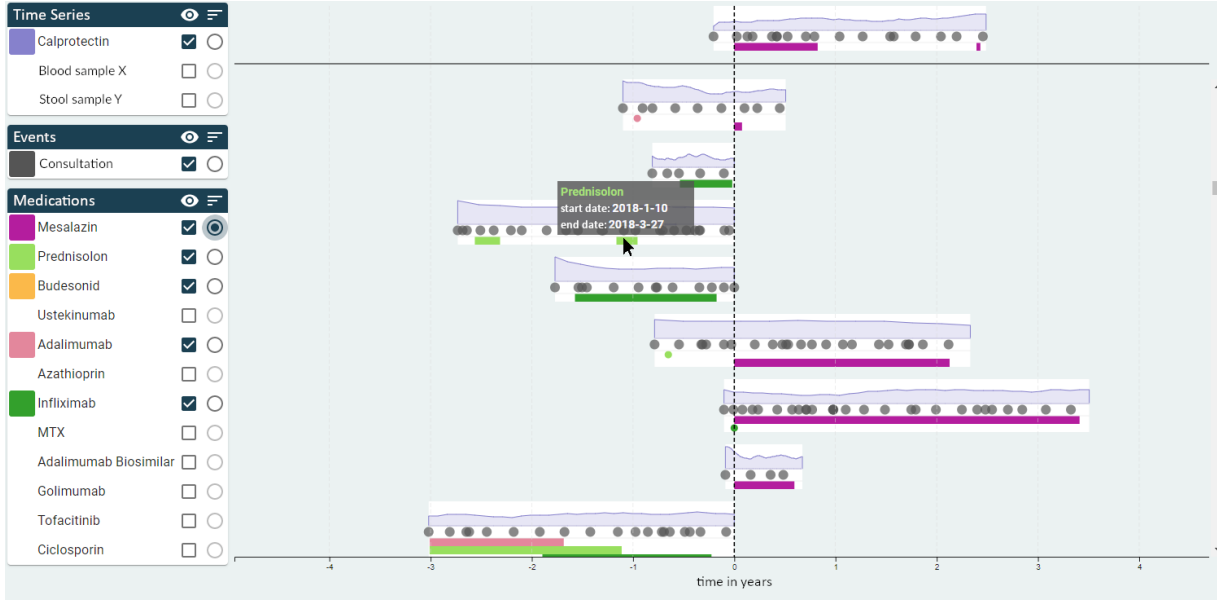


Figure 1: Visualization of a cohort of patients with inflammatory bowel disease with implemented feedback from the evaluations. Users can select data through the menu on the left. On the right side, this data is visualized for each patient in the cohort, with the focal patient at the top. Time series of blood or stool values, important events and prescribed medications are displayed in each patient's row. A tooltip shows additional information while hovering over an element. A timeline displays disease progression in years and can be synchronised to a specific element, in this case Mesalazin.

## ABSTRACT

This paper reports on a joint project with medical experts on inflammatory bowel disease (IBD). Patients suffering from IBD, e.g. Crohn's disease or ulcerative colitis, do not have a reduced life expectancy and disease progressions easily span several decades. We designed a visualization to highlight information that is vital for comparing patients and progressions, especially with respect to the treatments administered over the years. Medical experts can interactively determine the amount of information displayed and can synchronize the progressions to the beginning of certain treatments and medications. While the visualization was designed in close collaboration with IBD experts, we additionally evaluated our approach with 35 participants to ensure good usability and accessibility. The paper also highlights the future work on similarity definition and additional visual features in this on-going project.

## 1 INTRODUCTION

Inflammatory bowel disease (IBD) is a chronic, costly disease characterised by relapsing-remitting symptoms, causing inflammation of

the gastro-intestinal tract [2, 14]. Well-known varieties of IBD are Crohn's disease or ulcerative colitis with clinical features including diarrhea, abdominal pain, and, in the case of ulcerative colitis, perianal bleeding. The disease progression of IBD often spans several decades and its prevalence is increasing globally [6]. Managing this disease can be complex, since physicians usually only have access to written patient records of individual patients, which leads to a great amount of manual work if the complete medical history is to be considered. Collecting and visualizing this patient data can help physicians gain a quick overview of the patient and other similar patients. The IBD specialists in our collaboration explained to us that understanding the effects of biologic (protein-based) drugs that stimulate the body's response as part of an immunotherapy against IBD are of particular interest. The first biologic drug that is given to a patient seems to have a larger than expected impact on the disease progression, which makes the decision for a certain compound one of the most vital steps in the treatment of an IBD patient. Comparing patients and their disease progressions in relation to the chosen treatments is therefore an important IBD-specific analysis that our experts requested to help raise the standard of care and quality of life for their IBD patients.

Based on collaboration with IBD specialists we designed a visualization to clearly display multimodal information of patients of a cohort regarding disease progression and prior treatments. During development, we periodically carried out expert interviews to ensure that the visualization is moving in the appropriate direction. This included evaluation sessions with IBD specialists, an external eval-

\*e-mail: salmah.ahmad@igd.fraunhofer.de

†e-mail: david.sessler@igd.fraunhofer.de

‡e-mail: joern.kohlhammer@igd.fraunhofer.de

ation, and a usability study with university students. Fig. 1 shows the state of the application after implementing feedback gathered in all these evaluations.

## 2 RELATED WORK

In recent years, visualization in healthcare has become more widely used and prevalent. While analyses of IBD treatments and cohorts are a ubiquitous topic of research [16, 19], medical data pertaining this disease is rarely summarized in a comprehensive visualization. Instead, data tables and independent visualizations are still predominately used [17]. The workshop on visual analytics in healthcare has established itself as an important event showcasing new approaches in the visualization and analysis of medical data. Patient cohorts are an important mechanism for analyzing similar disease trajectories and drawing new conclusions about treatments.

Maf-tools by Mayacoda et al. [13] is a tool that focuses on visualizing a large cohort of the Mutation Annotation Format (MAF) data. Zhang et al. [20] developed a platform for Cohort Analysis via Visual Analytics (CAVA). This tool is designed to accelerate domain experts' cohort studies. Their visualization approach includes an interactive Sankey diagram to easily display complex analysis pathways that were chained together. Bernard et al. [3] have developed a visual-interactive system that enables physicians to define and analyze cohorts of prostate cancer patients. This system focuses on defining and visualizing patient cohorts and helping physicians and researchers increasing their analytical workflow. A visualization by Antweiler et al. [1] focuses on identifying, assessing and visualizing clusters in COVID-19 contact tracing networks. Their visualization displays multimodal data of events (contact, first symptoms, test results) and time periods (infectious periods, quarantine) in a single row per person. Events are displayed as colored circles and time spans as colored bars. Their approach is used in our visualization in a modified form. However, none of the previous work targeted IBD or the visualization of similarly long disease progressions.

## 3 VISUAL COHORT ANALYSIS

The goal of our visualization is to provide a quick overview of a disease progression over a long period of time. Fig. 1 shows our visualization filled with example data. The user can select relevant information through a menu on the left side. The selected information is displayed in multiple rows in the resulting visualization on the right side. A selected focal patient is always displayed at the top of the page and will stay there while the user may scroll through other patients of the cohort to ensure a good comparability to this focal patient. On the bottom of the page, a timeline shows the relative duration of the treatment history for all patients within the cohort. Additionally, a tooltip is shown on mouseover with further information on the corresponding event, e.g. the start and end date of a prescribed medication. Time series of blood or stool samples are displayed as a line chart at the top of each row. Below this, different events, e.g. consultations or surgeries can be displayed as icons on the timeline. Prescribed medications are shown in the bottom part of each patient row. Each medication is represented by a colored bar, corresponding to the color chosen in the menu on the left. Collecting ideas on how to visualize overlapping prescriptions and events was one part of the usability evaluation. In the current state of the visualization, overlapping prescriptions are stacked vertically and overlapping events are transparent. Different design ideas were collected and evaluated and will be implemented in subsequent iterations of the tool. These ideas are further elaborated in Sect. 4.3.

Furthermore, users are able to set the focus of the timeline at the bottom of the page to the peak in a time series of a measurement, a specific event or the start of a medication by pressing a button in the menu. In this case, the visualization will shift the timeline to the selected element. In Fig. 1 this alignment is shown for the medication Mesalazin. The user can now compare for example how

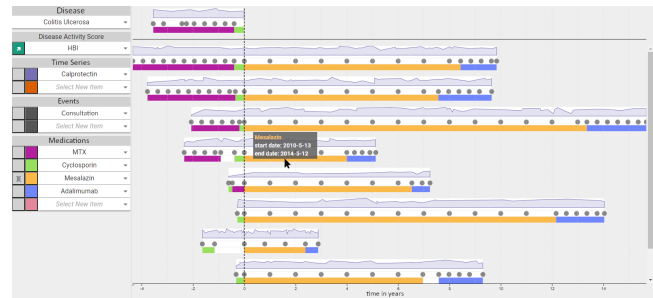


Figure 2: Our visualization in a previous iteration, which was used in the evaluations.

a specific blood level changed after prescribing a specific medication. Another example is examining disease progression after a surgery. By selecting and deselecting elements in the visualization, physicians can easily individualize patient care, after examining how treatments worked for other patients.

### 3.1 Technical Implementation

The basis for our visual-interactive system is data from the University Hospital Frankfurt [11]. A complete real-world data set was not yet available at the time of the evaluations. For this reason, we took the data of approx. 500 patients provided by our partners in Frankfurt and constructed a realistic, but simulated data set containing all relevant attributes for the evaluations. The department that specializes in treatment of IBD provided the data from their hospital information system (ORBIS) after technical, ethical, and GDPR approval. Our tool was developed as part of a larger project to advance cost-intelligence, data-driven medicine. Our cohort visualization is one module within a software framework that uses the data from Frankfurt to support decision making by IBD experts. Together with other modules our cohort analysis tool will be integrated into a dashboard providing the physicians with a powerful analysis tool set. To ensure the accessibility for all modules of the dashboard and to make the database easily extensible with data from additional sources, the ORBIS data was mapped into a knowledge graph by the data experts from our consortium. Our tool accesses this data via a secure connection to the database using SPARQL [18] as query language. The processing of the data to match the requirements of our visualization is performed on a Java backend. Here, we select a group of appropriate patients based on their similarity to the focal patient, thus creating a cohort that can be explored using our visualization. The visual-interactive tool is implemented as a web application. Notable frameworks we use are React.js [15] for the basis of the application, d3.js [4] for the event-based patient cohort visualization, and Material-UI [12] for the GUI components.

## 4 EVALUATION

During development expert interviews were held periodically. Since physicians usually have a very busy schedule, we scheduled feedback sessions as rare as possible and as often as needed. We were able to schedule five sessions with a senior expert at our partner clinic in Frankfurt and two meetings with the external advisory board to gather this expert advice. The functionality and user-friendliness of our tool was evaluated by an external company specialized in evaluating software solutions in the health sector. We also conducted a quantitative user evaluation with university students to collect feedback on the usability where domain expertise was not required. All evaluations were conducted with the state of the application as shown in Fig. 2.

**Data** The data set used in all evaluations contained a virtual

patient cohort with simulated multimodal data. It includes blood samples of Calprotectin, medical consultations as events and the medications MTX, Cyclosporin, Mesalazin and Adalimumab. This data was chosen in accordance to feedback from IBD specialists, in order to not distract from the visualization during the interviews. It was also constructed to be able to show all relevant features of the visualization.

#### 4.1 Expert Feedback

Feedback sessions with domain experts were conducted as an online video meeting, where IBD specialists were shown a live demonstration of the tool via screensharing. While it would have been preferable to have in-person meetings, we had to schedule online meetings due to the pandemic, which caused a more complex technical infrastructure in letting the experts use our application directly. The experts were able to ask questions about the tool at any time. After a demonstration of the features of the tool, we asked the domain experts about further features they may want to see in the tool (implemented as mock-ups). This approach allowed us to collect feedback on several design ideas before implementing them into the tool. In general, the feedback was positive. Physicians appreciated the clear and easy-to-read layout and the ability to quickly compare several patients. It was also noted that our tool could be used in teaching in order to explore long disease progressions and the impact of different treatments on the patient's wellbeing.

#### 4.2 Functional Evaluation

As part of an evaluation of all modules of the complete dashboard, our module was functionally evaluated by an external company specialized on evaluation in the health sector. First, we presented all current features of our tool with an outlook into future work. Afterwards, the evaluator asked specific questions about the future integration of the tool into the dashboard and assessed functionality and usability of the current state of the application. After the live interview, the application was made available to the evaluator for further testing. In general, the assessment of our tool was positive. There were no technical problems in using the application and especially the clear overview over a large patient cohort was commended.

#### 4.3 Usability Evaluation

We conducted a usability evaluation with 35 students on our tool. The students who participated in this evaluation were all taking the course on "user-centered design" at the time and they all study subjects related to computer science. Since the goal of the evaluation was to collect feedback and determine usability flaws in addition to the domain expert feedbacks, a medical background of the participating students was not required. Students were instructed to interact with the visualization with no prior knowledge about its features and only a short introduction to IBD and patient cohorts. While exploring the visualization we asked them to comment on perceived appealing and disruptive design elements and assess this using the AttrakDiff [10] and System Usability Scale [5] questionnaires. Using this evaluation approach helped us to understand which design elements worked well in guiding users without domain expertise. Further, participants were instructed to examine the visualization with respect to consistency, Gestalt laws [8] and reduction of memory load. Complementary to the AttrakDiff questionnaire and in preparation for creating new design ideas, participants also were asked to find specific pragmatic and hedonic qualities of the visualization. Almost all participants were in the age range of 20-30 years old with only one participant in the range of 30-40 years old. Of the 35 participants, 25 were male and 10 female. 62.9% of the participants have stated to have prior knowledge in information visualization. Feedback in general included improvements on visual aspects of the tool to create an intuitive workflow, impressions of

Type	Feedback	Impl.
E	Highlight important events like infections in a distinctive way.	<input checked="" type="radio"/>
E	Visualize when blood or stool values cross a threshold value.	<input type="radio"/>
E	Sort medications into a hierarchy to identify problematic administrations.	<input checked="" type="radio"/>
E	Visualize co-existing diseases and concomitant medications to ensure no harmful interactions during treatments.	<input checked="" type="radio"/>
E, F	Visualize concurrent prescriptions and events.	<input checked="" type="radio"/>
E, F	Save the current view as a screenshot.	<input type="radio"/>
F	The overall design should match the dashboard for future integration.	<input checked="" type="radio"/>
F	Manually arrange patients to provide a better overview.	<input type="radio"/>
F, U	Provide panning and zooming functionality.	<input checked="" type="radio"/>
F, U	Selected elements do not disappear from the drop-down menu.	<input checked="" type="radio"/>
F, U	A more prominent highlighting to further distinguish the focal patient from the other patients.	<input checked="" type="radio"/>
U	Add a higher contrast between the background color and the patient's color.	<input checked="" type="radio"/>
U	Indicate the mouse position to help reading the chart.	<input checked="" type="radio"/>
U	Add icons to the buttons.	<input checked="" type="radio"/>
U	Add an additional button to select custom colors for each element.	<input checked="" type="radio"/>
U	Permanently display all patients' IDs to be able to quickly locate patients again.	<input type="radio"/>
U	The menu bar should be expandable and collapsible.	<input type="radio"/>

Table 1: Most common feedback from the domain experts (E), the functional evaluation (F) and the usability evaluation (U). The circles indicate whether the feedback is implemented in the current iteration () being currently worked on () or not yet implemented ().

the usability while working with the tool and new design ideas to improve on perceived flaws.

#### 4.4 Results

The most common feedbacks and feature suggestions from all evaluations are collected in Table 1. Table 1 also shows which feedback is already implemented and being worked on in the current iteration as seen in Fig. 1.

The results of the AttrakDiff evaluation can be seen in Fig. 3. This scale is used to measure pragmatic and hedonic qualities [7] of a product. Pragmatic qualities describe how comprehensible, ergonomic and task-oriented a product is perceived. Hedonic qualities describe the innovativeness, enjoyment and general "appealingness" of a product [9]. On average, participants rated the pragmatic and hedonic quality as well as the attractiveness of the tool as neutral (PQ=3.96, HQI=4.25, HQS=4.1, ATT=3.8, on a likert scale from 1 (disagree) to 7 (agree)). As the participants of the usability evaluation had no expertise in the domain, these results were to be expected. Still, neutral values provide insight as this means that the application is not badly designed, but at the same time has room for improvement, which the students described in the feedback they provided. Participants commented positively on the clean interface of the visualization with no superfluous components. At the same time, some participants noted that the empty interface with no selected data felt "challenging" since they thought it would be demanding to find the data to display, but were pleasantly surprised

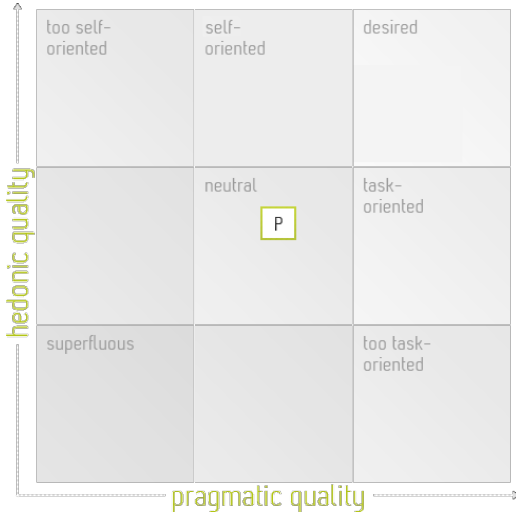


Figure 3: Results of the AttrakDiff evaluation with medium value of the dimension with prototype P [10].

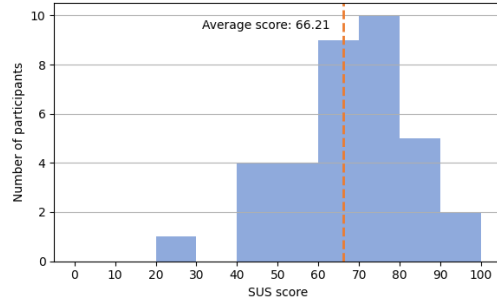


Figure 4: System Usability Scale scores. The average score (orange line) is 66.2 [5].

at the ease of displaying relevant data. The System Usability Score averaged at 66.2, with the lowest score of 22.5 and the highest of 97.5 (cf. Fig. 4). The large variance of SUS scores could be a result of the foreign domain of IBD for computer science students. While most participants placed importance on considering the tool from a physician's point of view, some did not see value in using the tool themselves and scored accordingly.

Fig. 5 shows different design ideas by participants for overlapping medications, concurrent events and improvements on the menu. Participants were directed to pay special attention to the limitation imposed by the limited screen space. For medications, a popular approach was to have the bars interlock. This way, two medications are easily distinguishable while keeping required space to a minimum. For more than two medications, many participants proposed decreasing the bar height or using texture to indicate further information to be accessed via tooltip. Icons were the most popular visualization technique proposed for events. Combined with color and transparency, two to three simultaneous events can comfortably be distinguished. For more than three events, displaying them vertically with smaller icons was often proposed. Since one frequent feedback was the inadequate depiction of the buttons, many design ideas featured improved menu elements. The button to remove an element from the visualization was often suggested as a bucket or "X". Another frequent suggestion included permanently displaying the icon for setting the focus of the timeline on all relevant buttons and

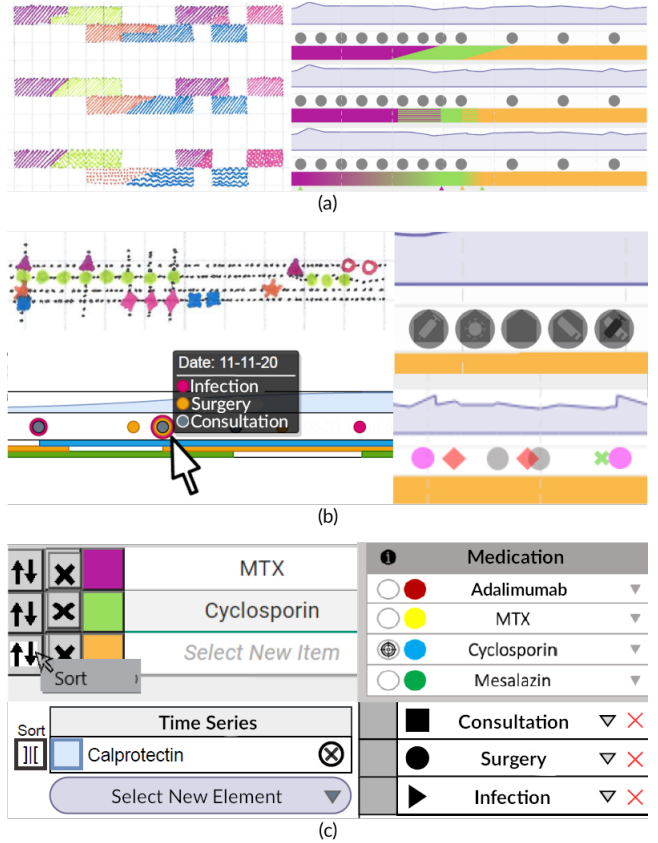


Figure 5: Different design ideas for overlapping medications (a), overlapping events (b) and menu improvements (c).

highlighting the element that is currently selected. Displaying icons on the buttons was commonly referenced in the task of reducing memory load for the user.

## 5 CONCLUSION AND FUTURE WORK

We presented a comprehensive visualization for cohorts of patients with IBD with the ability to display multimodal data. Domain experts gave quite positive feedback on the visualization and appreciated the ability to quickly gain an overview of the disease progression over a long period of time. Our visualization can help increase the standard of care by presenting complex information in a concise and easy to understand manner, allowing specialists to focus their expertise on patient care instead of manually browsing through patient records. We conducted a usability evaluation with university students to gain insight on aspects, where domain expertise was not a requirement. The usability evaluation showed that our visualization can be used without the need for an in-depth introduction.

Feedback from both domain experts and university students will be implemented in subsequent iterations of our tool. The collected design ideas for improvements and new features gave important impulses for future developments and will be evaluated again by our collaborating domain experts. Furthermore, in our future work we will work on the similarity definition for long disease progression coupled with an interactive filtering approach to allow our experts to quickly define a specific cohort of interest.

## ACKNOWLEDGMENTS

This work was funded by the Fraunhofer Lighthouse project on Medical Data for Individual Treatment and Cost Intelligence (MED<sup>2</sup>ICIN).

## REFERENCES

- [1] D. Antweiler, D. Sessler, S. Ginzel, and J. Kohlhammer. Towards the detection and visual analysis of covid-19 infection clusters. In *EuroVis Workshop on Visual Analytics (EuroVA)*. Submitted to the Eurographics Association, 2021.
- [2] D. C. Baumgart and S. R. Carding. Inflammatory bowel disease: cause and immunobiology. *The Lancet*, 369(9573):1627–1640, 2007.
- [3] J. Bernard, D. Sessler, T. May, T. Schlomm, D. Pehrke, and J. Kohlhammer. A visual-interactive system for prostate cancer cohort analysis. *IEEE Computer Graphics and Applications*, 35(3):44–55, 2015. doi: 10.1109/MCG.2015.49
- [4] M. Bostock, V. Ogievetsky, and J. Heer. D<sup>3</sup> data-driven documents. *IEEE transactions on visualization and computer graphics*, 17(12):2301–2309, 2011.
- [5] J. Brooke et al. Sus-a quick and dirty usability scale. *Usability evaluation in industry*, 189(194):4–7, 1996.
- [6] G. Collaborators et al. Global, regional, and national incidence, prevalence, and years lived with disability for 354 diseases and injuries for 195 countries and territories, 1990–2017: a systematic analysis for the global burden of disease study 2017. 2018.
- [7] S. Diefenbach, N. Kolb, and M. Hassenzahl. The ‘hedonic’ in human-computer interaction: history, contributions, and future research directions. In *Proceedings of the 2014 conference on Designing interactive systems*, pp. 305–314, 2014.
- [8] L. Graham. Gestalt theory in interactive media design. *Journal of Humanities & Social Sciences*, 2(1), 2008.
- [9] M. Hassenzahl. The effect of perceived hedonic quality on product appealingness. *International Journal of Human-Computer Interaction*, 13(4):481–499, 2001.
- [10] M. Hassenzahl, M. Burmester, and F. Koller. Attrakdiff: Ein Fragebogen zur Messung wahrgenommener hedonischer und pragmatischer Qualität. In *Mensch & computer 2003*, pp. 187–196. Springer, 2003.
- [11] KGU. University Hospital Frankfurt. <https://www.kgu.de/>, 2021. Accessed: July 2021.
- [12] Material-UI. React components that implement google’s material design. <https://material-ui.com/>, 2021. Accessed: July 2021.
- [13] A. Mayakonda and H. P. Koeffler. Maftools: Efficient analysis, visualization and summarization of maf files from large-scale cohort based cancer studies. *BioRxiv*, p. 052662, 2016.
- [14] D. Piovani, S. Danese, L. Peyrin-Biroulet, and S. Bonovas. Inflammatory bowel disease: estimates from the global burden of disease 2017 study. *Alimentary pharmacology & therapeutics*, 51(2):261–270, 2020.
- [15] React.js. Facebook inc. <https://reactjs.org/>, 2021. Accessed: July 2021.
- [16] D. Sahoo, L. Swanson, I. M. Sayed, G. D. Katkar, S.-R. Ibeawuchi, Y. Mittal, R. F. Pranadinata, C. Tindle, M. Fuller, D. L. Stec, et al. Artificial intelligence guided discovery of a barrier-protective therapy in inflammatory bowel disease. *Nature Communications*, 12(1):1–14, 2021.
- [17] L. A. Sceats, M. S. Dehghan, K. K. Rumer, A. Trickey, A. M. Morris, and C. Kin. Surgery, stomas, and anxiety and depression in inflammatory bowel disease: a retrospective cohort analysis of privately insured patients. *Colorectal Disease*, 22(5):544–553, 2020.
- [18] SPARQL. Sparql query language for rdf. <https://www.w3.org/TR/sparql11-query/>, 2013. Accessed: July 2021.
- [19] S. R. Vavricka, L. Brun, P. Ballabeni, V. Pittet, B. M. P. Vavricka, J. Zeitz, G. Rogler, A. M. Schoepfer, S. I. C. S. Group, et al. Frequency and risk factors for extraintestinal manifestations in the swiss inflammatory bowel disease cohort. *Official journal of the American College of Gastroenterology—ACG*, 106(1):110–119, 2011.
- [20] Z. Zhang, D. Gotz, and A. Perer. Iterative cohort analysis and exploration. *Information Visualization*, 14(4):289–307, 2015.

# Phoenix Virtual Heart: A Hybrid VR-Desktop Visualization System for Cardiac Surgery Planning and Education

Jinbin Huang\*

Arizona State University

Erik G. Ellsworth†

Phoenix Children's Hospital

Jonathan D. Plasencia‡

Phoenix Children's Hospital

Steven D. Zangwill||

Phoenix Children's Hospital

Dianna M.E. Bardo‡

Phoenix Children's Hospital

Chris Bryan, Member, IEEE\*\*

Arizona State University

Nicholas C. Rubert§

Phoenix Children's Hospital

## ABSTRACT

Physicians diagnosing and treating complex, structural congenital heart disease (CHD), i.e., heart defects present at birth, often rely on visualization software that scrolls through a volume stack of two-dimensional (2D) medical images. Due to limited display dimensions, conventional desktop-based applications have difficulties facilitating physicians converting 2D images to 3D intelligence. Recently, 3D printing of anatomical models has emerged as a technique to analyze CHD, but current workflows are tedious. To this end, we introduce and describe our ongoing work developing the Phoenix Virtual Heart (PVH), a hybrid VR-desktop software to aid in CHD surgical planning and family consultation. PVH is currently being integrated into a 3D printing workflow at a children's hospital as a way to increase physician efficiency and confidence, allowing physicians to analyze virtual anatomical models for surgical planning and family consultation. We describe the iterative design process that led to PVH, discuss how it fits into a 3D printing workflow, and present formative feedback from clinicians that are beginning to use the application.

**Index Terms:** Human-computer Interaction—Immersive Visualization—Virtual Reality—Interactive Data Analytics; Radiology—Surgical Planning—Medical Education—Medical Imaging

## 1 INTRODUCTION

Congenital heart disease (CHD) refers to a pathology of the heart which is present at birth. The most difficult cases are complex, structural defects, in general. Catheter, a mechanism that can be used to dilate / occlude anatomical structures or deliver other device types, and / or surgical interventions are often required during infancy for these complex cases [16]. For both catheter and surgical planning, physicians employ visualization tools for understanding of the spatial relationships of lesions and anatomy.

To reveal anatomical insights and plan clinical interventions, clinicians have traditionally employed desktop-based applications which show medical images as a volume stack of either 2D computed tomography (CT) or magnetic resonance (MR) slices [3]. These applications generally limit the viewing to the in-plane image stack and its two corresponding planes that are orthogonal to each other. A drawback to this method is that it can take physicians years to train themselves to “mentally construct” these three orthogonal image planes (called the axial, coronal and sagittal planes) into a 3D-space

of spatial knowledge [9]. Alternatively, while image stacks can also be visualized using volume rendering [14] or as 3D models, visualizing 3D anatomy on 2D displays has well-known drawbacks, including lack of depth perception and potential for misinterpretation [3].

Recently, the 3D printing of anatomical models based on CT/MR data has emerged as a strategy for CHD study. Allowing clinicians to hold a physical representation of a patient's anatomy has demonstrated trends for reduced operating room and case length of time [25] and promoting a high degree of engagement and therefore increased memorability [12, 30]. As an example, our collaborator hospital (Phoenix Children's Hospital, or PCH) was one of the first hospitals in the United States to develop a Cardiac 3D Print Lab to create life-size models of hearts from infants with complex forms of congenital heart disease to aid surgeons and physicians in surgical planning and family consultation. While this hospital is one of the first in the United States to support 3D anatomy printing in practice, the current workflow can become tedious (see Figure 1). First, a physician must dictate printing needs (including the identification of the anatomical features to reproduce, where cuts should be made, etc.) to an engineer who uses 3D printer software to produce the anatomical model. If changes are needed, the physician must specify additional print requests which are interpreted by the engineer and printed as additional models. The result is, for the physician, larger gulfs of execution and evaluation [21], as printing can take several hours for complex anatomies, as well as increased cost for using 3D printing material. Further, while the tactile nature of 3D printed models provides certain advantages compared to display on 2D monitors, such as improved conceptual understanding of complex anatomy [19] and informing the appropriate catheter course and device [22], these models also have drawbacks, such as low annotation capacity where only a surface area of interest can be highlighted with a marker pen. We have been interviewing physicians at PCH to learn how issues like these are considered bottlenecks in their 3D printing workflow. For example, instead of relying on engineers to update print requests and having to wait one or more hours every time a change is needed, physicians would prefer to plan first using software and make a print after being able to review the anatomy.

VR provides an attractive modality for this scenario, as it provides stereoscopic perspective of 3D anatomies with the benefit that virtual models can be explored or altered immediately (thus improving physician efficiency) [26]. VR is already being used for CHD tasks, including for treatment planning, training and practice simulation, and educational applications, and rehabilitation [27, 28].

Unfortunately, despite the emerging popularity of VR for cardiac use, there are questions as to the efficiency of such a technology. For example, VR software tend to employ hand-held controllers for interaction, which performs poorly in tasks such as text input and precise selection of small objects, where keyboard-and-mouse interfaces are much more effective [29]. As these are common actions in the 3D printing workflow (loading model and image stack files, manipulating item color and opacity, etc.), relying on VR as the only means of interaction is likely suboptimal compared to

\*e-mail: jhuan196@asu.edu

†e-mail: jplasencia@phoenixchildrens.com

‡e-mail: dbardo@phoenixchildrens.com

§e-mail: nrubert@phoenixchildrens.com

||e-mail: eellsworth@phoenixchildrens.com

||e-mail: szangwill@phoenixchildrens.com

\*\*e-mail: chris.bryan@asu.edu

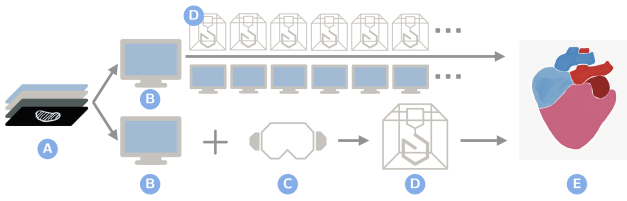


Figure 1: The 3D printing pipeline at PCH includes medical image acquisition (A), desktop data analysis (B) and potentially multiple iterations of 3D printing (D) to obtain a desired 3D anatomical model (E). The PVH software employs both desktop (B) and VR (C) to mitigate the need for multiple 3D prints, by allowing physicians to first virtually assess and modify anatomical models until satisfied. At that point, a print request can be made (D) to generate a 3D print of the model (E).

leveraging both VR and desktop modalities.

In this paper, we report on our ongoing work developing such a cross-device system that combines the strength of both VR and desktop tools to facilitate CHD surgical planning and education within a 3D printing workflow. Our software, called Phoenix Virtual Heart (PVH), is being built in an iterative manner with close collaboration with clinicians at PCH. It consists of two interfaces, a VR interface and the desktop interface, and has been integrated into the hospital’s existing 3D printing workflow. Each interface in PVH supports different tasks: spatial manipulations of medical models is done in VR to leverage its stereoscopic perspective and intuitive spatial interactions, while common operational tasks are done on a desktop computer with keyboard and mouse, taking advantage of familiarity of usage for these types of operations. Here, we report on the specific design goals of this system, and how it is being integrated into hospital use. We also report formative feedback from physicians who are beginning to use the tool as a supplement to the hospital’s existing 3D printing capabilities.

## 2 RELATED WORK

### 2.1 Immersive Analytics in Medical Field

Immersive analytics (IA) is “*the use of engaging, embodied analysis tools to support data understanding and decision making*” [4]. Though the idea behind IA goes back decades [6], it has recently gained attention due to advances in technology platforms [7]. IA applications in medical fields are also emerging. Javid et al. [13] surveyed applications of VR in the medical fields and identified four major application areas: virtual surgery, operation planning, diagnosis, and physical therapy. He et al. [10] developed a VR technique that creates an exploded view to enable interactive exploration of medical image ‘atlas’; (expert labeled tissues or structures) so as to enhance understanding of atlas. Pfeiffer et al. [24] proposed a framework that accommodates data of multiple modalities to aid in preoperative planning for liver surgery and enhances spatial understanding. Adams et al. [1] developed an commodity-level simulation where users can simultaneously interact with high resolution and temporal resolution CT and their corresponding 3D structures as well.

### 2.2 Visualization Technologies for CHD

Traditionally, CHD visualization has been done on the desktop using medical images (such as image stacks from CT or MR data) and/or anatomical reconstruction models to assist CHD procedures [3]. The use of 3D printing, which provides benefits such as tactile feedback and life-size reconstruction of anatomical models, is increasingly being used as a way to provide morphological information during surgical planning and medical education [17]. For example, Moore et al. [20] have demonstrated a clinical outcome benefiting from

digital reconstructions and 3D printed model and a discussion on how the advancement of virtual surgery and 3D printing will enhance decision making in CHD treatment.

Likewise, VR is a well-known technique in medicine, due to the fact that VR offers high embodiment, immersion, and realistic depth perception of the 3D-space occupied by human anatomy. Salavitzabar et al. [26] recently surveyed existing VR applications in CHD and summarized them into four categories: teaching, predicting, planning, and guiding. Our work lies in the line of using VR as a means of planning, with intended future usage in educational scenarios (such as family consultation and student education). Regarding the latter, VR is heavily used in medical education. For example, Maresky et al. [18] explored the usability of teaching cardiac anatomy to undergraduate students using VR, and Erolin et al. [5] ran a pilot study to test the usefulness of VR in various anatomies such as cranial structures. Silva et al. [27] provide an overview of most recent commercialized VR technologies in cardiovascular medicine such as the Stanford Virtual Heart that provides intuitive interactions for users to gain straightforward understanding of heart anatomy and Echopixel that employs stereoscopic techniques to simulate 3D volumes realistically to enhance surgical planning. Ong et al. explore the role of VR in CHD in [23] where they design interactions such as magnification and see-thru to facilitate exploration of 3D heart models in immersion. While we employ some of the same techniques as in these papers, our work differs in that we focus on a hybrid ecology specifically situated for integration into a 3D printing workflow.

### 2.3 Cross-device interaction

Cross-device interactions aim to facilitate users by combining the strength of different devices. In our case, this is motivated by the ease of some tasks when using traditional desktop peripherals such as mouse and keyboard, compared to VR where both the peripherals and the user’s hands are not visible [15]. Despite the overhead required in physically switching between devices, the idea of combining VR and desktop to take advantage of both interfaces is not new [2, 11]. To the best of our knowledge however, it has not yet been employed in CHD usage scenarios. In Section 3, we note how the hybrid desktop+VR system supports our design goals by providing different affordances to support different tasks. In other words, we take advantage of VR’s immersion, depth perception, and spatial interactions when visualizing and directly interacting with anatomical models, but utilize the familiarity and efficiency of the desktop for operational tasks.

## 3 DESIGN GOALS

To our knowledge, a systematic analysis of the design goals for incorporating VR into CHD usage scenarios has not yet been conducted. To understand how VR could help our collaborators, we conducted interviews with clinicians at PCH to understand how a VR software could be implemented to augment their existing 3D printing workflow. In particular, we honed in on the fact that engineers were required to “drive” the 2D desktop displays to analyze and position the anatomical models prior to 3D printing. A customized VR software application could have two advantages at this point in the workflow: (1) It could be tailored specifically to clinician expertise and requirements, allowing physicians to directly analyze and manipulate anatomies instead of relying on engineers. (2) By utilizing VR as a visual and interaction modality, clinicians will have realistic depth perception of the 3D anatomy, resulting in increased confidence when physicians analyzing the spatial relationships between lesions. Our discussions with our collaborators therefore led us to focus on supporting four design goals.

**(G1) Separate controls for desktop and VR for different tasks.** During our initial development, we quickly realized that a VR-only solution would be insufficient, and that a hybrid VR+desktop

application would better serve our collaborators. For example, an early prototype of PVH offloaded all functionality into the VR platform’s paddles. While physicians like the immersive viewpoints and intuitive manipulations afforded by VR, they had trouble with operations that were traditionally “desktop-based tasks,” such as precisely manipulating the intensity of medical images or navigating through the computer’s file system to load additional objects into the software. As a solution, PVH separates operations based on whether they are considered better suited for the VR or desktop modality.

#### (G2) Spatial manipulation of computer generated models.

CHD diagnosis and treatment relies heavily on understanding the 3D spatial relationships of heart lesions. Physicians often rotate and translate computer generated models to gain different views of the heart so as to synthesize a holistic view of the heart structure. Additionally, some surgeries rely on implanting artificial devices to replace malfunctioning heart tissues; planning for these operations require spatial knowledge which can be gained through spatial manipulation of different cardiac structures. The takeaways is that the heart’s anatomy is not considered a single object, but is instead composed of multiple subcomponents, which should be individually selectable and manipulatable within the VR space.

#### (G3) Alignment of models with medical images.

When planning for an operation (e.g., a surgery or a catheter procedure), physicians need to know what the inside of the heart looks like. CT and MR image slices are common techniques for obtaining structural information of a target organ and the surrounding anatomy (traditionally viewed as three orthogonal image planes). Surgeons planning for an operation and physicians planning for catheter interventions sometimes combine 3D computer generated models with images of three imaging planes to get situated knowledge of the patient’s heart [3]. It was therefore important to our collaborators that PVH includes functionality to superimpose CT and MR image slices within the VR space on top of the anatomical model.

#### (G4) Integrating devices into heart models.

Implantation is a common CHD-related procedure where physicians need to implant a medical device in the patient’s heart. The ability to study the heart’s structure first and preview a post-implantation heart is essential to the surgeons because it offers an immediate realistic feedback of how the heart structure will look after an operation; physicians can use this knowledge to evaluate and adjust implantation strategies. A major drawback of 3D printed anatomical models can be that it is difficult to simulate implantation, due to model rigidity and occlusion. The virtual, stereoscopic anatomy afforded by a VR space better supports this.

## 4 THE PHOENIX VIRTUAL HEART

PVH is developed using the Unity platform for HTC Vive Pro VR headsets via an iterative prototyping methodology [8] in close collaboration with several physicians at PCH. The system is being frequently tested by physicians and radiologists, who are providing immediate feedback for quick refinement, which allows us to adapt and change designs as difficulties are identified and new requirements emerge. We briefly describe the design of PVH as it reflects the four design goals listed in Section 3.

### 4.1 Separate Controls for Desktop and VR

A well-known drawback for extended reality devices, both VR and AR, is their inability to provide fast text entry and precise selection, which results in inefficiency of conducting 2D UI-based tasks [29]. In our initial development of PVH, the system was designed solely as a VR platform, however feedback from an early prototype quickly led us to realize that, in the context of the 3D printing workflow, a hybrid modality made the most sense. For example, physicians regularly must make precise adjustments to the intensity of CT and MR image slices when performing analysis, which was difficult to



Figure 2: PVH’s desktop interface supports operations that are efficient in traditional desktop UIs and inefficient in VR. The user can toggle between (A) the heart model (B) and any loaded devices (B). For the selected item, available interactions include (E-F) resizing the models, (G) toggling medical image planes, (H) toggling the visibility of model subcomponents, (I) changing color intensities, and (J) deleting model subcomponents. (K) The VR scene is also mirrored for coherence.

do in VR using paddles and much easier to do with numbers on a keyboard.

As a result, we decided to offloaded operations that were more natural with mouse-and-keyboard operations to a desktop modality (shown in Figure 2), such as file selections and slider bar interactions, as opposed to requiring these interactions via the use of paddles within the VR space. The desktop interface is used by physicians to load and delete models (or model subcomponents), and can be used to efficiently change image intensity, model color, and model size, and model opacity via the use of traditional UI affordances (checkboxes, sliders, input boxes, etc.) and windows, icons, mouses and pointers (WIMP) interactions. The physicians switch between desktop and VR control by mounting / unmounting the VR headset. Though such a setup – switching between modalities whilst using the application – temporarily breaks the user’s 3D immersion, the ultimate objective of PVH is not total or increased immersion and presence, but rather enhanced 3D intelligence and work efficiency. While we plan to conduct extensive empirical evaluations of this setup to understand the advantages and drawbacks of this approach in terms of task efficiency, insight, and cognitive load, the initial feedback from PCH personnel regarding this hybrid design is promising.



Figure 3: (A) Within the VR space, a user can select a heart model or device and then translate, rotate, or resize it. (B) Selecting a model allows the user to subsequently select its individual subcomponents, which can be further be moved around the space.

### 4.2 Spatially Manipulating Computer-Generated Models

Compared to using a mouse and keyboard on a desktop, VR supports more intuitive spatial manipulations of objects [3], such as allowing a user to virtually “grab” an object and translate it around by moving the user’s hand, or slice a model to simulate a cut plane. In PVH,

the user can raycast to select a model with a paddle. Once selected, a model can be manipulated with six degrees of freedom (DOF) by moving, rotating, or twisting the paddle to translate and rotate the model (see Figure 3(A)); rotation and toggling a slice plane are additionally supported by scrubbing a control on the paddle.

Manipulation of individual parts that make up an anatomy is enabled by switching to a subcomponent manipulation mode. Individual features that make up the heart can be freely moved within the virtual space (see Figure 3(B)), allowing the user to examine them in detail. Subcomponents can be moved back to their original position i.e., inside the heart model via a trigger on the VR paddle.

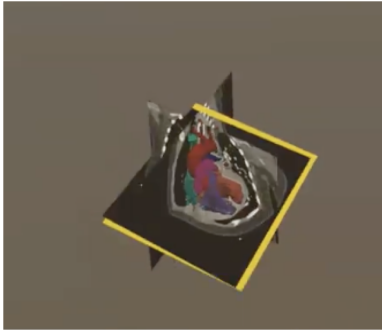


Figure 4: CT and MR image data can be overlaid onto the heart's 3D anatomy, shown as three orthogonal image planes. The user can select and scroll individual planes along their axes.

### 4.3 Aligning Heart Models and Image Slices

In addition to 3D models, CT and MR-based medical images act as a major source of spatial insight into the heart's anatomy. PVH supports overlaying this data onto the 3D heart model inside the VR space. The medical image stack is shown as three orthogonal planes (axial, coronal, and sagittal) that intersect the heart model's geometry. Each plane can be selected via paddle raycasting and moved along its axis.

PVH supports overlaying image slice data onto anatomy models in VR space — the user load an image stack CT or MR slices using the desktop interface, which are then spatially aligned with the 3D models as shown in Figure 4. Individual image planes can be selected and manipulated via the VR paddle to adjust the depth of each of the three orthogonal planes (up and down, left and right, back and forth).

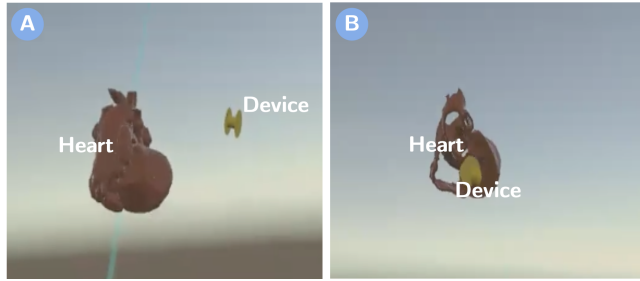


Figure 5: In these images, (A) the user is inserting a 3D model of a device into the VR space, and (B) moving it inside the heart's geometry to assess if a device fits the heart anatomy. The user has also toggled off several subcomponents of the heart model for better visibility.

### 4.4 Integrating Devices into Heart Models

Finally, PVH supports adding additional medical devices into the VR space to simulate implantation scenarios. Devices can be loaded

from the desktop interface and manipulated within the VR space. Figure 5 shows an example of inserting an Amplatzer ventricular septal occluder device into the interventricular septum of the heart. To provide additional visibility, the user has toggled off several subcomponents of the heart, so they can better see how the device fits into the anatomy.

## 5 DISCUSSION AND CONCLUSION

PVH is an ongoing project, and this paper primarily focuses on highlighting a set of four primary design goals that were considered while implementing this tool. While we plan to conduct extensive evaluations with PCH physicians to learn in detail about how the system supports surgical planning, family consultation, and educational training, a formative survey with three clinicians (one interventionalist and two pediatric radiologists, all with working experience in CHD of more than 24 years) has provided positive feedback about PVH's tailored user experience.

For example, the hybrid VR+desktop interface was well-regarded, and the physicians are planning to expand their use of PVH in their own clinical work. General system usability was rated as high, and all participants felt confident using the system, though as expected, there was a higher learning curve for the users who lacked prior experience in VR. Despite this, during demonstrations all were able to use the software to find pathologies in patient anatomies. We also plan to investigate the design and use of novel affordances and interactions to support physicians using the tool.

In terms of integrating PVH into the 3D printing workflow at PCH, the potential to mitigate scenarios where multiple prints are done, thus requiring multiple consultations between physician and engineer, as well as several hours of wait time, is significant. As PVH is designed specifically to sit inside the 3D printing workflow, we see it as an example of how interactive visualization tools provide exploratory and sensemaking insights without having to create expensive and time-consuming 3D prints. However, if desired, users can export analyzed and manipulated models (both anatomies and devices) to 3D prints and receive additional benefits not offered in VR such as tactile response. We expect our future empirical studies will also shed light into how PVH can act both as an alternative and a precursor to 3D printing of models, and better characterize the types of situations that are best served in the VR space as compared to the 3D printed space or by using a combination of both modalities.

## ACKNOWLEDGMENTS

This work is supported in part by a Phoenix Children's Hospital Foundation's Leadership Circle grant.

## REFERENCES

- [1] H. Adams, J. Shinn, W. G. Morrel, J. Noble, and B. Bodenheimer. Development and evaluation of an immersive virtual reality system for medical imaging of the ear. In *Medical Imaging 2019: Image-Guided Procedures, Robotic Interventions, and Modeling*, vol. 10951, p. 1095111. International Society for Optics and Photonics, 2019.
- [2] B. Brown, I. MacColl, M. Chalmers, A. Galani, C. Randell, and A. Steed. Lessons from the lighthouse: collaboration in a shared mixed reality system. In *Proceedings of the SIGCHI conference on Human factors in computing systems*, pp. 577–584, 2003.
- [3] J. L. Byl, R. Sholler, J. M. Gosnell, B. P. Samuel, and J. J. Vetukattil. Moving beyond two-dimensional screens to interactive three-dimensional visualization in congenital heart disease. *The international journal of cardiovascular imaging*, pp. 1–7, 2020.
- [4] T. Dwyer, K. Marriott, T. Isenberg, K. Klein, N. Riche, F. Schreiber, W. Stuerzlinger, and B. H. Thomas. Immersive analytics: An introduction. In *Immersive analytics*, pp. 1–23. Springer, 2018.
- [5] C. Erolin, L. Reid, and S. McDougall. Using virtual reality to complement and enhance anatomy education. *Journal of visual communication in medicine*, 42(3):93–101, 2019.

- [6] M. A. Fisherkeller, J. H. Friedman, and J. W. Tukey. An interactive multidimensional data display and analysis system. Technical report, SLAC National Accelerator Lab., Menlo Park, CA (United States), 1974.
- [7] A. Fonnet and Y. Prié. Survey of immersive analytics. *IEEE transactions on visualization and computer graphics*, 2019.
- [8] N. Goldman and K. Narayanaswamy. Software evolution through iterative prototyping. In *Proceedings of the 14th international conference on Software engineering*, pp. 158–172, 1992.
- [9] A. Guillot, S. Champely, C. Batier, P. Thiriet, and C. Collet. Relationship between spatial abilities, mental rotation and functional anatomy learning. *Advances in Health Sciences Education*, 12(4):491–507, 2007.
- [10] L. He, A. Guayaquil-Sosa, and T. McGraw. Medical image atlas interaction in virtual reality. In *Immersive analytics workshop. IEEE Vis*. <http://immersiveanalytics.net>, 2017.
- [11] R. Holm, E. Stauder, R. Wagner, M. Priglinger, and J. Volkert. A combined immersive and desktop authoring tool for virtual environments. In *Proceedings IEEE Virtual Reality 2002*, pp. 93–100. IEEE, 2002.
- [12] Y. Jansen, P. Dragicevic, and J.-D. Fekete. Evaluating the efficiency of physical visualizations. In *Proceedings of the SIGCHI Conference on Human Factors in Computing Systems*, pp. 2593–2602, 2013.
- [13] M. Javaid and A. Haleem. Virtual reality applications toward medical field. *Clinical Epidemiology and Global Health*, 8(2):600–605, 2020.
- [14] A. E. Kaufman and K. Mueller. Overview of volume rendering. *The visualization handbook*, 7:127–174, 2005.
- [15] P. Knierim, V. Schwind, A. M. Feit, F. Nieuwenhuizen, and N. Henze. Physical keyboards in virtual reality: Analysis of typing performance and effects of avatar hands. In *Proceedings of the 2018 CHI Conference on Human Factors in Computing Systems*, pp. 1–9, 2018.
- [16] J. E. Lock, J. F. Keane, and S. B. Perry. *Diagnostic and interventional catheterization in congenital heart disease*, vol. 221. Springer Science & Business Media, 2000.
- [17] S. Marconi, L. Pugliese, M. Botti, A. Peri, E. Cavazzi, S. Latteri, F. Auccio, and A. Pietrabissa. Value of 3d printing for the comprehension of surgical anatomy. *Surgical endoscopy*, 31(10):4102–4110, 2017.
- [18] H. Maresky, A. Oikonomou, I. Ali, N. Dikofsky, M. Pakkal, and B. Ballyk. Virtual reality and cardiac anatomy: Exploring immersive three-dimensional cardiac imaging, a pilot study in undergraduate medical anatomy education. *Clinical Anatomy*, 32(2):238–243, 2019.
- [19] J. S. Matsumoto, J. M. Morris, T. A. Foley, E. E. Williamson, S. Leng, K. P. McGee, J. L. Kuhlmann, L. E. Nesberg, and T. J. Vrtiska. Three-dimensional physical modeling: applications and experience at mayo clinic. *Radiographics*, 35(7):1989–2006, 2015.
- [20] R. A. Moore, K. W. Riggs, S. Kourtidou, K. Schneider, N. Szugye, W. Troja, G. D’Souza, M. Rattan, R. Bryant III, M. D. Taylor, et al. Three-dimensional printing and virtual surgery for congenital heart procedural planning. *Birth defects research*, 110(13):1082–1090, 2018.
- [21] D. A. Norman and S. W. Draper. User centered system design: New perspectives on human-computer interaction. 1986.
- [22] L. Olivieri, A. Krieger, M. Y. Chen, P. Kim, and J. P. Kanter. 3d heart model guides complex stent angioplasty of pulmonary venous baffle obstruction in a mustard repair of d-tga. *International journal of cardiology*, 172(2):e297–e298, 2014.
- [23] C. S. Ong, A. Krishnan, C. Y. Huang, P. Spevak, L. Vricella, N. Hibino, J. R. Garcia, and L. Gaur. Role of virtual reality in congenital heart disease. *Congenital heart disease*, 13(3):357–361, 2018.
- [24] M. Pfeiffer, H. Kenngott, A. Preukschas, M. Huber, L. Bettscheider, B. Müller-Stich, and S. Speidel. Imhotep: virtual reality framework for surgical applications. *International journal of computer assisted radiology and surgery*, 13(5):741–748, 2018.
- [25] J. Ryan, J. Plasencia, R. Richardson, D. Velez, J. J. Nigro, S. Pophal, and D. Frakes. 3d printing for congenital heart disease: a single site’s initial three-yearexperience. *3D printing in medicine*, 4(1):1–9, 2018.
- [26] A. Salavatabar, C. A. Figueroa, J. C. Lu, S. T. Owens, D. M. Axelrod, and J. D. Zampi. Emerging 3d technologies and applications within congenital heart disease: teach, predict, plan and guide. *Future Cardiology*, 16(6):695–709, 2020.
- [27] J. N. Silva, M. Southworth, C. Raptis, and J. Silva. Emerging applications of virtual reality in cardiovascular medicine. *JACC: Basic to Translational Science*, 3(3):420–430, 2018.
- [28] M. K. Southworth, J. R. Silva, and J. N. A. Silva. Use of extended realities in cardiology. *Trends in cardiovascular medicine*, 30(3):143–148, 2020.
- [29] M. Speicher, A. M. Feit, P. Ziegler, and A. Krüger. Selection-based text entry in virtual reality. In *Proceedings of the 2018 CHI Conference on Human Factors in Computing Systems*, pp. 1–13, 2018.
- [30] S. Stusak, J. Schwarz, and A. Butz. Evaluating the memorability of physical visualizations. In *Proceedings of the 33rd Annual ACM Conference on Human Factors in Computing Systems*, pp. 3247–3250, 2015.

# Communicating Performance of Regression Models Using Visualization in Pharmacovigilance

Ashley Suh\*  
Tufts University

Gabriel Appleby†  
Tufts University

Erik W. Anderson‡  
Data Science and AI  
Novartis Pharmaceuticals

Luca Finelli§  
Data Science and AI  
Novartis Pharmaceuticals

Dylan Cashman¶  
Data Science and AI  
Novartis Pharmaceuticals

## ABSTRACT

Statistical regression methods can help pharmaceutical organizations improve the quality of their pharmacovigilance by predicting the expected quantity of adverse events during a trial. However, the use of statistical techniques also changes the risk profile of any downstream tasks, due to bias and noise in the model’s predictions. That risk profile must be clearly understood, documented, and communicated across many different stakeholders in a highly regulated environment. Aggregated performance metrics such as explained variance or mean average error fail to tell the whole story, making it difficult for subject matter experts to feel confident in deciding to use a model. In this work, we describe guidelines for communicating regression model performance for models deployed in predicting adverse events. First, we describe an interview study in which both data scientists and subject matter experts within a pharmaceutical organization describe their challenges in communicating and understanding regression performance. Based on the responses in this study, we develop guidelines for which visualizations to use to communicate performance, and use a publicly available trial safety database to demonstrate their use.

**Keywords:** Visual Communication, Regression Models, Pharmacovigilance

## 1 INTRODUCTION

Advanced analytics and statistical methods have seen increasing use by pharmaceutical organizations to improve the quality of their pharmacovigilance [1, 11]. Notably, regression models have been shown to accurately predict and detect the under-reporting of adverse events (AEs) in clinical trials [16, 20, 21] – a persistent and recurrent issue raised by the FDA and GCP [33]. By identifying outliers in AE reporting through advanced regression methods, pharmaceutical companies can improve the early-detection of data collection or processing issues at trial sites, prevent delays in the required approval process, and ultimately improve patient safety [15].

Although regression methods can augment traditional pharmacovigilance approaches, a new challenge emerges: how can a diverse set of stakeholders and subject matter experts (SMEs) assess a model’s risk profile in a highly regulated space, such as clinical safety? Stakeholders and SMEs often rely on model builders themselves to translate the reliability and limitations of predictive models, under the assumption that these translations will be accessible by the audience [14]. However, empirical studies suggest that even SMEs can be overwhelmed and disappointed during presentations by data scientists, particularly when metrics alone are presented as an assessment of the model’s performance [14, 23, 31]. Without a

more careful consideration for the communication of model performance between data scientists and SMEs, pharmacovigilance groups can fail to capitalize on the predictive power of modern machine learning and artificial intelligence techniques. It has been suggested that similar conditions limited the use of machine learning in other applications and domains, such as cybersecurity [30].

In this workshop paper, we present a design study on effective communication of regression models deployed for pharmacovigilance. First, we describe a preliminary interview study within a pharmaceutical corporation conducted with two participant groups: data scientists who build regression models, and SMEs who make decisions based on a regression model’s performance and outputs. From our interviews, we outline common challenges that occur when communicating and assessing regression models, and offer guidelines for visual communication methods for a regression model’s performance. Lastly, we demonstrate the use of our guidelines with a pharmacovigilance use case, illustrating the performance of three different regression models trained on a publicly available trial safety database for predicting AEs in clinical trials.

## 2 RELATED WORK

The interpretability and transparency of machine learning models is an active field being tackled at every level of industry and academia. We take a more targeted approach, focusing on the specific needs of users within a pharmaceutical corporation. However, we still review related works to identify previous examples of the use of statistical methods in pharmacovigilance. We then offer a high-level summary of relevant work in model communication to understand if any current solutions address our use case.

### 2.1 Predictive Models in Pharmacovigilance

Advanced analytics have been in use in pharmacovigilance for decades to investigate both the risks and benefits of medicines [1, 8, 11]. For example, Ménard et al. developed a predictive model that enables the oversight of AE reporting in clinical trials at the program, study, site, and patient levels [20, 21]. The authors describe that the deployment of these predictive models can lessen the labor-intensive load of manual investigations by pharmaceutical sponsors [33], however, the authors do not detail whether challenges occurred in the model’s actual adoption by end-users. Previous studies suggest that these techniques are rarely deployed in practice at healthcare and pharmaceutical organizations, regardless of their ability to improve pharmacovigilance and QA practices [4, 7, 29].

Seneviratne et al. call to bridge the implementation gap of machine learning in healthcare by merging ML algorithms into the ‘socio-technical’ milieu of the organization [27]. Shah et al. suggests that the utility of ML algorithms could be better demonstrated in practice if stakeholders and healthcare patients could better assess the performance of a predictive model without relying on standard performance metrics [28]. In this work, we intentionally study how the performance of a regression model can be effectively communicated to SMEs and decision-makers, with the goal of improving the accessibility and use of predictive models in pharmacovigilance.

\*e-mail: ashley.suh@tufts.edu

†e-mail: gabriel.appleby@tufts.edu

‡e-mail: erik.anderson@novartis.com

§e-mail: luca.finelli@novartis.com

¶e-mail: dylan.cashman@novartis.com

## 2.2 Model Communication

Effective presentation of a predictive model’s performance to domain scientists, SMEs, and other stakeholders is of ongoing study in literature. Researchers in explainable AI seek to help users interpret and explain the inferences of AI models by visualizing the internal workings of those models [6, 19, 22, 34]. Metrics and principles are posed for explainable AI [12, 25], guidelines for defining *interpretability* are suggested [5, 36], and visual analytic tools enhance machine learning and AI transparency [2, 13, 17, 26]. While much of this research is relevant to the use case in this paper, they target explainability at too low of a level – the proposed solutions are typically complex and often require training. From our interview study, we found that there was a need for better solutions at a higher level to facilitate communication between data scientists and SMEs.

Our work is closer to the user-centered approaches that interview and observe builders and consumers of AI models for improved ML workflows. For example, previous work has examined the workflow for machine learning practitioners to characterize common challenges faced by those in industry settings [14, 23]. Similarly, Suresh et al. suggest improving ML workflows by characterizing stakeholders by their personal knowledge and expertise outside of ML [31]. Our work attempts to consider both ‘expert’ and ‘non-expert’ roles, and examine the bridge of communication between them within a small scope of regression models for pharmacovigilance.

While most related work at least touches on how visualization can be used as a communication method for the interpretability of ML models, to our knowledge, no previous work aims to understand the communication gap between data scientists and SMEs who must make decisions based on a regression model’s performance. To address this, we identify what data scientists who build models and SMEs that use their predictions find most valuable in the interpretation of a regression model’s outcome. Our interviews with members of both groups, described in Section 3, lead us to create guidelines (Section 3.3) that can be used broadly by the community for communicating regression model performance to SMEs.

## 3 INTERVIEW STUDY

To identify visualization techniques that are most effective in communicating a regression model’s performance, we conducted an interview study within a pharmaceutical company with two participant groups: data scientists who regularly build regression models, and SMEs who make decisions with regression models in their daily work. In this section, we describe our study design, interview protocol, and identify our participants’ priorities when communicating and interpreting the capabilities of a regression model.

### 3.1 Study Design

**Participants:** In total, 6 data scientists and 6 subject matter experts were recruited via email. During our email exchange, potential participants were informed that the purpose of the interview was to discuss their experiences interpreting and communicating a regression model’s performance. When recruiting SMEs, we specifically targeted those without direct expertise in statistics, but who have worked with or seen a regression model in the past. For data scientists, we targeted those who have developed or assessed regression models at some point in their daily work. Demographics for our participants, including their area of expertise and level of familiarity with regression models, can be seen in Table 2.

**Procedure:** All of our interviews were semi-structured and took 45-60 minutes to complete. Each interview was conducted virtually on Microsoft Teams with audio only. Shortly before each interview, participants were given a copy of the consent form which contained information about the study, its design, and their rights as participants. Each participant verbally consented to the study over a recording and was given an anonymous demographics survey to complete. At the start of each interview, participants were given a

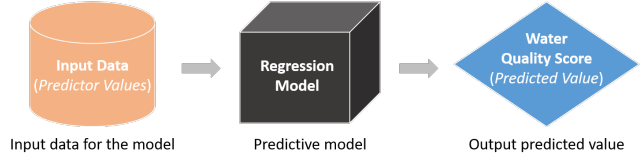


Figure 1: Visual representation provided to participants for the regression model they are tasked with assessing in the first part of our interview study (Section 3). Participants were shown 10 rows of the input data, with labeled attributes for each predictor variable.

refresher on regression models which included: (1) a definition, (2) an example of a regression model being used at a weather station to predict daily temperature, (3) the semantic difference between regression and classification models.

Participants were shown the same set of prepared slides to walk through three different scenarios of assessing and communicating the performance of a regression model, one question at a time. Regardless of the participant’s organizational role (data scientist or SME), the same questions were given during the interview. For time sensitivity, we did not ask all data scientists and SMEs every question that was included in our slide deck. Our slides and interview questions are included as supplementary material.

**Interviews:** While previous work has investigated common machine learning interpretability challenges faced by data scientists [23], machine learning practitioners [14] and stakeholders [31], our work focuses directly on how communication can be improved between data scientists and subject matter experts when the end-goal is to use a regression model in their workflow. Our interviews consider three major topics, presented as individual scenarios we stepped through with participants during the interview:

1. **What would you need to know about a regression model to recommend its use?** Participants were described a theoretical scenario in which a new regression model was being presented at their workplace. In our slides, we illustrated the regression model as one that predicts a water potability score based on a set of input predictor values (e.g., pH, sulfate). A subset of the input data was shown to participants, and the output of the model displayed a predicted water potability score as a numerical value. The visual representation of the scenario shown to participants is available in Figure 1. Participants described what they would need to know about the model to recommend and trust its use.
2. **How have you assessed and communicated a regression model at work previously?** We asked participants to think of a time when a regression model was introduced to their daily work. In our slides, we presented examples of regression models commonly deployed for pharmacovigilance. Once the participant had a particular model in mind, they described how its performance was assessed, communicated, and scrutinized.
3. **How could communicating a regression model’s performance with data scientists and subject matter experts be improved?** We asked participants to describe what they would like the opposite role to better communicate or give feedback on when assessing the performance of a regression model together. In other words, SMEs were asked what they would like data scientists to communicate to them regarding a model’s performance, and data scientists were asked what they would like SMEs to communicate to them regarding a model’s performance.

For the first scenario of our interview study, we asked participants how they would assess a regression model that they had never seen before. Our goal was to engage participants in a broad discussion on factors that influence their trust and interpretation of a regression model when being presented on its performance. In the second sce-

nario, a number of data scientists and SMEs elaborated on projects related to modeling adverse events in clinical trials, which we consider for our use case in Section 4. For the remainder of the section, we summarize results for all three interview scenarios.

### 3.2 Study Results

A preliminary analysis of our interviews revealed several high-level differences and similarities between the experiences and concerns of data scientists and SMEs. In this workshop paper, we highlight the findings that were most relevant to our use case, and present guidelines based on these findings. We hope to provide further analysis of our interview results in future work.

To recommend a model's use, we found data scientists strongly valued performance metrics, the distribution and correlation of features, and overall data quality when assessing regression models. On the other hand, SMEs were primarily concerned with the limitations of the regression model, particularly where the model might fail. One SME detailed the risks that he must consider when using a regression model to predict under-reporting of AEs in clinical trials: “*Under-reporting is very critical for clinical trials because it's safety information... which needs to be notified from the scientists, to the teams, to the company... There can be a risk to the patient's safety, [if] we have not addressed a safety issue which has come up on time, that may have an impact on changing the safety profile of the drug. So, it [the model's performance] has quite an impact.*”

Another SME working in pharmacovigilance was strongly concerned about the reliability of the model's outputs, particularly when it affects patient safety. She was the only interviewee of ours to adamantly question how the predicted water potability score, described in the first scenario of our interview, would be used in the real world. In particular, she noted that she would need to exhaustively know the limitations and risks of the model before recommending its use: “*If we're telling people that water is potable, that means they're going to use it for washing, cooking, cleaning, drinking... there are consequences to that decision. You know, there is a human being at the end of it. That's the reason why I'd want as much information about the model as possible. So if I'm going to make a decision about applying this in the real world, then at least I know exactly what its limitations are before making a decision on something.*”

During the second scenario of our interview, all participants mentioned charts, graphs, or interfaces that would be or have been useful to them in assessing a model's performance. Overwhelmingly, SMEs requested the ability to see how certain inputs (or features) affected the output of a model to test out its performance. This offers evidence that there is an appetite for the interactive explainable systems that are seen in literature, e.g., the What-if tool [35] for black box models, and similar tools for classification models [24, 37].

When discussing how communication could be improved, data scientists told us they expected to spend time explaining the technical details of their models' performance to SMEs. They did not expect SMEs to already know regression metrics by name, noting that slides are prepared in advance to cover questions about quantifying performance. However, SMEs stated they did not always feel comfortable asking questions during presentations, often due to the pacing of the explanation: “*Data scientists show a regression curve and it's so normal for them... they don't always realize that people don't understand some of the visuals for the models and what they really mean. Sometimes it just goes over your head, and I think the end-user a good chunk of the time would be too embarrassed to say - I don't get what you're talking about*” (SME).

Similar feedback from interview participants suggests that there can be a mismatch in the interpretation of the conversation between data scientists and SMEs, where visualization could more effectively act as an explanatory bridge. Further, it suggests that commonly used charts for visualizing regression performance may not be as easily interpretable or recognizable to SMEs as data scientists perceive.

### 3.3 Guidelines

From the analysis of our interviews, we derive a set of guidelines for communicating the performance of a regression model to SMEs.

The first two guidelines address a lack of context and comfort identified by SMEs: “*You have to make the end-user feel comfortable both in the data scientist's language, and also that if they don't understand something they can easily ask, what is this?*” (SME).

**G1: When articulating results, start slow and offer to speed up.** All SMEs we interviewed suggested that data scientists could spend more time highlighting aspects of their presentation that could be considered “obvious”, in order to establish a common baseline for the language spoken and understood. For example, data scientists could define common performance metrics or potentially nuanced visual encodings before detailing their results.

**G2: Tie in use cases for the model by illustrating real-life, objective-driven examples.** Across all of our interviews, when asked what they would want to know about a model's performance to recommend its use, a common request made by SMEs was to understand how a regression model's performance relates to their end-goals for the model. This request is especially critical when using regression models that affect patient and/or public safety.

The next three guidelines relate to the choice of visualization style when communicating and presenting regression model performance to SMEs: “*Some people don't have experience with visualization outside of BBC infographics. I do realize it can be hard for me to remove my data scientist hat and put myself into the role of somebody who's not looking at a log plot every day*” (data scientist).

**G3: Provide context for performance by annotating plots with stories.** Each annotated story serves to decode the intended message of the visualization, beyond the visualized data and provided legend. By guiding the audience through sensible conclusions on a provided visualization, an SME could more quickly arrive at new conclusions with the same visualization.

**G4: For any chart that communicates a model's performance, provide a range of comparisons.** SMEs found that assessing the results of a regression model's performance is easier if it is compared against their current practices, an interpretable naive baseline model, and if possible, an oracle or perfect model.

**G5: Visually explain significance of global metrics.** Global metrics such as explained variance or mean absolute error can seem abstract and removed from the use case. Showing metrics in visual context can help ground them; for example, visualizing the enveloping ellipse in a correlation scatterplot can give a proxy for the correlation between predicted and actual values.

The final three guidelines address concerns by both data scientists and SMEs in understanding the caveats, edge cases, outliers, and limitations of the model: “*If data scientists said, 'when you run these models, here is the area where we think you're going to have the most problems, or the most risk. And here's the explanation for why we think that's happening...' I think upfront and transparent communication about why we should expect those issues is a very big way for us to build trust and confidence in the model*” (SME).

**G6: Point to outliers in the model's performance with known or plausible explanations.** The source of outliers and anomalies is often dependent on the scenario, therefore, data scientists should point SMEs to known or potential outliers, and include at least reasonable speculations behind their anomalous behavior.

**G7: Be descriptive about the data used for training and testing a model, and provide examples.** The distribution, weighting, correlation, and availability of the data used in the modeling process were notable concerns from both SMEs and data scientists. Many data scientists agreed that SMEs provide essential context

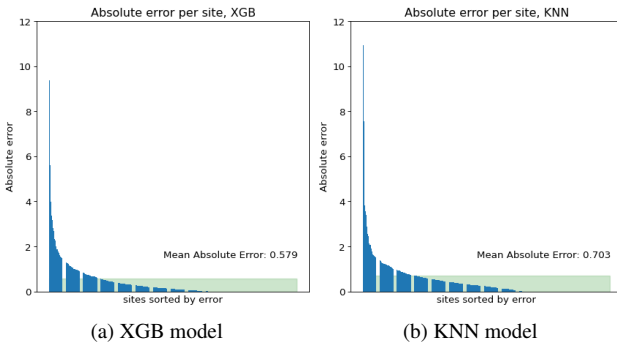


Figure 2: Absolute error plots for two models predicting adverse event rate. To explain the mean absolute error global metric, the average error is shown as a green rectangle compared with the sorted errors of individual sites, showing that approximately 80% of sites have better than average error with the XGB model. Residual plots for the remaining models can be seen in Figure 5 of the appendix.

for the data domain, ultimately leading to improvements in model performance and transparent communication.

**G8: Explicitly demonstrate the error, limitations, and weaknesses of the model, not just the strengths.** From our interviews, SMEs want transparent information regarding the limitations of a model with both qualitative and quantitative assessments of those errors or weaknesses. Both SMEs and data scientists noted that they were able to help each other improve a model’s performance once the limitation of the model was fully understood.

#### 4 USE CASE: MODELING ADVERSE EVENTS

To demonstrate how our guidelines for communicating regression model performance can be used, we present a use case on modeling AEs in clinical trials. We train three different models and two baselines, then provide example visualizations that could be used in explaining the performance of these models. A write-up of our modeling process is included in our appendix, and error metrics for the regressors trained are available in Table 1. A subset of visualizations for our models are provided in the main text, however, examples for each can be found in the appendix (Figures 4, 5, 6).

##### 4.1 Communicating Model Performance

For the remainder of this section, we provide examples of visualizations and explanations that follow the proposed guidelines in Section 3.3 for the five models described above.

**Adding context and comfort:** To address **G1** and **G2**, we suggest starting with an explanation of the model’s basic functions. For example, if a KNN model was used, it could be explained that the model looks at the rates of similar historical trials based on multiple aspects: the program, patient, site, and study phases. Walking through a single example of inference, or a simplified illustration, can establish a level of comfort with SMEs and better tie the model to the use case at hand. For context on the data used in the modeling process (**G7**), a description of the data can be provided, as in Table 3.

**Provide annotated visualizations explaining global metrics:** For the use case of predicting the rate of AEs, we propose using a bar chart showing the residuals between predicted and actual, sorted by size of the residual. The shape of this plot shows how error is apportioned globally (**G5**). Explanatory annotations (**G3**) can show the mean absolute error and a comparison against a baseline (**G4**) can show the different shapes of error, as seen in

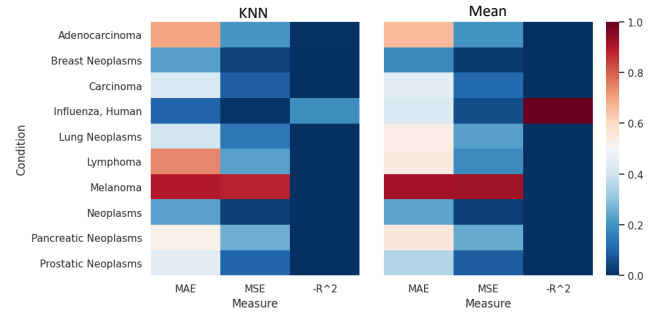


Figure 3: Heat map showing the apportionment of error of a KNN model vs. a baseline (mean), split by treatment in each row. This visualization explains whether the model is biased towards certain subgroups in the data. An annotation could be added to point out that the KNN model has a better  $r^2$  for Influenza trials than the mean, but a worse mean absolute error for Lymphoma trials. Heat maps for remaining models can be seen in Figure 4 of the appendix.

Figure 2. A containing ellipse can also be shown to provide a visual of the  $r^2$  of the regression model (e.g., Figure 6) [10].

**Caveats, edge cases, outliers, and limitations:** Examples of the input data should be provided, with special focus given to trials where the model has greatest error (**G6**). SMEs also want to know if there are segments of the data that the model has high error on; we recommend looking at the most important features of the model and using a heat map to show which categories have high error (**G7**), as seen in Figure 3. This heat map can show multiple error metrics across all categories. However, different error metrics have different scales, so some normalization must be applied to make outliers visually salient. The most important limitations of a model can be communicated textually or visually (**G8**). For example, if a KNN model is used, it should be explained that they are highly sensitive to noisy or junk data, while it can be communicated that an XGB model might be slower to train.

#### 5 CONCLUSION AND FUTURE WORK

In this work, we present guidelines for communicating regression model performance within a pharmaceutical organization. Based on interviews with both data scientists and subject matter experts, we identify common gaps in communication and suggest broadly applicable solutions for data scientists to use in communicating their results to SMEs. Lastly, we demonstrate how our guidelines could be used in practice by illustrating a pharmacovigilance use case.

We hope to have future work in several directions. First, we would like to quantitatively analyze our interview data to better understand mismatches in language between data scientists and SMEs. Characterizing these gaps could lead to more pointed recommendations about common language to use, or a visual language to facilitate translation. We would also like to evaluate commonly used regression visualizations, including those suggested in this workshop paper, to evaluate if SMEs indeed find them helpful when interpreting a model’s performance. Finally, empirical studies can comparatively analyze the efficacy of our suggested guidelines.

#### ACKNOWLEDGMENTS

We thank our collaborators at Novartis for their time and participation in our study, as well as the reviewers for their helpful feedback.

#### REFERENCES

- [1] J. S. Almenoff. Innovations for the future of pharmacovigilance. *Drug safety*, 30(7):631–633, 2007.

- [2] A. Chatzimpampas, R. M. Martins, I. Jusufi, K. Kucher, F. Rossi, and A. Kerren. The state of the art in enhancing trust in machine learning models with the use of visualizations. In *Computer Graphics Forum*, vol. 39, pp. 713–756. Wiley Online Library, 2020.
- [3] T. Chen and C. Guestrin. XGBoost: A scalable tree boosting system. In *Proceedings of the 22nd ACM SIGKDD International Conference on Knowledge Discovery and Data Mining*, KDD ’16, pp. 785–794. ACM, New York, NY, USA, 2016. doi: 10.1145/2939672.2939785
- [4] K. Cresswell and A. Sheikh. Organizational issues in the implementation and adoption of health information technology innovations: an interpretative review. *International journal of medical informatics*, 82(5):e73–e86, 2013.
- [5] B. Davis, M. Glenski, W. Sealy, and D. Arendt. Measure utility, gain trust: Practical advice for xai researchers. In *2020 IEEE Workshop on TRust and EXPertise in Visual Analytics (TREX)*, pp. 1–8. IEEE, 2020.
- [6] F. Doshi-Velez and B. Kim. Towards a rigorous science of interpretable machine learning. *arXiv preprint arXiv:1702.08608*, 2017.
- [7] E. J. Emanuel and R. M. Wachter. Artificial intelligence in health care: will the value match the hype? *Jama*, 321(23):2281–2282, 2019.
- [8] S. J. Evans. Pharmacovigilance: a science or fielding emergencies? *Statistics in medicine*, 19(23):3199–3209, 2000.
- [9] E. Fix and J. L. Hodges. Discriminatory analysis. nonparametric discrimination: Consistency properties. *International Statistical Review / Revue Internationale de Statistique*, 57(3):238–247, 2021/07/09/ 1989. Full publication date: Dec., 1989. doi: 10.2307/1403797
- [10] M. Friendly, G. Monette, and J. Fox. Elliptical insights: understanding statistical methods through elliptical geometry. *Statistical Science*, 28(1):1–39, 2013.
- [11] M. Hauben and X. Zhou. Quantitative methods in pharmacovigilance. *Drug safety*, 26(3):159–186, 2003.
- [12] R. R. Hoffman, S. T. Mueller, G. Klein, and J. Litman. Metrics for explainable ai: Challenges and prospects. *arXiv preprint arXiv:1812.04608*, 2018.
- [13] F. Hohman, A. Srinivasan, and S. M. Drucker. Telegam: Combining visualization and verbalization for interpretable machine learning. In *2019 IEEE Visualization Conference (VIS)*, pp. 151–155. IEEE, 2019.
- [14] S. R. Hong, J. Hullman, and E. Bertini. Human factors in model interpretability: Industry practices, challenges, and needs. *Proceedings of the ACM on Human-Computer Interaction*, 4(CSCW1):1–26, 2020.
- [15] ICH. E26(r2) guideline for good clinical practices. *International Conference on Harmonisation of Technical Requirements for Registration of Pharmaceuticals for Human Use.*, 2:1–60, 2016.
- [16] B. Koneswarakantha, T. Ménard, D. Rolo, Y. Barmaz, and R. Bowling. Harnessing the power of quality assurance data: can we use statistical modeling for quality risk assessment of clinical trials? *Therapeutic innovation & regulatory science*, 54(5):1227–1235, 2020.
- [17] J. Krause, A. Dasgupta, J. Swartz, Y. Aphinyanaphongs, and E. Bertini. A workflow for visual diagnostics of binary classifiers using instance-level explanations. In *2017 IEEE Conference on Visual Analytics Science and Technology (VAST)*, pp. 162–172. IEEE, 2017.
- [18] A. Legendre. *Nouvelles méthodes pour la détermination des orbites des comètes*. Nineteenth Century Collections Online (NCCO): Science, Technology, and Medicine: 1780–1925. F. Didot, 1805.
- [19] Z. C. Lipton. The mythos of model interpretability: In machine learning, the concept of interpretability is both important and slippery. *Queue*, 16(3):31–57, 2018.
- [20] T. Ménard, Y. Barmaz, B. Koneswarakantha, R. Bowling, and L. Popko. Enabling data-driven clinical quality assurance: predicting adverse event reporting in clinical trials using machine learning. *Drug safety*, 42(9):1045–1053, 2019.
- [21] T. Ménard, B. Koneswarakantha, D. Rolo, Y. Barmaz, L. Popko, and R. Bowling. Follow-up on the use of machine learning in clinical quality assurance: can we detect adverse event under-reporting in oncology trials? *Drug safety*, 43(3):295–296, 2020.
- [22] S. Mohseni, N. Zarei, and E. D. Ragan. A survey of evaluation methods and measures for interpretable machine learning. *arXiv preprint arXiv:1811.11839*, 1, 2018.
- [23] S. Passi and S. J. Jackson. Trust in data science: Collaboration, translation, and accountability in corporate data science projects. *Proceedings of the ACM on Human-Computer Interaction*, 2(CSCW):1–28, 2018.
- [24] D. Ren, S. Amershi, B. Lee, J. Suh, and J. D. Williams. Squares: Supporting interactive performance analysis for multiclass classifiers. *IEEE transactions on visualization and computer graphics*, 23(1):61–70, 2016.
- [25] C. Rudin, C. Chen, Z. Chen, H. Huang, L. Semenova, and C. Zhong. Interpretable machine learning: Fundamental principles and 10 grand challenges. *arXiv preprint arXiv:2103.11251*, 2021.
- [26] D. Sacha, M. Kraus, D. A. Keim, and M. Chen. Vis4ml: An ontology for visual analytics assisted machine learning. *IEEE transactions on visualization and computer graphics*, 25(1):385–395, 2018.
- [27] M. G. Seneviratne, N. H. Shah, and L. Chu. Bridging the implementation gap of machine learning in healthcare. *BMJ Innovations*, 6(2), 2020.
- [28] N. H. Shah, A. Milstein, and S. C. Bagley. Making machine learning models clinically useful. *Jama*, 322(14):1351–1352, 2019.
- [29] S. Shilo, H. Rossman, and E. Segal. Axes of a revolution: challenges and promises of big data in healthcare. *Nature medicine*, 26(1):29–38, 2020.
- [30] R. Sommer and V. Paxson. Outside the closed world: On using machine learning for network intrusion detection. In *2010 IEEE symposium on security and privacy*, pp. 305–316. IEEE, 2010.
- [31] H. Suresh, S. R. Gomez, K. K. Nam, and A. Satyanarayan. Beyond expertise and roles: A framework to characterize the stakeholders of interpretable machine learning and their needs. *Proceedings of the 2021 CHI Conference on Human Factors in Computing Systems*, May 2021. doi: 10.1145/3411764.3445088
- [32] A. Tasneem, L. Aberle, H. Ananth, S. Chakraborty, K. Chiswell, B. J. McCourt, and R. Pietrobon. The database for aggregate analysis of clinicaltrials.gov (aact) and subsequent regrouping by clinical specialty. *PloS one*, 7(3):e33677–e33677, 2012. 22438982[pmid]. doi: 10.1371/journal.pone.0033677
- [33] F. R. Varallo, S. d. O. P. Guimarães, S. A. R. Abjaude, and P. d. C. Mastroianni. Causes for the underreporting of adverse drug events by health professionals: a systematic review. *Revista da Escola de Enfermagem da USP*, 48(4):739–747, 2014.
- [34] H. J. Weerts, W. van Ipenburg, and M. Pechenizkiy. A human-grounded evaluation of shap for alert processing. *arXiv preprint arXiv:1907.03324*, 2019.
- [35] J. Wexler, M. Pushkarna, T. Bolukbasi, M. Wattenberg, F. Viégas, and J. Wilson. The what-if tool: Interactive probing of machine learning models. *IEEE transactions on visualization and computer graphics*, 26(1):56–65, 2019.
- [36] F. Yang, Z. Huang, J. Scholtz, and D. L. Arendt. How do visual explanations foster end users’ appropriate trust in machine learning? In *Proceedings of the 25th International Conference on Intelligent User Interfaces*, pp. 189–201, 2020.
- [37] J. Zhang, Y. Wang, P. Molino, L. Li, and D. S. Ebert. Manifold: A model-agnostic framework for interpretation and diagnosis of machine learning models. *IEEE transactions on visualization and computer graphics*, 25(1):364–373, 2018.

## A APPENDIX

### A.1 Modeling Process

The data used is a small subset of the ClinicalTrials.gov data accessed through the AACT database [32], which contains a large quantity of basic trial summary and results information. We use this information to predict the number of AEs per enrolled person.

The dataset was filtered by requiring all values to be filled, in addition to the study being a completed interventional study that lasted one or more years. We also filtered the dataset by removing any studies that did not have a MeSH<sup>1</sup> term for the condition, or an intervention in the 40 most popular within the current subset. Finally, all categorical features were transformed into a one-hot encoding. The resulting dataset totals 2572 instances with 96 derived features, 88 of which are one-hot encodings of categorical features.

Three basic regression models were chosen: Linear Regression [18] (OLS), K-Nearest Neighbors Regression [9] (KNN), and Gradient Boosting Tree Regression [3] (XGB). Two ‘dummy’ regression models were included as interpretable baselines: one that always predicts the mean, and one that always predicts the median.

Some hyperparameter tuning was done for two of the regression models, KNN and XGB. We split the dataset into a train and test set of 75% and 25%. The training set was then used to perform three fold cross validation grid search to find the best hyperparameters based on mean squared error. For the KNN we looked for the number of nearest neighbors, and for XGB we examined different max depths. We found the best value for the nearest neighbors to be 25, and the best value for max depth to be 3.

Each of the regression models were then trained on the full training set, using the best hyperparameter values found with the grid search where appropriate. Finally, the mean squared error (MSE), mean absolute error (MAE), and coefficient of determination ( $R^2$ ) on the test set was recorded. Error metrics for all regressors trained are available in Table 1.

### A.2 Additional Tables and Figures

Regressor	MAE	MSE	$R^2$
OLS	0.564	1.064	0.283
XGB	0.579	1.090	0.266
KNN	0.703	1.364	0.082
Mean	0.788	1.486	-0.001
Median	0.736	1.621	-0.091

Table 1: Error metrics across the three regressors, and two heuristic methods used as baselines. In order of lowest mean squared error, regressors were Linear Regression (OLS), Gradient Boosting Trees (XGB), and K-Nearest Neighbors Regression (KNN). The two baseline methods were Mean and Median, which predicted the Mean and Median of the training set respectively.

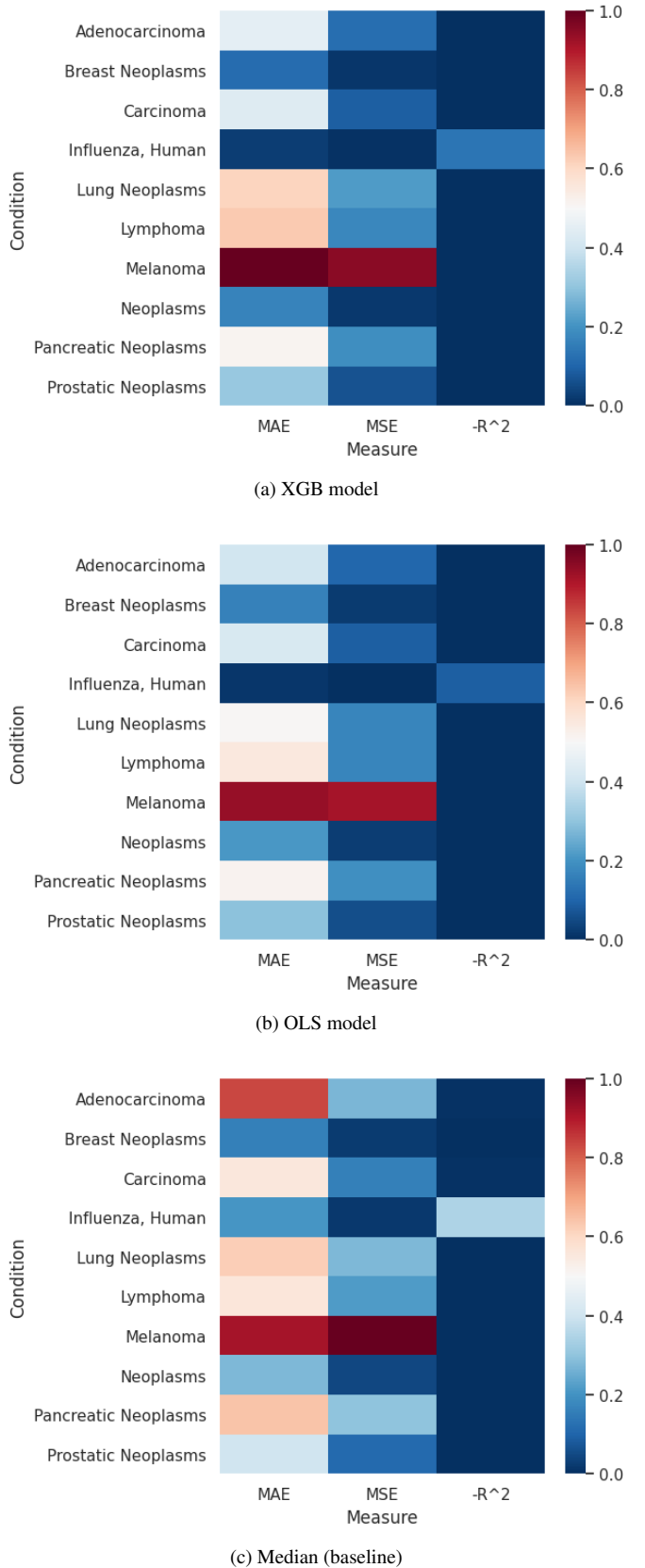


Figure 4: Heat maps for the remaining three models described in Section 4.

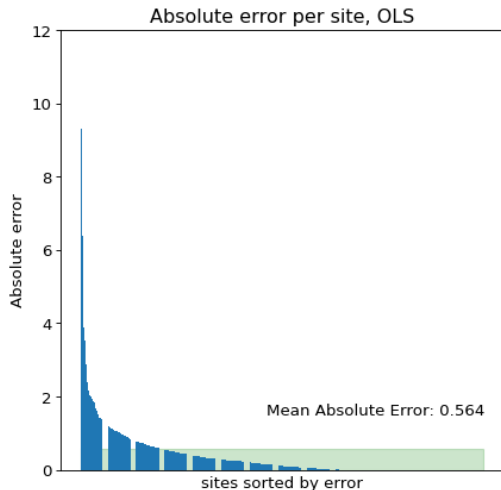
<sup>1</sup><https://www.ncbi.nlm.nih.gov/mesh/>

Measure	Count
N	12
Age	18-29: 1, 30-39: 5, 40-49: 5, 50-59: 1, 60-69: 0
Gender	Female: 5, Male: 7, Non-binary: 0
Education	Associates: 0, Bachelors: 1, Masters: 7, Doctorate: 4
Role	Data scientist: 6, Subject matter expert: 6
Data science experience	No experience: 0, Somewhat familiar: 1, Familiar: 5, Very familiar: 3, Expert: 5
Frequency using data tools	Never: 0, 1-3x/month: 0, 1-3x/week: 4, 1-3x/day: 2, All day: 6
Frequency using regression	Never: 1, 1-3x/month: 4, 1-3x/week: 1, 1-3x/day: 5, All day: 1
Expertise (SMEs only):	Finance 1, Commercial: 1, Pharmacovigilance: 2, Quality Assurance: 2

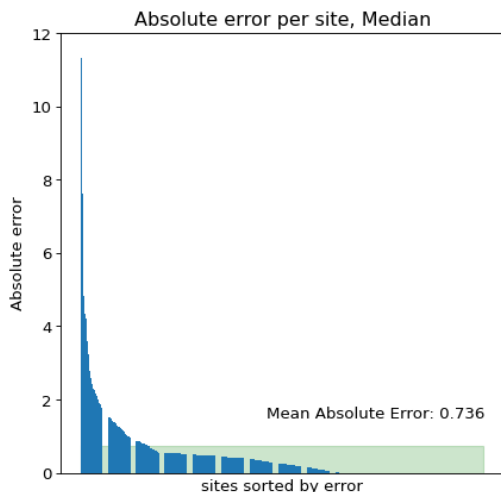
Table 2: Demographics table for the interview study described in Section 3.

Feature	Description
Phase	For a clinical trial of a drug product (including a biological product), the numerical phase of such clinical trial, consistent with terminology in 21 CFR 312.21 and in 21 CFR 312.85 for phase 4 studies.
Enrollment	The estimated total number of participants to be enrolled (target number) or the actual total number of participants that are enrolled.
Number of Arms	The number of arms in the clinical trial. For a trial with multiple periods or phases that have different numbers of arms, the maximum number of arms during all periods or phases.
Has Expanded Access	Whether there is expanded access to the investigational product for patients who do not qualify for enrollment in a clinical trial. Expanded Access for investigational drug products (including biological products) includes all expanded access types under section 561 of the Federal Food, Drug, and Cosmetic Act: (1) for individual participants, including emergency use; (2) for intermediate-size participant populations; and (3) under a treatment IND or treatment protocol.
Number of Facilities	The number of participating facility in a clinical study.
Actual Duration	Number of months between the start date and primary completion date. Start date: the estimated date on which the clinical study will be open for recruitment of participants, or the actual date on which the first participant was enrolled. Primary completion date: the date that the final participant was examined or received an intervention for the purposes of final collection of data for the primary outcome, whether the clinical study concluded according to the pre-specified protocol or was terminated. In the case of clinical studies with more than one primary outcome measure with different completion dates, this term refers to the date on which data collection is completed for all of the primary outcomes.
Months to Report Results	Number of months between primary completion date and first received results date.
Minimum Age	The numerical value, if any, for the min. age a potential participant must meet to be eligible for the clinical study. (Years only for us)
Number of Primary Outcomes	“Primary outcome measure” means the outcome measure(s) of greatest importance specified in the protocol, usually the one(s) used in the power calculation. Most clinical studies have one primary outcome measure, but a clinical study may have more than one.
Number of Secondary Outcomes	“Secondary outcome measure” means an outcome measure that is of lesser importance than a primary outcome measure, but is part of a pre-specified analysis plan for evaluating the effects of the intervention(s) under investigation in a clinical study, and is not specified as an exploratory or other measure. A clinical study may have more than one secondary outcome measure.
Condition Mesh Term	Condition MeSH terms generated by NLM algorithm
Intervention Mesh Term	Intervention MeSH terms generated by NLM algorithm

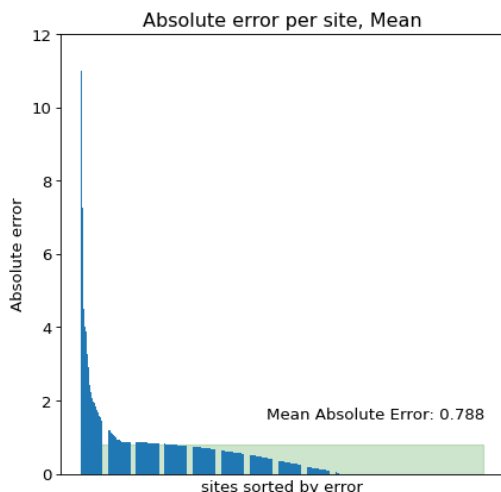
Table 3: Descriptions of the data used for training in Section 4.



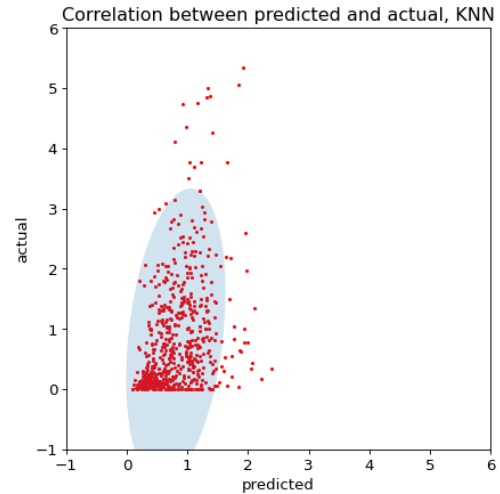
(a) OLS model



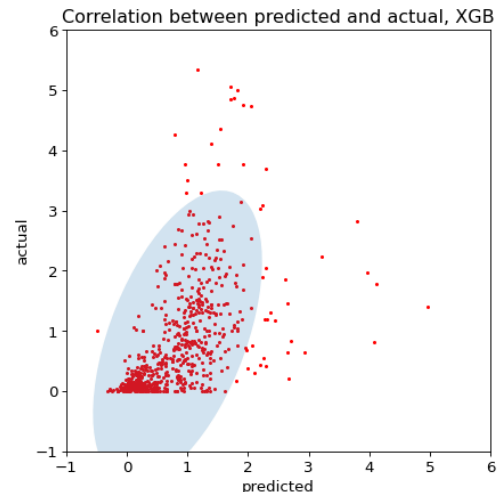
(b) Median (baseline)



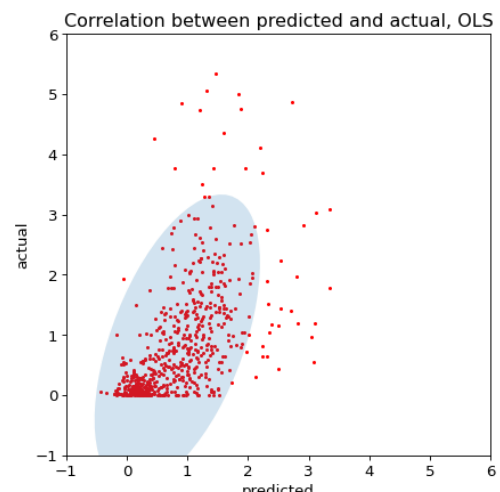
(c) Mean (baseline)



(a) KNN model



(b) XGB model



(c) OLS model

Figure 5: Absolute error plots for the three remaining models described in Section 4.

Figure 6: Correlation scatter plots for three of the models described in Section 4.

# Interactive Cohort Analysis and Hypothesis Discovery by Exploring Temporal Patterns in Population-Level Health Records

Tianyi Zhang\*  
Purdue University

Thomas H. McCoy Jr.<sup>†</sup> Roy H. Perlis<sup>‡</sup>  
Massachusetts General Hospital  
Harvard Medical School

Finale Doshi-Velez<sup>§</sup> Elena Glassman<sup>¶</sup>  
Harvard University

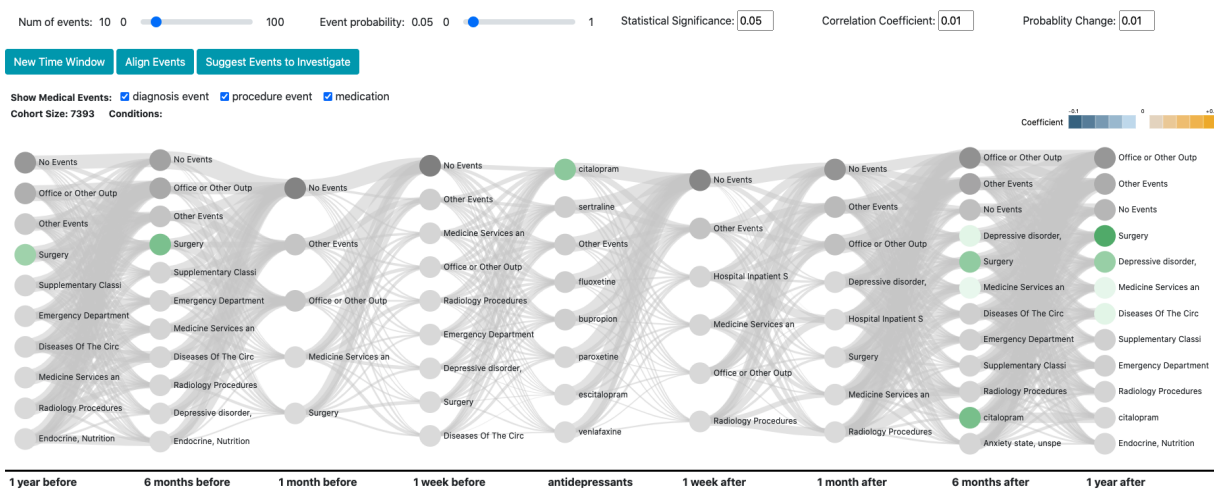


Figure 1: A holistic view of medical events with information scents (green) in different time windows

## ABSTRACT

It is challenging to visualize temporal patterns in electronic health records (EHRs) due to the high volume and high dimensionality of EHRs. In this paper, we conduct a formative study with three clinical researchers to understand their needs of exploring temporal patterns in EHRs. Based on those insights, we develop a new visualization interface that renders medical event trajectories in a holistic timeline view and guides users towards interesting patterns using an information scent based method. We demonstrate how a clinical researcher can use our tool to discover interesting sub-cohorts with unique disease progression and treatment trajectories in a case study.

**Index Terms:** Human-centered computing—Visualization—Visualization techniques; Human-centered computing—Visualization—Visualization design and evaluation methods

## 1 INTRODUCTION

The availability of electronic health records (EHRs) enables clinical researchers to discover data-driven insights about diseases and treatments. However, EHRs often include data spanning several years from hundreds of thousands of patients (i.e., large volume), which are encoded using hundreds of thousands of unique medical event types (i.e., high dimensionality). As a result, clinical researchers cannot easily gain insights from EHRs with bare eyes or primitive data analysis tools [10]. For example, it is hard to answer questions like “What are the patients with similar disease progression patterns?”,

“What are the commonality among them and how are they different from other patients?”, “What comorbidities have they developed?”, “Does the ordering of drugs tried matter?”, etc.

Over the years, the information visualization community has made great efforts to visualize EHRs. Of particular interest to us are the visualization techniques that identify and render temporal patterns in EHRs [4, 6, 7, 9, 13, 14, 17, 18, 20, 25, 29–32]. To understand how clinical researchers use such visualization tools in exploratory cohort analysis, we conducted a formative study with three clinical researchers at Massachusetts General Hospital and asked them to try out a state-of-the-art visualization tool called Cadence [13]. Participants gave three major pieces of feedback. First, they wished the visualization could make interesting patterns more recognizable or at least provide some hints about which medical events to consider investigating first, instead of users composing their own hypotheses or queries with little assistance or information scent from the system. Second, instead of only showing relative temporal ordering, they suggested time be better represented in the visualization, as an event occurring a week vs. a month after another event has significantly different clinical implications. Third, they found it difficult to translate their clinical questions into queries supported by Cadence. For example, they found it hard to define a *meta-event* like “seizure” using several diagnosis codes, and they were also not able to define a query to answer an exploratory question such as “What symptoms did patients develop while taking a drug over a time period?”

Based on the formative study, we designed an interactive visualization interface for exploring temporal patterns in electronic health records. Figure 1 shows an overview of our tool. Our tool provides a holistic view of disease and treatment trajectories in a timeline view, where users are given the flexibility to bin medical events into different time windows. Frequent medical events are rendered in each time window. The flow between two events in adjacent time windows indicates the conditional probability of having one event given another event, which is computed based on the frequency of each event in the cohort. We also developed a novel algorithm to

\*e-mail: tianyi@purdue.edu

<sup>†</sup>e-mail: tmccoy@mgh.harvard.edu

<sup>‡</sup>e-mail: rperlis@mgh.harvard.edu

<sup>§</sup>e-mail: finale@seas.harvard.edu

<sup>¶</sup>e-mail: glassman@seas.harvard.edu

identify medical events that may lead to a sub-cohort with unique temporal patterns. These medical events are highlighted to guide the data exploration process, inspired by the idea of information scents in the information foraging theory [8]. Furthermore, our tool supports a rich set of user interactions to allow clinical researchers to create a query that answers their clinical questions. For example, users can group multiple events to form a meta-event. Users can also define the inclusion or exclusion of an event to filter the cohort of patients. Clinical researchers can further run statistical tests to assess the correlation between two medical events.

This paper is organized as follows. Section 2 discusses related work and elaborates on how our tool is different from existing visualization, clustering, and data mining techniques for EHRs. Section 3 describes the formative study and our findings. Section 4 describes the tool design. Section 5 demonstrates how a clinical researcher can use our tool to arrive at a sub-cohort of patients with interesting and unique temporal patterns. Section 6 concludes this work and discusses future work.

## 2 RELATED WORK

### 2.1 Visualization for temporal patterns in EHRs

Many visualization techniques have been proposed to discover temporal patterns in EHRs [1, 4, 6, 7, 9, 13, 17, 18, 20, 25, 29–32]. To reduce the volume and dimensionality of medical records, many of these techniques require a priori event selection, e.g., only including a small set of events for analysis and ignoring the rest. While several tools such as EventFlow [20] provide a faithful overview of event sequences in medical records, the resulting sequence view can be quite complex and cluttered given the high dimensional structure of medical events and the rich variations in individual patients’ medical histories. Therefore, users have to manually filter and aggregate medical events before they can arrive at a simple and clean sequence view with recognizable patterns. This manual process is tedious and time-consuming. OutFlow [30] and Cadence [13] use automated hierarchical event aggregation algorithms to simplify event sequences, where users can control the aggregation level through a slider. However, clinical researchers in our formative study found such automated aggregation obscure. They wished to have more transparency and control over the automated aggregation process.

Query-based visualization tools [11, 13, 16, 17, 21] allow users to define a query to filter a dataset and then visualize the query result for further investigation. However, our formative study shows that, for exploratory analysis, clinical researchers found it difficult to decide where to start and which event to further investigate on. They wished the tool could provide some hints to guide them towards interesting patterns, rather than coming up with their own hypothesis or queries. To support this need, we propose a novel algorithm to compute the information scent of a medical event based on how likely patients having this event have unique patterns compared with patients without this event. By following the information scent of medical events, users can interactively filter the dataset and identify a sub-cohort of patients with unique temporal patterns.

### 2.2 Clustering and sequence mining approaches

Clustering-based approaches have been proposed to identify patients that follow the same or similar patterns [2, 3, 5, 12, 14, 19, 22]. These approaches rely on feature selection and predefined metrics to measure the similarity between patients. This may hinder opportunities of identifying latent patterns that are not captured by selected features or similarity metrics. Furthermore, it may not be readily determinable by the user why some patients are grouped together while others are not. As a result, clinical researchers still need to dig into each cluster of patients’ records to make sense of these clusters. In fact, given the complexity and temporal nature of medical records, they are often distributed in a high-dimensional space without clear boundaries as the basis for clustering.

Frequent sequence mining techniques have also been applied to identify temporal patterns from EHRs [15, 23–26]. However, these techniques often require careful data preprocessing, aggregation, or filtering to simplify the raw EHRs, e.g., removing disease and procedure events that are not related to a specific disease under investigation. Otherwise, these mining techniques often identify too many patterns. For example, we identified over 321K sequence patterns supported by at least 100 patients by running a frequent sequence mining algorithm [28] on a fully dimensional, non-filtered EHR dataset of 7K patients. A key challenge is to distill useful insights from the over-abundance of patterns. Instead of directly visualizing the large number of sequence patterns identified from an EHR dataset, we choose to use these patterns to compute the information scents of medical events and guide users to interactively narrow down to a sub-cohort of patients with unique sequence patterns.

## 3 FORMATIVE STUDY

To understand how well existing visualization techniques support temporal pattern discovery in exploratory cohort analysis, we conducted a formative study with three psychiatrists at Massachusetts General Hospital. During the study, participants did an exploratory analysis of a large EHR dataset that they were familiar with, using a state-of-the-art visualization tool called Cadence [13]. The EHR dataset contains medical records of 7393 patients diagnosed with major depressive disorders. In this dataset, diagnosis events are encoded with ICD-9 codes, procedures are encoded with CPT-4 codes, and drug prescriptions are encoded with RxNorm codes.

While the participants felt excited about the visualization support provided by Cadence, they gave three major pieces of feedback based on their experience of using Cadence.

**The tool should provide more hints to guide users towards interesting patterns.** Given a temporal query, Cadence visualizes the trajectories of events specified in the query. Users can interactively add more events to the timeline view and refine the query by exploring co-occurring events in a list view or a scatter plot. Due to the high dimensionality of EHRs, there are often many events in the list view and the scatter plot. As a result, participants found it difficult to navigate through these many events and figure out which event to investigate for the next step. Even though the list view shows the frequency of co-occurring events and the scatter plot also renders the statistical significance value of correlated events, such information scents are not sufficient for users to decide whether further investigation on an event would lead them to a sub-cohort of patients with interesting patterns. P1 said, “*The distribution bars of co-occurring events do not really tell me how many patients get it one time, two times, or many times. We really care about the time density of these events, not just their frequency.*”

**Time should be better represented.** Though the visualization in Cadence shows the relative ordering between different events, it is hard to tell how long an event occurred before another. In clinical settings, an event occurring one week before another is quite different from the event occurring one year before another. In addition, the timeline view in Cadence does not show co-occurring events other than those specified in the query. When investigating what happened to patients who got seizure after taking bupropion, P3 wished to see co-occurring events in the timeline view so she could easily recognize other possible reasons for seizure such as a recent diagnosis of alcoholic disorder. While the scatter plot shows the correlation between events, it is hard to tell when a correlated event occurs. Participants commented that what they really cared about was the chronicity of events. They wished to see trajectories of co-occurring events in the timeline view.

**The tool should provide more support to express exploratory queries and sophisticated temporal patterns.** The query interface in Cadence can be used to specify temporal patterns such as “dis-

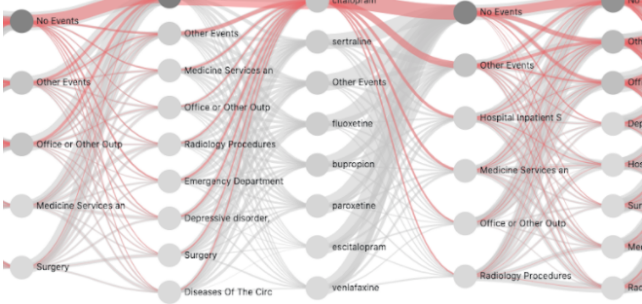


Figure 2: Hovering over an event shows the flow of patients conditioned on this event.

charged from a hospital ten days after transferred into the ICU.” However, participants found it hard to define a query to answer more open-ended questions such as “are there groups of patients that are different from other groups of patients in the way that we are not aware of?” Furthermore, since medical events in the EHR dataset were encoded with low-level codes in CPT, ICD, and RxNorm, participants often had to manually bundle multiple low-level codes based on their clinical questions. It is cumbersome since there are many codes. While Cadence allows users to aggregate events using a slider, participants found it hard to interpret which events were aggregated together when moving the slider. Furthermore, when informed that this dynamic event aggregation feature was based on ICD and CPT hierarchies, P2 said, “*ICD and CPT hierarchies should not be used to infer event aggregation strategies, since these hierarchies are primarily designed for billing. They do not reflect the appropriate bundling clinicians need to answer their questions.*” Participants wished to have better tool support for medical event bundling.

#### 4 TOOL DESIGN

Based on the feedback from the formative study, we designed an interactive visualization interface for exploring temporal patterns in EHRs, as shown in Figure 1.

##### 4.1 A Holistic View of Temporal Patterns

To help users recognize temporal patterns in a large EHR dataset, our interface provides a holistic view of medical events in different timeline windows. Users need to first define an anchoring point to initiate the visualization, such as the first prescription of any antidepressants. We choose to ask users to provide an anchoring point since patients’ health record often span across many years and the resulting timeline view can be extremely lengthy and complex without a focus. By default, our interface shows frequent medical events in multiple time windows up to a year before and after the anchoring point. Users are allowed to add or delete a time window to adjust the timeline view. The width of the flow between two events indicates how likely patients having one event would then have another event, which is a kind of conditional probability.

$$\text{Flow}(x_{t1} \rightarrow y_{t2}) = \frac{|\text{Patient}(x_{t1}) \cap \text{Patient}(y_{t2})|}{|\text{Patient}(x_{t1})|}$$

In the formula above, the function  $\text{Patient}(x_t)$  returns the set of patients who have medical event  $x$  in the time window  $t$ . An alternative way to compute the flow width is to use the relative frequency of having  $x_{t1}$  and  $y_{t2}$ , i.e.,  $\frac{|\text{Patient}(x_{t1}) \cap \text{Patient}(y_{t2})|}{|\text{Cohort Size}|}$ . After consulting our clinician collaborators, we decided to use conditional probability since it was more preferred to interpret the time dependency between events in a temporal pattern. In addition, when a user hovers over an

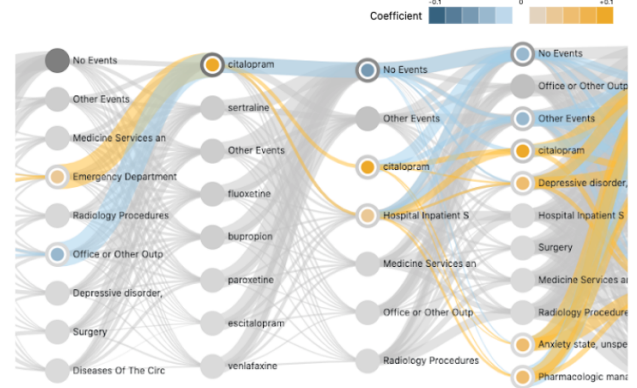


Figure 3: A user pinned an event and viewed positively or negatively correlated events in the timeline view.

event in the timeline view, the flows in a sub-cohort with that event are highlighted and overlaid on the current timeline view, as shown in Figure 2.

If a user is interested in one particular event, she can pin the event in the timeline view. Our interface will then test the correlation between the pinned event and every other events in the timeline view. Currently, we use chi-squared test of independence to calculate the coefficients and p-values. For example, if a user pins the first prescription of citalopram, other correlated events with statistical significance, such as admitted to an emergency room a week before the citalopram prescription, are highlighted in the timeline view, as shown in Figure 3. Yellow color indicates a positive correlation, while blue indicates a negative correlation. The color hue is adjusted based on the correlation coefficient value. The default p-value and coefficient thresholds are 0.05 and 0.01 respectively. A user can adjust these thresholds along with other thresholds, such as the number of events rendered in each time window, using the control knobs on top of the interface.

##### 4.2 Information Scents

Due to the high dimensionality of EHRs, the timeline view often renders many medical events in different time windows. Based on our formative study, users may find it hard to navigate through these many events and decide which one to investigate for the next step. To address this challenge, we have developed a novel algorithm that identifies medical events that will lead to a sub-cohort with unique temporal sequence patterns compared to other sub-cohorts without these events.

$$\text{Scent}(x_t) = |\text{PSet}(x_t) - \text{PSet}(\neg x_t)| \times |\text{PSet}(\neg x_t) - \text{PSet}(x_t)|$$

The formula above shows the method to calculate the information scent of an event  $x$  in a time window  $t$ . The function  $\text{PSet}(x_t)$  returns the set of temporal patterns in a sub-cohort of patients with  $x_t$ , while  $\text{PSet}(\neg x_t)$  returns the set of temporal patterns in a sub-cohort without  $x_t$ . We choose to multiply the number of unique temporal patterns in the sub-cohort with  $x_t$  and the number of unique patterns in the sub-cohort without  $x_t$ , since during the experiment, we observed that selecting an event sometimes split the cohort to two sub-cohorts, one of which contains a super set of temporal patterns of another. Currently, we use a frequent closed sequence mining algorithm called BIDE [28] to identify temporal sequence patterns in a cohort. Since it is computationally expensive to run frequent sequence mining on the fly, we precompute all frequent sequence patterns in the entire cohort using a minimum support threshold of 100. In other word, each identified pattern is followed by at least 100 patients. For each sequence pattern, we also cache the IDs of



Figure 4: An example inclusion criterion that bundles multiple events

those patients who follow the pattern. In this way, we can efficiently compute  $PSet(x_t)$  by checking whether there are at least 100 patients in the intersection of the patients with  $x_t$  and the patients that support a pattern  $p$  in the pre-computed pattern set.

As shown in Figure 1, the events with information scent scores above a threshold are highlighted in green. The green color hue is adjusted based on the information scent score. For example, the surgery events in multiple time windows are highlighted in Figure 1. This indicates that further investigation of these surgery events will lead to a sub-cohort of patients with unique temporal sequence patterns. A user can filter the dataset by selecting one or more of these events and make further investigation.

### 4.3 Event bundling

While navigating through medical events in the timeline view, users can bundle multiple events using conjunction and disjunction operators to filter events and create a sub-cohort. Users can either add an event via drag and drop or through a look up table. Our interface also supports specifying exclusion criteria such as not including an event  $x_t$ . Figure 4 shows an example inclusion criterion that bundles three events. Filtering the dataset with this criterion creates a sub-cohort of 320 patients who were given either citalopram or sertraline in their first antidepressant prescription and were then diagnosed with depressive disorder again a month after the first prescription. Every time the dataset is filtered, the set of pre-computed sequence patterns and their supporting patients are also filtered accordingly.

## 5 DEMONSTRATION

This section describes a usage scenario to demonstrate how clinical researchers can use our tool to discover interesting temporal patterns in a cohort. We use the same psychiatry dataset as in Section 3 in this usage scenario. Suppose Alex is a psychiatry researcher who is conducting an exploratory analysis on the psychiatry dataset. He wants to find some interesting patterns that he is not aware of before and use them to form new hypotheses in his research. Alex defines the first prescription of any antidepressants as an anchoring point. Then a timeline view is rendered in the interface. While it is interesting to see the trajectories of patients in such a timeline view, Alex finds it tedious to look into so many events one by one. Alex clicks on the “Suggest Events to Investigate” button to solicit some recommendations from the tool. Several medical events are highlighted in green to indicate what to investigate next (Figure 1). Alex notices that patients whose first antidepressant prescription is citalopram are likely to have unique temporal patterns. He decides to make some further investigation and pins this event in the timeline view. Then, several events that are correlated with the first prescription of citalopram are highlighted in the timeline view (Figure 3). Alex finds that there is a strong positive correlation between the first prescription of citalopram and the subsequent prescriptions of citalopram, which is not surprising. On the other hand, Alex is surprised to see a positive correlation between the prescription of citalopram and being admitted to an emergency. This makes Alex wonder whether this is because citalopram is a common antidepressant choice for those ER doctors. Alex also wonders whether other kinds of antidepressants also have such a positive correlation with ER. He pins the first prescription of another antidepressant, sertraline, in the timeline view. This time, the timeline view highlights a different set of correlated events for sertraline, as shown in Figure 5. Alex notices the first prescription of sertraline has a positive correlation with radiology procedures

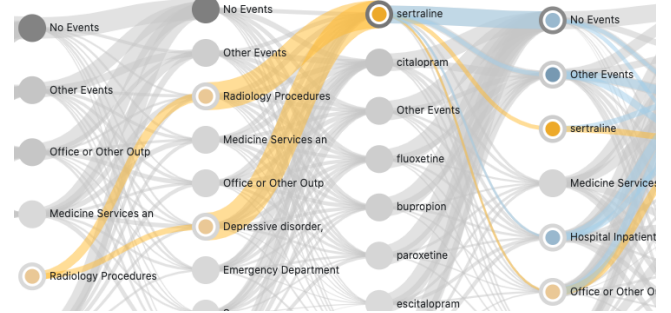


Figure 5: Medical events correlated with the first sertraline prescription

a week and a month before the first sertraline prescription. This implies a contrastingly different trajectory compared with patients who were given citalopram as the first antidepressant. Alex finds this observation quite interesting. He decides to conduct more rigorous experiments to validate this hypothesis and check if any scientific conclusions can be reached.

## 6 CONCLUSION

This paper presents an interactive visualization interface for exploring temporal sequence patterns in population-level electronic health records (EHRs). The design of this interface is informed by a formative study with clinical researchers on their needs and experiences of using a state-of-the-art visualization tool for EHRs. Three key features in this tool include: (1) a holistic view of medical events in different time windows, (2) information scents that guide users towards sub-cohorts of patients with unique sequence patterns, (3) a rich set of interactions that allow users to identify statistically correlated events, bundle multiple events, and define sophisticated inclusion and exclusion criteria to filter the dataset. Using this tool, we identified several interesting temporal patterns that were not known before in a psychiatry dataset.

In future work, we will continue to implement several tool features suggested by our clinician collaborators to further support exploratory cohort analysis. For example, our clinician collaborators found it hard to compare patterns in two sub-cohorts, e.g., a sub-cohort of patients who prescribed citalopram and another sub-cohort who prescribed sertraline. They wished they could compare the timeline views of multiple sub-cohorts side by side. Some existing work such as LifeLines2 [29] allows users to compare temporal summaries of two cohorts. It is worth investigating how well such cohort comparison design can support clinicians’ need. Another promising tool feature is to recommend what events to bundle together using concept learning or ontology learning. In addition, we will conduct case studies with clinical researchers to comprehensively evaluate the usability and effectiveness of our tool, following the evaluation guidelines from prior work [27].

## ACKNOWLEDGMENTS

We would like to thank anonymous participants for the formative study and anonymous reviewers for their valuable feedback. This work was supported in part by NIH R01 MH123804-01A1.

## REFERENCES

- [1] R. Bade, S. Schlechtweg, and S. Miksch. Connecting time-oriented data and information to a coherent interactive visualization. In *Proceedings of the SIGCHI conference on Human factors in computing systems*, pp. 105–112, 2004.
- [2] I. Batal, G. F. Cooper, D. Fradkin, J. Harrison, F. Moerchen, and M. Hauskrecht. An efficient pattern mining approach for event detection in multivariate temporal data. *Knowledge and information systems*, 46(1):115–150, 2016.
- [3] G. Bruno, T. Cerquitelli, S. Chiusano, and X. Xiao. A clustering-based approach to analyse examinations for diabetic patients. In *2014 IEEE International Conference on Healthcare Informatics*, pp. 45–50. IEEE, 2014.
- [4] H. S. G. Caballero, A. Corvò, P. M. Dixit, and M. A. Westenberg. Visual analytics for evaluating clinical pathways. In *2017 IEEE Workshop on Visual Analytics in Healthcare (VAHC)*, pp. 39–46. IEEE, 2017.
- [5] N. Cao, D. Gotz, J. Sun, and H. Qu. Dicon: Interactive visual analysis of multidimensional clusters. *IEEE transactions on visualization and computer graphics*, 17(12):2581–2590, 2011.
- [6] A. T. Chen, J. H. Chang, S. Hallinan, and D. C. Mohr. Mapping user trajectories to examine behavior and outcomes in digital health intervention data. In *2019 IEEE Workshop on Visual Analytics in Healthcare (VAHC)*, pp. 1–8. IEEE, 2019.
- [7] R. Chen, P. Ryan, K. Natarajan, T. Falconer, K. D. Crew, C. G. Reich, R. Vashisht, G. Randhawa, N. H. Shah, and G. Hripcsak. Treatment patterns for chronic comorbid conditions in patients with cancer using a large-scale observational data network. *JCO clinical cancer informatics*, 4:171–183, 2020.
- [8] E. H. Chi, P. Pirolli, K. Chen, and J. Pitkow. Using information scent to model user information needs and actions and the web. In *Proceedings of the SIGCHI conference on Human factors in computing systems*, pp. 490–497, 2001.
- [9] F. Dabek, E. Jimenez, and J. J. Caban. A timeline-based framework for aggregating and summarizing electronic health records. In *2017 IEEE Workshop on Visual Analytics in Healthcare (VAHC)*, pp. 55–61. IEEE, 2017.
- [10] F. Du, B. Shneiderman, C. Plaisant, S. Malik, and A. Perer. Coping with volume and variety in temporal event sequences: Strategies for sharpening analytic focus. *IEEE transactions on visualization and computer graphics*, 23(6):1636–1649, 2016.
- [11] D. Gotz and H. Stavropoulos. Decisionflow: Visual analytics for high-dimensional temporal event sequence data. *IEEE transactions on visualization and computer graphics*, 20(12):1783–1792, 2014.
- [12] D. Gotz, J. Sun, N. Cao, and S. Ebadollahi. Visual cluster analysis in support of clinical decision intelligence. In *AMIA Annual Symposium Proceedings*, vol. 2011, p. 481. American Medical Informatics Association, 2011.
- [13] D. Gotz, J. Zhang, W. Wang, J. Shrestha, and D. Borland. Visual analysis of high-dimensional event sequence data via dynamic hierarchical aggregation. *IEEE transactions on visualization and computer graphics*, 26(1):440–450, 2019.
- [14] M. Grace Shin, M. Samuel McLean, and M. June Hu. Visualizing temporal patterns by clustering patients. pp. 41–46, 2014.
- [15] Z. Huang, X. Lu, and H. Duan. On mining clinical pathway patterns from medical behaviors. *Artificial intelligence in medicine*, 56(1):35–50, 2012.
- [16] J. Jin and P. Szekely. Interactive querying of temporal data using a comic strip metaphor. In *2010 IEEE Symposium on Visual Analytics Science and Technology*, pp. 163–170. IEEE, 2010.
- [17] J. Krause, A. Perer, and H. Stavropoulos. Supporting iterative cohort construction with visual temporal queries. *IEEE transactions on visualization and computer graphics*, 22(1):91–100, 2015.
- [18] S. Malik, F. Du, M. Monroe, E. Onukwugha, C. Plaisant, and B. Shneiderman. Cohort comparison of event sequences with balanced integration of visual analytics and statistics. In *Proceedings of the 20th International Conference on Intelligent User Interfaces*, pp. 38–49, 2015.
- [19] B. M. Marlin, D. C. Kale, R. G. Khemani, and R. C. Wetzel. Unsupervised pattern discovery in electronic health care data using probabilistic clustering models. In *Proceedings of the 2nd ACM SIGHIT international health informatics symposium*, pp. 389–398, 2012.
- [20] M. Monroe, R. Lan, H. Lee, C. Plaisant, and B. Shneiderman. Temporal event sequence simplification. *IEEE transactions on visualization and computer graphics*, 19(12):2227–2236, 2013.
- [21] M. Monroe, R. Lan, J. Morales del Olmo, B. Shneiderman, C. Plaisant, and J. Millstein. The challenges of specifying intervals and absences in temporal queries: A graphical language approach. In *Proceedings of the SIGCHI Conference on Human Factors in Computing Systems*, pp. 2349–2358, 2013.
- [22] A. Mustaqueem, S. M. Anwar, and M. Majid. A modular cluster based collaborative recommender system for cardiac patients. *Artificial intelligence in medicine*, 102:101761, 2020.
- [23] G. N. Norén, J. Hopstadius, A. Bate, K. Star, and I. R. Edwards. Temporal pattern discovery in longitudinal electronic patient records. *Data Mining and Knowledge Discovery*, 20(3):361–387, 2010.
- [24] A. Perer and F. Wang. Frequence: Interactive mining and visualization of temporal frequent event sequences. In *Proceedings of the 19th international conference on Intelligent User Interfaces*, pp. 153–162, 2014.
- [25] A. Perer, F. Wang, and J. Hu. Mining and exploring care pathways from electronic medical records with visual analytics. *Journal of biomedical informatics*, 56:369–378, 2015.
- [26] H. Scheuerlein, F. Rauchfuss, Y. Dittmar, R. Molle, T. Lehmann, N. Pienkos, and U. Settmacher. New methods for clinical pathways—business process modeling notation (bpmn) and tangible business process modeling (t. bpm). *Langenbeck's archives of surgery*, 397(5):755–761, 2012.
- [27] B. Shneiderman and C. Plaisant. Strategies for evaluating information visualization tools: multi-dimensional in-depth long-term case studies. In *Proceedings of the 2006 AVI workshop on BEyond time and errors: novel evaluation methods for information visualization*, pp. 1–7, 2006.
- [28] J. Wang, J. Han, and C. Li. Frequent closed sequence mining without candidate maintenance. *IEEE Transactions on Knowledge and Data Engineering*, 19(8):1042–1056, 2007.
- [29] T. D. Wang, C. Plaisant, B. Shneiderman, N. Spring, D. Roseman, G. Marchand, V. Mukherjee, and M. Smith. Temporal summaries: Supporting temporal categorical searching, aggregation and comparison. *IEEE transactions on visualization and computer graphics*, 15(6):1049–1056, 2009.
- [30] K. Wongsuphasawat and D. Gotz. Exploring flow, factors, and outcomes of temporal event sequences with the outflow visualization. *IEEE Transactions on Visualization and Computer Graphics*, 18(12):2659–2668, 2012.
- [31] K. Wongsuphasawat, J. A. Guerra Gómez, C. Plaisant, T. D. Wang, M. Taieb-Maimon, and B. Shneiderman. Lifeflow: visualizing an overview of event sequences. In *Proceedings of the SIGCHI conference on human factors in computing systems*, pp. 1747–1756, 2011.
- [32] Y. Zhang, K. Chanana, and C. Dunne. Idmvis: Temporal event sequence visualization for type 1 diabetes treatment decision support. *IEEE transactions on visualization and computer graphics*, 25(1):512–522, 2018.

# Enabling Longitudinal Exploratory Analysis of Clinical COVID Data

David Borland\* Irena Brain † Karamarie Fecho ‡ Emily Pfaff § Hao Xu ¶  
RENCI, UNC-Chapel Hill UNC-Chapel Hill RENCI, UNC-Chapel Hill UNC-Chapel Hill RENCI, UNC-Chapel Hill  
James Champion ‡ Chris Bizon\*\* David Gotz ††  
UNC-Chapel Hill RENCI, UNC-Chapel Hill UNC-Chapel Hill

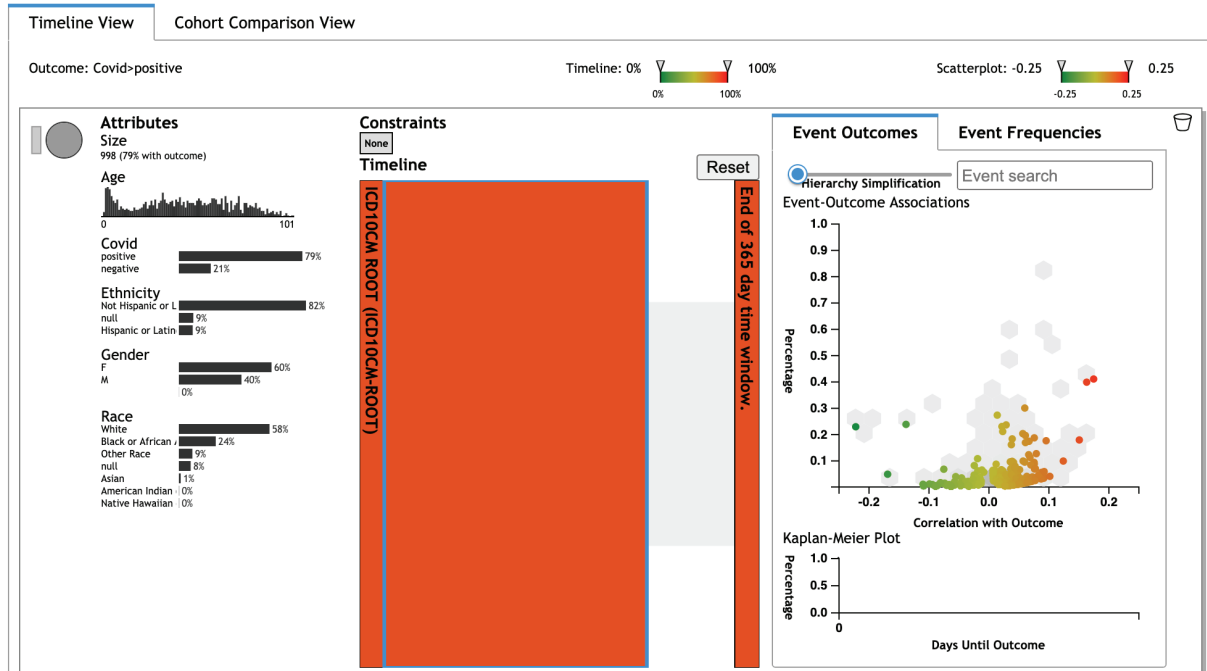


Figure 1: The Cadence visual analytics system in use to examine data from a cohort of 998 patients from early in the COVID-19 pandemic. Because no official COVID diagnosis was available in the standard coding systems at that point in the pandemic, a temporal query of “First ICD-10 Diagnosis” followed by a one year time window was issued to select all patients and all events in the available data. As the visualization shows, the patients were 79% COVID-positive (based on a standardized COVID phenotype), 60% female, and represented a wide variety of ages, from infants to elderly adults. An exploration of potential risk factors based on this cohort is presented within this paper.

## ABSTRACT

As the COVID-19 pandemic continues to impact the world, data is being gathered and analyzed to better understand the disease. Recognizing the potential for visual analytics technologies to support exploratory analysis and hypothesis generation from longitudinal clinical data, a team of collaborators worked to apply existing event sequence visual analytics technologies to a longitudinal clinical data from a cohort of 998 patients with high rates of COVID-19 infection. This paper describes the initial steps toward this goal, including: (1) the data transformation and processing work required to prepare the

data for visual analysis, (2) initial findings and observations, and (3) qualitative feedback and lessons learned which highlight key features as well as limitations to address in future work.

**Keywords:** Visual analytics, temporal event sequence visualization, human-computer interaction, medical informatics, COVID-19

**Index Terms:** Human-centered computing [Visualization]: Visualization systems and tools—; Human-centered computing [Visualization]: Visualization application domains—Visual analytics

## 1 INTRODUCTION

Beginning in late 2019, the emergence of the SARS-CoV-2 virus and its corresponding disease COVID-19 triggered a quickly spreading global pandemic. The crisis has caused health and economic harms to billions of people around the world, and resulted in millions of deaths in less than two years of existence. As of this writing, novel variants are emerging and continue to ravage unvaccinated populations [6]. As a result, and despite the development of effective vaccines, it appears that the virus is becoming endemic [25].

This ongoing health crisis has led to significant investments in research to better understand the nature of the SARS-CoV-2 virus, the novel disease it causes, risk factors that relate to severe outcomes, and the efficacy of potential treatments. One major initiative spon-

\*email: borland@renci.org

†e-mail: irenab@live.unc.edu

‡e-mail: kfecho@renci.org

§e-mail: epfaff@email.unc.edu

¶e-mail: xuhao@renci.org

||e-mail: champioj@email.unc.edu

\*\*e-mail: bizon@renci.org

††e-mail: gotz@unc.edu

sored by the National Institutes of Health in the United States is the National COVID Cohort Collaborative (N3C) [2, 18]. N3C is a multi-institutional effort to collect and share longitudinal clinical data in support of urgent research related to the pandemic.

Given the novelty of the COVID-19 disease—including many unknowns surrounding long and short-term symptoms, risk factors, and response to treatments—there is great interest among researchers in finding effective tools that can facilitate exploratory analysis and hypothesis generation based on complex longitudinal clinical data. These requirements align well with the general goals of visual analytics technologies [12, 24], and fit particularly closely with the capabilities of certain visual analytics tools developed for understanding event sequence data [15].

Motivated by this alignment in analytic requirements and system capabilities, a collaborative project was initiated to apply Cadence [14], an existing prototype visual analytics tool for event sequence analysis, to COVID-centric clinical data gathered at UNC Health using the N3C phenotype definition. This paper describes key aspects of this project, including: (1) the data transformation and preparation work required to ready the COVID cohort data for visual analysis, (2) initial findings and observations from a visual analysis of the data, and (3) qualitative feedback and lessons learned which include observations that motivate future research opportunities.

## 2 RELATED WORK

This section provides an overview of two key areas of research that provide a context for the work presented in this paper: applications of visualization to support the response to the COVID-19 pandemic, and visual analytics techniques for event sequence analysis.

### 2.1 Visualization and COVID-19

The value of visualization for health-focused applications has been well-studied [12], including both clinical use cases [27] and public health applications [22]. Accordingly, visualization has played a key role in the ongoing response to the COVID-19 pandemic. Examples include visualizations for managing the rise in telehealth activity [8], surveillance tools for tracking infection prevalence geographically and over time [9], and fatality management tools for managing the worst of the pandemic’s impacts [17]. One common theme in these efforts is the need for rapid development and innovation to meet the needs of a quickly changing environment. Our work follows a similar rapid development process. However, in contrast to the COVID-related articles cited above, which primarily focus on situational awareness and crisis management for on-the-ground response, the work presented in this paper aims to support COVID research activities for analysts working to better understand the nature of the disease.

### 2.2 Event Sequence Analysis

Event sequence data has been the focus of a large number of visual analytics research efforts [15]. From techniques for individual event sequences (e.g., [21]) to those for large collections of sequences (e.g., [28, 29]), many of these technologies have been developed with medical data analysis as a primary application. More recent work has focused on solving scalability challenges for these types of visual analytics tools [10]. Such challenges are especially pronounced in medical data, such as the extensive number of event types that arise from large medical coding systems [13, 14].

Reflecting the need for rapid progress, the work reported in this paper leverages Cadence [30], an existing visual analytics platform. Cadence employs a scalable visual design similar to the earlier DecisionFlow design [13], but adds selection bias quantification tools [3, 4] and data aggregation and navigation features for hierarchical event types such as those found in coded medical data [14]. This hierarchical aggregation and navigation feature proved especially useful for the work reported in this paper because, beyond the

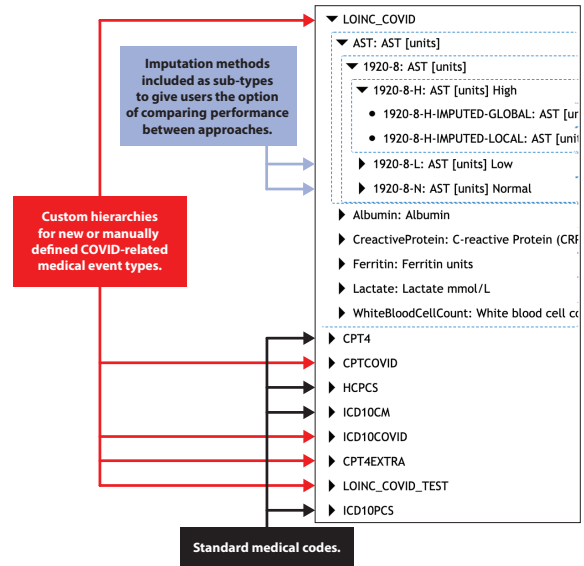


Figure 2: The type hierarchy for this project includes a combination of standard coding systems, custom hierarchies for new COVID-specific concepts, and representations of different imputation methods.

normal benefits for high-dimensional health data, it provided a way to allow users to optionally distinguish between different imputation methods during as part of their analysis.

## 3 METHODS AND FINDINGS

To support exploratory analysis and hypothesis generation by researchers investigating the clinical nature of COVID-19, we applied the Cadence visual analytics system to longitudinal medical data from UNC Health that was collected using the N3C phenotype definition in collaboration with the Integrated Clinical and Environmental Exposures Services (ICEES) [1, 11] team at UNC-Chapel Hill.

ICEES is an open regulatory-compliant service that exposes sensitive clinical data (e.g., EHR data, survey data, research data) that have been integrated at the patient level with a variety of public environmental exposures data (e.g., airborne pollutants, major roadways/highways, socio-economic factors, landfills, CAFOs). ICEES provides disease-agnostic capabilities for data access and analysis, and was recently adapted to support research activities surrounding coronavirus infections.

This section details the key steps required to apply the Cadence visual analytics system in this context, and describes an initial set of interesting findings. This work represents the first steps towards the ultimate aim of fully integrating Cadence capabilities within the larger ICEES platform for longitudinal analysis of large scale clinical data.

### 3.1 Data Preparation

Data for an initial set of 999 patients were obtained from the N3C team at UNC-Chapel Hill. The data included patient demographic attributes (including ethnicity, gender, race, and age), diagnoses, procedures, and laboratory tests. One patient was excluded because there were zero diagnoses present in that patient’s data, resulting in an overall cohort of 998 patients. The cohort was 60% female and included patients of all ages from infants to elderly adults. These figures are visible in the Attributes sidebar on the left side of Figure 1. The data were represented using standard medical coding systems (e.g., ICD-10, CPT4, and LOINC), and included several newly added codes created specifically for COVID-related concepts.

The data also contained labels for each patient identifying their COVID-19 status (COVID positive or COVID negative). Because the data for this cohort was captured early in the pandemic, few patients had actual COVID tests. Instead, labels were assigned to each patient based on a specific set of criteria regarding combinations of diagnoses and lab test results. In all, 79% of the cohort was labeled as COVID positive.

Data was provided in a set of JSON-encoded FHIR format files [16] and transformed into the Cadence data model. This model represents time-specific events as  $\langle ID, Date, EventType \rangle$  triples where the *EventType* has both a class and a code component (e.g.,  $\langle ICD-10, B34.2 \rangle$  to represent a coronavirus infection using the ICD-10 coding system). As part of this process, all diagnosis and procedure data was included. However, only LOINC data specifically related to COVID was included in the transformation from FHIR to Cadence formats. This includes LOINC-coded data about COVID tests (for those that had access, which was limited at the time) and other lab tests thought to be associated with COVID-related outcomes based on published literature [2]. Other LOINC lab tests were excluded from the analysis due to the manual work required to include these values (see the next section for more details).

### 3.2 Data Imputation and Categorization

Unlike diagnoses or procedures, which are represented as categorical events (e.g., a pneumonia diagnosis made on a specific date), lab tests are typically associated with attributes. For example, a white blood cell count test would include not only the fact that the test occurred, but also the value of the result. To fit this type of data into the triplet format used by Cadence, the lab results needed to be converted into categorical values. To achieve this goal, we used reference ranges for the test results to map observed numerical values to either High, Normal, or Low categories. Then, within the data, we created three types for each lab test (e.g., White-Blood-Cell-HIGH, White-Blood-Cell-NORMAL, White-Blood-Cell-LOW).

This process worked predictably and reliably when reference range data was available in the original FHIR data. However, we found information about High or Low ranges were often missing. Moreover, the specific ranges used to determine High or Low values can vary from patient to patient in complex ways based on their medical condition.

We therefore applied a two-phase imputation algorithm to fill in missing high or low reference range information. First, in a *local imputation phase*, if a given occurrence of a lab test was missing a reference range, we looked at the same patient's data to see if there were any records of the same test being performed on different dates that included a reference range. If so, we applied the reference range most frequently used for that patient on other dates to the lab test that was missing a reference range. Second, in a *global imputation phase*, if a given occurrence of a lab test was missing a reference range and all occurrences of that lab test for the same patient were also missing reference ranges, we applied the most frequent reference range from the overall population to that lab test.

### 3.3 Event Type Metadata

Cadence leverages event type hierarchies to manage complexity by performing aggregation of similar event types. The system recommends informative levels of aggregation while enabling users to manually move up or down the hierarchy of event types as desired during analysis. Standard medical codes are used as much as possible by leveraging the open-source Athena vocabulary database maintained by OHDSI [20]. However, the advent of COVID has led to the introduction of a number of extremely new codes. One key feature of Cadence is that it allows manually defined type hierarchies to supplement those in Athena, and this feature was used to add support for any new codes found in the data that were not present in Athena. These event types are shown in Figure 2.

The manually defined type hierarchy feature of Cadence was also critical for maintaining transparency for imputed event types. The imputation process described in Section 3.2 produces a High, Normal, or Low label for all lab tests. It was important to ensure that analysts could both: (1) treat all High (or Normal, or Low) values the same regardless of imputation method to maximize statistical power, and (2) distinguish between imputation methods to identify batch effects for validation of the various approaches. This was accomplished by inserting multiple event types into the hierarchy for each categorized lab test result, one for each imputation method. This can be seen in the user interface snapshot shown in Figure 2 for the AST lab test. The expanded hierarchy shows three subtypes of AST tests: High, Low, and Normal. The expanded High value section shows subtypes which can be used to represent High values obtained via the two types of imputation. This approach enables comparisons of different imputation methods as shown in Figure 4(b).

### 3.4 Findings

Once the data processing stage was complete, the data were loaded into the Cadence event sequence visual analysis platform for analysis. The data were initially explored by developers of the Cadence system. Then two interactive meetings were held with members of the collaborating ICEES team at UNC-Chapel Hill. The first meeting included two developers and five other full-time research staff collaborators, including three PhD-level researchers involved in medical data analysis. The second meeting included two developers and one PhD-level researcher in medical data analysis. During these meetings, the visualization was displayed to all attendees using Zoom screen sharing and jointly analyzed as we discussed the findings.

The first step in using Cadence was to issue a query. Event sequence visualization tools, including Cadence, generally aim to temporally align event sequences by a sentinel event (e.g., first diagnosis of COVID-19) to see patterns in how patients evolve before or after the alignment point. However, in the early days of the pandemic, patients were not often formally diagnosed with COVID-19. The disease was novel and not yet represented as a coded diagnosis within the EHR systems. Therefore, data were retrieved by issuing a temporal query that asked for one year of medical data following the first occurrence of any ICD-10 code. The generic nature of this query ensured that all 998 patients in the cohort matched the query, and the one year duration of the time window was sufficiently long to ensure that all available data was included in the analysis. The COVID-19 label value for these patients was used as the outcome with a positive COVID-19 value representing a negative outcome for the purposes of analysis.

The result from this initial query is shown in Figure 1. The Attributes column provides a summary of key non-temporal patient data including gender, ethnicity, race, and age distributions. In addition, the summary view showed that 79% of patients were labeled as COVID-positive.

Analysts were next drawn to the event scatterplot on the right side of the Cadence interface. Each circle in this plot represents a specific event type or higher-level event type group (e.g., a range of closely related ICD-10 codes) as determined by a dynamic hierarchical aggregation algorithm that aims to maximize informativeness of the visualized representation with respect to the outcome (in this case, a patient's COVID-19 label) [14]. The x-axis represents the event type's correlation with the outcome, and the y-axis represents the proportion of the population that exhibits the corresponding event type. Given this encoding, the most "interesting" events tend to be those on the left/right extremes (higher correlation) and toward the top of the scatterplot (high frequency).

Via interactive probing of this plot, the team was able to quickly confirm that well-publicised COVID-19 symptoms were indeed among the most strongly associated factors with a positive COVID-

19 label. Factors standing out at the periphery of the scatterplot included cough, fever, pneumonia, and a range of respiratory issues including general difficulty in breathing. The very quick identification and confirmation of these well-known symptoms raised the team's confidence in the system's analysis capabilities.

Similarly, a strong negative indicator for COVID-19 was a negative COVID test. These tests were rare early in the pandemic, and some patients who tested negative later tested positive. However, a negative test was by far the strongest negatively associated factor.

Not all findings were confirmatory, however, with the visualization highlighting some surprising discoveries. For example, there was a strong negative association between an “exposure to communicable disease” ICD-10 diagnosis and a positive COVID-19 status. Given the focus on contact tracing and our understanding of how disease spreads, this is opposite from what might be initially expected. However, surprisingly, the statistics for this diagnosis placed it quite close to a negative COVID-19 test in the scatterplot. A discussion within the team ensued to interpret this finding, and the leading hypothesis was that early in the pandemic, fearful patients with no symptoms were arriving for medical care because of potential exposure as their only risk factor. Without observable symptoms or the availability of confirmatory tests, these patients were not considered COVID-positive.

Similarly, the team was somewhat surprised to see a lack of strong support for some lab tests that had been expected to be predictive indicators for positive COVID cases: AST, Albumin, C-Reactive Protein, Ferritin, Lactate, and White Blood Cell Count [2]. Abnormal tests did show some correlation with positive COVID cases, but the strength of the effect was very small. For example, Figure 4(a) shows the data for AST tests in our cohort. This screenshot from Cadence shows that the High AST test results did have a stronger correlation than Normal or Low tests, but all were close to zero.

This could be caused in part by the imbalance in our cohort (70% COVID-positive) as well as the fact that these patients were from early in the pandemic before standards of care were developed. However, we can also see another potential problem from the visualization. The gray triangle beneath the High circle in Figure 4(a) is wide. This is a scenting clue provided by Cadence that variation exists within children event types.

Clicking on the High circle brought us to the view in Figure 4(b). Here we can see that not all High lab tests are the same. Locally imputed high AST test results were statistically similar to those found in the raw data. Globally imputed values, however, were quite different. This suggests a potential problem with the global imputation algorithm which may be obscuring more meaningful relationships between labs and a patient's COVID status. This shows the critical value in ensuring that analysts can distinguish between observed data, imputed values, and the different methods used for imputation.

Other interesting findings included a surprising-to-the-team link between sleep apnea and COVID-19 status. As shown in Figure 3, the general class of diseases of the nervous system (ICD codes in range G00-G99) had a positive correlation with COVID-19. Drilling down via the visualization, we found sleep apnea to be the predominant diagnoses within this category. This was a new discovery for those of us in the meeting, but a subsequent literature search demonstrated that this finding is in fact in line with recently published research [23]. In a similar way, we found relatively strong links between various hyperlipidemia diagnoses and COVID-19 status. This too was confirmed by a subsequent literature search as an exacerbating factor [5, 26].

## 4 DISCUSSION

Beyond the specific findings about the data, our analyses and the two interactive team meetings described in Section 3 yielded several insights about both the utility of various event sequence analysis

features and open challenges that would be valuable to address in future work.

For example, the collaborators found the attribute summaries useful to ground the work. “That’s handy, the demographics.” Commenting on the gender breakdown, “that’s about the hospital breakdown.” This along with confirmation of known symptoms increased user confidence in the system.

The ability to browse visually up and down the event type hierarchy as part of the visualization was seen to be especially valuable. A collaborator commented “that’s a nice feature I think, often you care about the higher level” aggregation. In addition, it enabled users to search for generic terms (e.g., ‘vent’ for ‘ventilator’) and then browse from that point to find a specific code or code group. Relatedly, the ability to leverage the type hierarchy to distinguish between observed values and different types of imputed values proved extremely valuable. As described in Section 3 with the AST lab test example, this approach provided essential transparency as to the batch effects between different methods of imputation.

Beyond these useful capabilities, the surprise findings were often most exciting for users. Remarking on the previously described sleep apnea observation, one user exclaimed “Oh, OK. That’s interesting!” Users would then immediately begin thinking about the potential validity of the discovery. Showing her internal thought process, a user commented about the sleep apnea discovery by stating “it makes sense. It’s a big risk factor for anesthesiology too.”

In terms of limitations, there were several that would benefit from additional research. One key constraint was the requirement that events with attribute values (e.g. lab tests) be mapped to categorical values (e.g., High, Normal, Low). This forces an analyst to impose arbitrary thresholds. This can obscure potentially valuable information such as trending in labs performed multiple times, or differences in thresholds for different patients. There has been some past research exploring events with attributes [7] but continued research is needed. Similarly, the pre-defined type hierarchy imposes constraints on the units of analysis. Support for more dynamic and flexible grouping would bring these tools closer to allowing arbitrary value sets [19] during analysis.

Finally, one of our collaborators mentioned that we could “do cool stuff with other outcomes and a better dataset.” For future work, we aim to apply Cadence to a larger 100,000 patient cohort from UNC Health that has a more balanced case/control population and which includes samples from later in the pandemic. This will enable us, as requested by our collaborators, to look more closely at different outcomes, such as mortality, ventilation, or other indicators of severe disease.

## 5 CONCLUSION

A collaborative effort was undertaken to adapt and apply existing visual analytics technologies to support exploratory analysis and hypothesis generation from UNC Health data gathered using the COVID phenotype definition developed by the National COVID Cohort Collaborative (N3C). This paper describes the initial steps toward this goal, including: (1) the data transformation and preparation work required to prepare the data for visual analysis, (2) initial findings and observations, and (3) qualitative feedback and lessons learned about the visual analytics system which highlight both useful features and limitations to address in future work.

## ACKNOWLEDGMENTS

The research reported in this article was supported in part by a grant from the United States National Science Foundation (#1704018). Partial support was also provided by the United States National Institutes of Health (NCATS OT2TR003430, NCATS UL1TR002489, NCATS UL1TR002489-03S4, and NCATS OT3TR002020).

## REFERENCES

- [1] S. C. Ahalt, C. G. Chute, K. Fecho, G. Glusman, J. Hadlock, C. O. Taylor, E. R. Pfaff, P. N. Robinson, H. Solbrig, C. Ta, N. Tatonetti, and C. Weng. Clinical Data: Sources and Types, Regulatory Constraints, Applications. *Clinical and Translational Science*, 12(4):329–333, 2019. doi: 10.1111/cts.12638
- [2] T. D. Bennett, R. A. Moffit, J. G. Hajagos, B. Amor, A. Anand, M. M. Bissell, K. R. Bradwell, C. Bremer, J. B. Byrd, A. Denham, P. E. DeWitt, D. Gabriel, B. T. Garibaldi, A. T. Girvin, J. Guinney, E. L. Hill, S. S. Hong, H. Jimenez, R. Kavuluru, K. Kostka, H. P. Lehmann, E. Levitt, S. K. Mallipattu, A. Manna, J. A. McMurry, M. Morris, J. Muschelli, A. J. Neumann, M. B. Palchuk, E. R. Pfaff, Z. Qian, N. Qureshi, S. Russell, H. Spratt, A. Walden, A. E. Williams, J. T. Wooldridge, Y. J. Yoo, X. T. Zhang, R. L. Zhu, C. P. Austin, J. H. Saltz, K. R. Gersing, M. A. Haendel, and C. G. Chute. The National COVID Cohort Collaborative: Clinical Characterization and Early Severity Prediction. *medRxiv*, p. 2021.01.12.21249511, Jan. 2021. doi: 10.1101/2021.01.12.21249511
- [3] D. Borland, W. Wang, J. Zhang, J. Shrestha, and D. Gotz. Selection Bias Tracking and Detailed Subset Comparison for High-Dimensional Data. *IEEE Transactions on Visualization and Computer Graphics*, 26(1), 2020.
- [4] D. Borland, J. Zhang, S. Kaul, and D. Gotz. Selection-Bias-Corrected Visualization via Dynamic Reweighting. *IEEE Transactions on Visualization and Computer Graphics*, 27(2):1481–1491, 2021. doi: 10.1109/TVCG.2020.3030455
- [5] J. H. Butt, T. A. Gerds, M. Schou, K. Kragholm, M. Phelps, E. Havers-Borgersen, A. Yafasova, G. H. Gislason, C. Torp-Pedersen, L. Køber, and E. L. Fosbøl. Association between statin use and outcomes in patients with coronavirus disease 2019 (COVID-19): a nationwide cohort study. *BMJ Open*, 10(12):e044421, Dec. 2020. doi: 10.1136/bmjopen-2020-044421
- [6] E. Callaway. Could new covid variants undermine vaccines? labs scramble to find out. *Nature*, 589(7841):177–178, 2021.
- [7] B. C. Cappers and J. J. van Wijk. Exploring multivariate event sequences using rules, aggregations, and selections. *IEEE transactions on visualization and computer graphics*, 24(1):532–541, 2017.
- [8] R. A. Dixit, S. Hurst, K. T. Adams, C. Boxley, K. Lysen-Hendershot, S. S. Bennett, E. Booker, and R. M. Ratwani. Rapid development of visualization dashboards to enhance situation awareness of COVID-19 telehealth initiatives at a multihospital healthcare system. *Journal of the American Medical Informatics Association*, 27(9):1456–1461, Sept. 2020. doi: 10.1093/jamia/ocaa161
- [9] B. E. Dixon, S. J. Grannis, C. McAndrews, A. A. Broyles, W. Mikels-Carrasco, A. Wiensch, J. L. Williams, U. Tachinardi, and P. J. Embi. Leveraging data visualization and a statewide health information exchange to support COVID-19 surveillance and response: Application of public health informatics. *Journal of the American Medical Informatics Association*, 28(7):1363–1373, July 2021. doi: 10.1093/jamia/ocab004
- [10] F. Du, B. Shneiderman, C. Plaisant, S. Malik, and A. Perer. Coping with Volume and Variety in Temporal Event Sequences: Strategies for Sharpening Analytic Focus. *IEEE Transactions on Visualization and Computer Graphics*, 23(6):1636–1649, June 2017. doi: 10.1109/TVCG.2016.2539960
- [11] K. Fecho, E. Pfaff, H. Xu, J. Champion, S. Cox, L. Stillwell, D. B. Peden, C. Bizon, A. Krishnamurthy, A. Tropsha, and S. C. Ahalt. A novel approach for exposing and sharing clinical data: the Translator Integrated Clinical and Environmental Exposures Service. *Journal of the American Medical Informatics Association*, 26(10):1064–1073, Oct. 2019. doi: 10.1093/jamia/ocz042
- [12] D. Gotz and D. Borland. Data-Driven Healthcare: Challenges and Opportunities for Interactive Visualization. *IEEE Computer Graphics and Applications*, 36(3):90–96, May 2016. doi: 10.1109/MCG.2016.59
- [13] D. Gotz and H. Stavropoulos. DecisionFlow: Visual Analytics for High-Dimensional Temporal Event Sequence Data. *IEEE Transactions on Visualization and Computer Graphics*, 20(12):1783–1792, 2014. doi: 10.1109/TVCG.2014.2346682
- [14] D. Gotz, J. Zhang, W. Wang, J. Shrestha, and D. Borland. Visual Analysis of High-Dimensional Event Sequence Data via Dynamic Hierarchical Aggregation. *IEEE Transactions on Visualization and Computer Graphics*, 26(1), 2020.
- [15] Y. Guo, S. Guo, Z. Jin, S. Kaul, D. Gotz, and N. Cao. A survey on visual analysis of event sequence data. *IEEE Transactions on Visualization and Computer Graphics*, Early Access, 2021. doi: 10.1109/TVCG.2021.3100413
- [16] HL7 FHIR Community. JSON - FHIR v4.0.1. <https://www.hl7.org/fhir/json.html>, Jul 2021.
- [17] S. Kaul, C. Coleman, and D. Gotz. A rapidly deployed, interactive, online visualization system to support fatality management during the coronavirus disease 2019 (COVID-19) pandemic. *Journal of the American Medical Informatics Association*, 27(12):1943–1948, Dec. 2020. doi: 10.1093/jamia/ocaa146
- [18] NIH National Center for Advancing Translational Sciences. National COVID Cohort Collaborative (N3C). <https://ncats.nih.gov/n3c>, Jun 2021.
- [19] NIH National Library of Medicine. Value Set Authority Center. <https://vsac.nlm.nih.gov/>, Jul 2021.
- [20] OHDSI. ATHENA Standardized Vocabularies. <https://www.ohdsi.org/analytic-tools/athena-standardized-vocabularies/>, Jul 2021.
- [21] C. Plaisant, R. Mushlin, A. Snyder, J. Li, D. Heller, and B. Shneiderman. LifeLines: using visualization to enhance navigation and analysis of patient records. *Proceedings of the AMIA Symposium*, pp. 76–80, 1998.
- [22] B. Preim and K. Lawonn. A Survey of Visual Analytics for Public Health. *Computer Graphics Forum*, 39(1):543–580, 2020. doi: 10.1111/cgf.13891
- [23] S. Strausz, T. Kiiskinen, M. Broberg, S. Ruotsalainen, J. Koskela, A. Bachour, FinnGen, A. Palotie, T. Palotie, S. Ripatti, and H. M. Ollila. Sleep apnoea is a risk factor for severe COVID-19. *BMJ Open Respiratory Research*, 8(1):e000845, Jan. 2021. doi: 10.1136/bmjjresp-2020-000845
- [24] J. Thomas and K. Cook. *Illuminating the Path: The Research and Development Agenda for Visual Analytics*. National Visualization and Analytics Ctr, 2005.
- [25] I. Torjesen. Covid-19 will become endemic but with decreased potency over time, scientists believe. *BMJ: British Medical Journal (Online)*, 372, 2021.
- [26] H. Wang, Z. Yuan, M. A. Pavel, S. M. Jablonski, J. Jablonski, R. Hobson, S. Valente, C. B. Reddy, and S. B. Hansen. The role of high cholesterol in age-related COVID19 lethality. *bioRxiv*, p. 2020.05.09.086249, June 2021. doi: 10.1101/2020.05.09.086249
- [27] V. L. West, D. Borland, and W. E. Hammond. Innovative information visualization of electronic health record data: a systematic review. *Journal of the American Medical Informatics Association*, 22(2):330–339, Mar. 2015. doi: 10.1136/amiainjnl-2014-002955
- [28] K. Wongsuphasawat and D. Gotz. Outflow: Visualizing Patient Flow by Symptoms and Outcome. In *IEEE VisWeek Workshop on Visual Analytics in Healthcare*. Providence, Rhode Island, USA, 2011.
- [29] K. Wongsuphasawat, J. A. Guerra Gómez, C. Plaisant, T. D. Wang, M. Taieb-Maimon, and B. Shneiderman. LifeFlow: visualizing an overview of event sequences. In *Proceedings of the 2011 annual conference on Human factors in computing systems*, CHI ’11, pp. 1747–1756. ACM, New York, NY, USA, 2011. doi: 10.1145/1978942.1979196
- [30] J. Zhang, D. Borland, W. Wang, J. Shrestha, and D. Gotz. Dynamic Hierarchical Aggregation, Selection Bias Tracking, and Detailed Subset Comparison for High-Dimensional Event Sequence Data. In *2019 IEEE Workshop on Visual Analytics in Healthcare (VAHC)*, pp. 56–57, Oct. 2019. doi: 10.1109/VAHC47919.2019.8945029

## A ADDITIONAL FIGURES

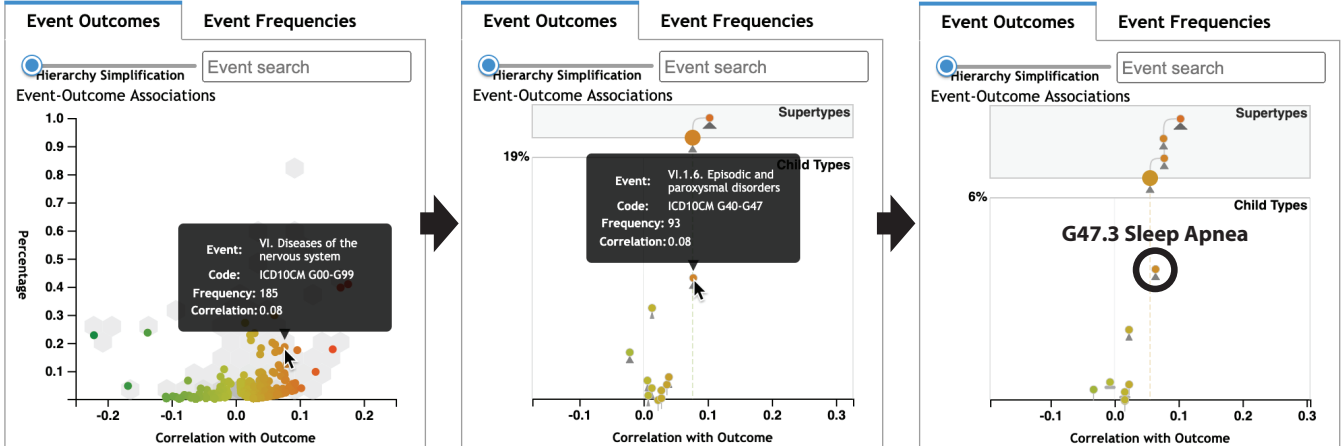


Figure 3: Diagnoses for diseases of the nervous system showed positive correlation with COVID-19-positive status. Drilling down via the interactive scatterplot, it was found that Sleep Apnea was the most common diagnosis code within that category and exhibited a positive correlation.

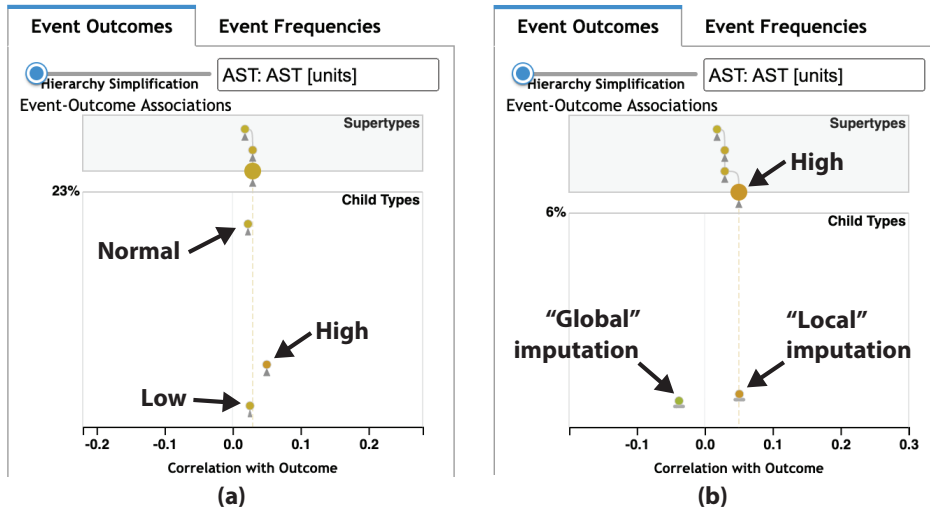


Figure 4: Several lab tests that were thought to be associated with COVID-19 infection proved to have weaker association than expected in the study cohort. (a) This example screenshot shows that high AST tests had a stronger positive correlation with COVID than normal or low tests, but the effect was very weak. Meanwhile, the scatting feature of Cadence (the gray triangular glyph underneath the High dot in the plot) suggests that variation exists between subtypes of High AST. Clicking on the High dot brings up (b) a visualization of the High result's subtypes which correspond to different methods of imputation. The plot shows that local imputation methods perform well in that the locally imputed High lab values have similar correlation statistics to the High test results found in the raw data. However, global imputation appears to have performed poorly as indicated by the large difference in correlation to COVID-positive patients. In fact, the sign of the correlation is reversed. This suggests a potential flaw in the global imputation approach, a key insight for analysts.

# Visual Analytics for Decision-Makers and Public Audiences within the United States National COVID-19 Response

Elisha Peterson, Philip Graff, Peter Gu, Max Robinson \*

Johns Hopkins University  
Applied Physics Laboratory

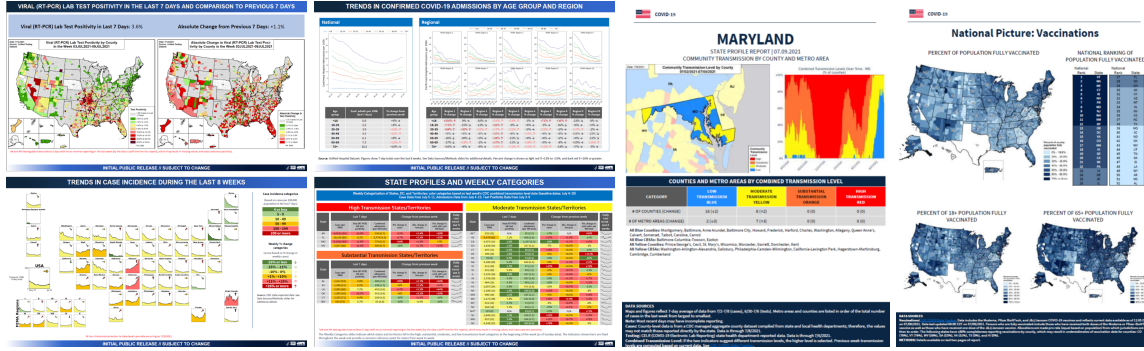


Figure 1: Selected elements of the publicly available *Community Profile Report* (left) and *State Profile Report* (right), highlighting COVID-19 indicators of interest at the national, regional, state, metropolitan, and county levels.

## ABSTRACT

The COVID-19 pandemic launched a worldwide effort to collect, process, and communicate public health data at unprecedented scales, and a host of visualization capabilities have been launched and maintained to meet the need for presenting data in ways that the general public can understand. This paper presents a selection of visualizations developed in support of the United States National COVID-19 Response, describes the unique set of constraints and challenges of operational visualization in this context, and reflects on ways the visualization community might be able to support public health operations moving forward.

**Index Terms:** Human-centered computing—Visualization—Empirical studies in visualization; Applied computing—Life and medical sciences—Health informatics

## 1 INTRODUCTION

The COVID-19 pandemic launched a worldwide effort to collect, process, and communicate public health data at unprecedented scales, and a host of visualization capabilities have been launched and maintained to meet the need for presenting data in ways that the general public can understand [3,5,7,9,12–14]. While there was a substantial body of work on epidemic visualizations prior to 2020 [6,8,11], the current pandemic lead to the near-simultaneous creation of national and sub-national dashboards and visuals targeted at a variety of audiences. Information visualization has been critical at every level and a fundamental tool to convey data to decision-makers in a way that lets them understand data, limitations, and take appropriate action. It has also been vital for communicating data and public health messaging to the general public in a way that is understandable and trusted [14]. It has also been an opportunity for visualization methods to evolve in response to a dynamic environment, with operational needs driving improvements.

\*e-mail: elisha.peterson@jhuapl.edu, philip.graff@jhuapl.edu, peter.gu@jhuapl.edu, max.robinson@jhuapl.edu

Within the United States National COVID-19 Response, the Data Strategy and Execution Workgroup (DSEW) was launched to provide a cross-agency focal point for data integration, analytics, and communication. Inside DSEW, the Integrated Surveillance Analysis (ISA) team was created to design, maintain, and deliver a common set of analytical products across government audiences and the public. In support of this response effort, a JHU/APL team designed, implemented, and maintained numerous visualizations targeted at a variety of audiences, evolving them as needed to keep up with the changing demands of the pandemic, and delivering them within daily and weekly reports. Two of the reports, the *Community Profile Report* (CPR) and the *State Profile Report* (SPR) were made public in December 2020 and January 2021, respectively, and are currently available on COVID Data Tracker [2]<sup>1</sup>, hosted by the US Centers for Disease Control (CDC).

This paper describes unique constraints and challenges associated with developing visualizations within an operational emergency response effort. We begin by discussing some of these challenges and how the unique needs of visualization consumers or “users” of our products informed our design choices. We then survey four specific visualizations created over the course of the pandemic, discussing the key information elements and questions addressed in each case. We close with some lessons learned as practitioners within this operational setting, and reflect on how the visualization community informed the effort.

## 2 METHODOLOGY

### 2.1 Constraints

The COVID-19 pandemic brought a unique set of constraints and challenges for visual analytics, for both data and process. When designing visualizations for products, it was important to be as focused as possible on the specific questions being asked and answered by a visualization, minimize distractions, and ensure the result met needs of the intended user, all while operating within the context of a constantly evolving environment, rapid response requests, and constant product deliveries.

<sup>1</sup><https://covid.cdc.gov/covid-data-tracker>

Data challenges related to the *variety*, *rapid evolution*, and *quality* of sources. Dozens of data sources have been available through the pandemic, most of them updated daily and frequently adding or changing reporting fields. Reporting criteria for specific fields shifted throughout the pandemic, and localities followed these inconsistently. There were often multiple reporting sources providing different values, sometimes varying substantially.

Operational/process challenges related primarily to *speed*, *scale*, and *consistency*. Visualizations needed to be designed and delivered on a quick-turn basis (hours to days). Within a national response, *consistency* is key to building trust and to keeping users focused on the question being answered rather than “why do these two numbers disagree?” To that end, it was important to consider whether existing methods were already in use for certain questions, to select common datasets where there were multiple options, and to align data cleaning methods with other products or pipelines.

Over the course of the pandemic, the “library” of visualizations grew to over 100 unique daily visualizations; these needed to be fully automated, regenerated each time a dataset was updated, and always kept production-ready. The data pipeline needed to be similarly automated and reliable. Beyond that, products and visualizations needed to be *archivable*, stored to serve as a historical document of what was known at certain points in time.

## 2.2 Visualization Design

Visualization design and evolution within the response was almost always driven by decision-maker needs. Where was the disease burden the highest? Where are hospitals running out of supplies? Where could interventions be most effective? What communities need to be targeted for vaccine outreach? Do we expect to see cases increasing or decreasing? A secondary goal in creating visualizations was to provide a set of common methods that would be applicable across all states and geographic levels.

During the response, we designed and refined numerous visualizations to address some of these questions. We routinely followed four design phases: (i) understand the precise question being asked/answered, (ii) survey existing tools and literature for best visualization methods, while keeping the approach simple, (iii) develop a quick mockup with sample data for review, and (iv) automate. As mentioned above, this process would need to be completed within a few days, or sometimes a few hours, to keep up with the rapidly changing needs within the response.

In addition to the initial design process, we solicited and received frequent feedback from stakeholders through email and remote collaboration. Feedback often included alignment issues such as wording and color choice or methodological improvements such as the addition of trajectory arrows in Figure 6 and explicit numbers in Figure 8. Frequently, feedback also involved removal of visualizations that were no longer necessary, or the creation of entirely new visualizations, as the analytic needs of the response evolved significantly over time.

## 3 IMPLEMENTATION

Two of the key products within the national response are the *Community Profile Report* (CPR) and the *State Profile Report* (SPR), both produced and made available each week for the general public [2].

The CPR, originally a daily spreadsheet and Portable Document Format (PDF) report and now generated twice-weekly, was designed to provide key indicators of interest across all geographic levels (national, regional, state, metropolitan, and county), with accompanying visuals to answer questions of interest related to trends, current disease burden, historical values, and more. It includes both a spreadsheet component, with color coding to help users understand variations in reporting across hundreds of indicators, and a PDF component with visualizations.

The SPR is a weekly PDF report designed to be used by state leaders and health officials, with a separate report prepared for each state, plus the District of Columbia and Puerto Rico, and currently contains 426 pages and hundreds of visualizations each week.

This section presents four of the visualizations within the CPR, as a representative sample of the kinds of questions that visual analytics have been best able to answer within the context of public health response efforts as well as some of the decision-making that goes into them. These four are taken from the CPR, but there are similar visuals and methods within the SPR.

### 3.1 Choropleth Geospatial Visualizations

Geospatial visualizations provide quick insight into the variation of indicators at different local levels, and were a staple of every response product. There are currently 19 national geospatial choropleth visualizations in the CPR, and several hundred within the SPR, showing incidence rates, utilization, change, and more (Figures 4 and 5).

These visualizations were primarily oriented at the US county level, as the finest unit of geography with good reporting, but sometimes would use states, zip codes, or other area types such as Hospital Service Areas (HSAs) [4]. Where variations in reporting might cause confusion, data notes were added to ensure context was provided. In addition to the primary metric, these visualizations would often be accompanied by *stacked area charts* (Figure 5) to provide users context regarding how the distribution of counties (or other area) by category changed over time.

#### 3.1.1 Color Selection

When selecting categories for Figure 4, we originally selected palettes with no more than six colors, and made it clear where areas were either missing data, or contained so little data that the resulting color could not be reliably interpreted. However, since the initial selection of categories in August 2020, the winter surge made it necessary to introduce two additional levels of “red” while retaining existing color mappings. Ideally, color palettes would be selected with color blindness in mind; however, given the operational context, decision-makers felt it more important to adopt the red-yellow-green color scale because it better resonated with expectations of the original audience.

The numeric thresholds in color palettes used here were chosen based on two criteria: (i) they needed to provide a simply-computed answer to the question about which areas are experiencing “high” or “low” disease spread, with color boundaries informed by epidemiological observations of past data, and (ii) they needed to agree with all other products used in the response that associated colors with the same metric. This latter point often required aligning methods, down to rounding methods and specific red-green-blue color definitions, with partner organizations.

### 3.2 Geofacet Visualizations

Given the visualizations were static, we often designed faceted visualizations to enable explicit comparisons between metrics, geographies, or demographics. This facetting enables users to make comparative visual queries much like they would with interactive dashboards, but also sometimes has the advantage of enabling *gestalt* perception of the whole.

Geofacet visualizations are a useful tool for showing *trends* across a variety of geographic areas [10]. Within the response, these were used to illustrate differences between US states and regions and to draw attention to those areas with the most concerning indicators. The CPR contains versions of these for eight key metrics of interest: case incidence, mortality rate/forecast, test positivity, emergency department visits, hospital admission rate, hospital inpatient COVID utilization, hospital ICU COVID utilization, and vaccine dose administration (Figures 6, 7).

Each geofacet visualization includes the following components: (i) a visual element for each state and HHS/FEMA region, along with a national plot, showing a normalized metric of interest for the most recent 8 weeks, (ii) color coding based on the most recent 7-day period, and (iii) indicators of trajectory based on week-on-week change (percent change from last 7-day period to current 7-day period), designed to quickly answer the question “how many states are trending up?”

The mortality version of this visualization (Figure 7) also included a 4-week forecast from the CDC ensemble forecast, indicating which states are likely to see increases of decreases in the near future [1]. The forecast was visualized based on the median projection, along with the 50% and 95% confidence intervals. The confidence intervals make it clear that there is a significant uncertainty with expected outcomes, especially for smaller states.

### 3.3 Small Multiple Region/Age Plots

A common challenge throughout the pandemic was to provide visualizations with concrete, quantitative, actionable indicators. For this purpose, small multiples were extremely useful, particularly for digging into more specific demographics that provide a more explanatory look at why disease spread might be occurring.

The hospital admissions chart in Figure 8 shows trends in confirmed COVID-19 admissions by age group and region, with small multiples alongside a chart showing week-on-week percentage change for each age group. This visual was launched in Spring 2021 to provide a quick way to capture the shift in hospital admissions from primarily older age groups to more middle aged groups.

This chart was enthusiastically received by the CPR’s audiences because it provided clear indicators of what age groups might be driving hospitalizations. While weekly percent change metrics are often noisy, at the regional and national level, these have been proven to be fairly stable for this metric.

### 3.4 State Category Table

In many cases, users are interested in quickly comparing multiple indicators for a given area, and for comparing these indicators to each other. For this purpose, simple tables of values are one of the most effective ways to present information. Figure 9 shows states grouped into categories, with six key indicators and a sparkline showing the recent case trajectory for each state.

As above, colors and thresholds in this table are selected to align with other visualizations throughout the response. Color palettes across different indicators are also aligned, so red/pink always indicates high burden or increasing trajectory, orange/yellow always indicate moderate burden or stable trajectory, and green always indicates low burden or declining trajectory. The high, substantial, moderate, and low transmission categories are set within the CDC Community Transmission guidelines<sup>2</sup>, but align where possible.

This slide is information-dense and can answer numerous questions about where disease burden is highest, whether it’s increasing or decreasing, whether increases in cases are matched by increases in test positivity or hospitalizations, whether case rates are generally trending up or down, and more, making it one of the most actionable visuals within the CPR. While not shown, the spreadsheet version of the CPR, provided as an Excel document, is essentially an expanded version of this with dozens of color-coded indicators for each region, state, metropolitan area, and county within the United States.

### 3.5 Data and Visualization Pipeline

The above visualizations were all fully automated over the course of the pandemic, along with hundreds of other pages presented in DSEW daily and weekly reports. Our team developed a data processing pipeline to meet the unique needs of the public health

response, with dozens of data sources updated multiple times per day, the need to maintain an independent history for every day of the response, and the need to deliver products every day even while they were being developed and refined.

The pipeline was built using primarily Python, with some elements in Java and Kotlin, and uses a tiered architecture with strong separation of concerns between its core components: data acquisition, data cleaning, quantitative analytics, visual analytics, geospatial visualization, product generation, and quality control (Figure 2). Visualizations were built primarily using ArcGIS and python arcpy for geospatial visualization and python matplotlib<sup>3</sup> for other visualizations, with pandas<sup>4</sup> for data processing.

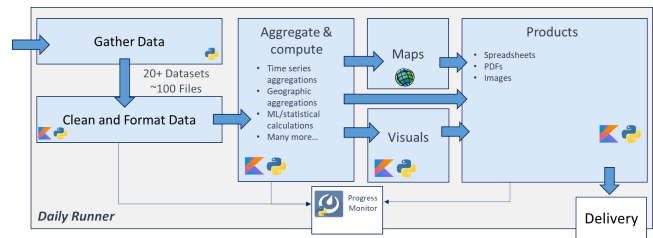


Figure 2: Daily processing pipeline used to generate ISA visualizations and products.

Unique operational requirements meant the pipeline needed to (i) be *scalable*, processing roughly 20 gigabytes of data each day, (ii) be *efficient*, running from end-to-end each day within a few hours, (iii) be *reliable/repeatable*, able to run multiple times per day as needed, and (iv) have a robust *change management* and *quality control* process, able to integrate numerous changes per day while ensuring no incorrect data and no unintended consequences, with any failures identified and resolved before production time.

#### 3.5.1 Map Production in ArcGIS

Templates and automation with ArcGIS<sup>5</sup> enabled repeatable, fast, and detailed map production at scale. Initially, geospatial layers with geographical region boundaries were brought into map documents (.mxd files). Choropleth data tables were joined to appropriate layers such that simply updating the table and refreshing the map would load the new data into the map. Then, the map layout was designed. In many cases, these documents served as templates to create similar maps without starting from scratch.

The python library arcpy<sup>6</sup> provided further control of the map generation. Title dates could be updated each day, layers could be turned on and off to create multiple types of maps from each map document, and the maps could be generated automatically in a pipeline. In some products, python code even created new layers or transferred additional information from text files to the map legend.

One common, but extremely important, use of automation was in creating maps of every state. Some products, such as the SPR, required multiple maps showing every state one at a time. Another use case was for emerging conditions localized in a list of counties or metropolitan areas. Rather than make a custom map responding to each request, maps centered on every state were created beforehand, and the appropriate maps were used for each request. Maps for every state were created by enabling *Data Driven Pages* in ArcGIS, where a layer was created specifying the zoom and positioning of every page, one for each state. By referencing the page name, a transparent mask covered areas outside of that state (Figure 3).

<sup>3</sup><https://matplotlib.org/>

<sup>4</sup><https://pandas.pydata.org/>

<sup>5</sup><https://www.arcgis.com/>

<sup>6</sup><https://pro.arcgis.com/en/pro-app/latest/arcpy/get-started/what-is-arcpy-.htm>

<sup>2</sup><https://covid.cdc.gov/covid-data-tracker/#county-view>

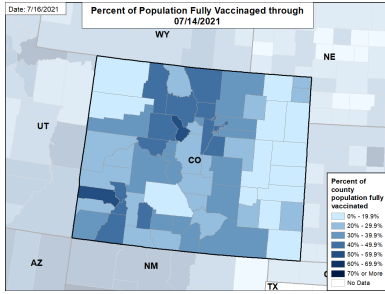


Figure 3: Single state vaccination map used within the *State Profile Report*. Each map highlights the state of interest by covering other areas with a transparent mask.

## 4 DISCUSSION

The visualizations here all evolved over the course of the pandemic, based on near continuous user feedback and changing priorities, and could likely be improved further. Based on this experience, five key attributes were needed for successful public health visualization: simplicity, explanatory power, consistency, deliverability, and timeliness. These observations mirror some of the findings in [14], in particular the need to maintain *trust* and ensure visualizations are clear and not misleading.

**Simplicity.** When communicating with decision-makers and the general public, visuals should be easily interpreted and consistent with past experience or general knowledge wherever possible. Methods should be clear and easily replicated wherever possible. This excludes several visualization types from consideration, for instance scatterplots that are designed to convey correlations.

**Explanatory Power.** Metrics/indicators should be communicated along with an “explanation.” If there are 100 cases, is that good or bad? In practice, the most critical element providing this explanation is the choice of a metric that allows for comparison across geographic areas (like normalizing COVID-19 case counts by population), along with a color palette that is shared across all visualizations using that metric. For displaying trajectory, simple visual indicators can explain whether a given percentage change in a metric indicates an increase, decrease, or stability.

**Consistency.** Reports provide a historical record and anchor discussion around a common set of values along with methods for interpreting those values. For decision-makers that base discussions on a set of “daily numbers,” visualizations need to agree on those numbers. Any discrepancies, whether due to reporting or data access time or cleaning methods, serve as a distraction (unless the conversation is about data reporting!). Visualizations should also maintain a consistent layout and look-and-feel so that they can be easily compared or viewed together.

**Deliverability.** As in many operational settings, visual analytics were best received and used when delivered to the email inboxes of users. Many decision-makers have limited time to access dashboards, but can quickly review a key set of visual analytics that arrive in their inbox.

**Timeliness.** Throughout the pandemic, conditions rapidly changed across the country, and due to the novel nature of COVID-19, having up to date information was of utmost importance. This meant that most products needed to be regenerated each day, quickly becoming too much to create manually. To this end, we heavily automated as much of the process as possible. The daily pipeline runs automatically every day, generating most of the recurring visualizations and freeing up the team for handling new requests.

In addition to these, visualizations need to be maintained over time in response to changing needs, data sources, or data quality. As one example, over the course of 2021, states continually shifted

reporting frequencies and policies. Because of this, reporting methods also needed to change to ensure displayed weekly averages and weekly changes were not misleading. Where methods couldn’t change due to the need for consistency, we added high visibility data notes as in Figures 4 and 6.

### 4.1 Needs

We also found there are two areas where current methods do not adequately address needs:

**Uncertainty.** Communicating uncertainty and risk in operational settings remains a challenge. Some of our visualizations depicted uncertainty, such as the confidence intervals for model projections shown alongside recent data in Figure 7 to illustrate the range of likely outcomes. However, most of the time either appropriate models/methods were not available to communicate uncertainty, or the inclusion of uncertainty added too much complexity to a visualization.

As an example, we primarily relied on week-over-week percent change to highlight changes in metrics. While simple, this metric can often provide misleading values, particularly when reporting dumps occur and in smaller states or counties, leading some users to the wrong conclusions. This could be resolved in part by better methods for estimating trajectory, better methods for filtering data to remove reporting dumps, or methods that indicate confidence intervals rather than a single number.

**Shared Methods.** Given the need to align data processing and reporting methods with partner organizations, many of whom used different platforms, we often faced significant challenges aligning methods. This is particularly true for more complex datasets, such as hospital data, where state data is “rolled up” from daily reports by individual hospitals with frequent missing or inaccurate data, changes in bed counts, and even changes in which hospitals should be included. A grammar for time series data methods, similar to what vega-lite<sup>7</sup> does for visualization, might help bridge this gap.

## 5 CONCLUSION AND FUTURE WORK

This paper described some of the unique challenges associated with developing operational visualizations in support of a pandemic public health response, with selected visualizations reviewed as exemplars of the questions and methods used.

In an operational public health setting, there is constant change and visualizations must often be designed and deployed on quick timelines. For decision-makers, the best visualizations answer questions clearly and directly, with minimal distractions. Often, this means visualizations that help them understand, diagnose, or pinpoint a problem, whether by geography or demographic, and often this means providing multiple indicators together as a bulwark against problematic data reporting.

In future pandemic response efforts, visualization could be improved by providing clearer, more accessible explanations of methods and do a better job of conveying uncertainty and risk. In addition, the practitioner community would benefit greatly from better tools for sharing methods, ensuring that common data cleaning, processing, and presentation methods are available to a wide range of partners and platforms.

## ACKNOWLEDGMENTS

This work was supported by the U.S. Department of Health and Human Services, Office of the Assistant Secretary for Preparedness and Response. The authors wish to thank the Integrated Surveillance Analysis team as well as the JHU/APL COVID-19 Response team, many of whom played major roles in the development and automation of these visualizations.

<sup>7</sup><https://vega.github.io/vega-lite/>

## REFERENCES

- [1] CDC COVID-19 Forecasts: Deaths. <https://www.cdc.gov/coronavirus/2019-ncov/science/forecasting/forecasting-us.html>. Accessed: 2021-07-19.
- [2] CDC COVID Data Tracker. <https://covid.cdc.gov/covid-data-tracker>. Accessed: 2021-07-19.
- [3] CovidActNow U.S. COVID Risk & Vaccine Tracker. <https://covidactnow.org>. Accessed: 2021-07-19.
- [4] Dartmouth Atlas of Health Care. <https://www.dartmouthatlas.org/faq/>. Accessed: 2021-07-19.
- [5] JHU CSSE COVID Dashboard. <https://www.arcgis.com/apps/dashboards/index.html#/bda7594740fd40299423467b48e9ecf6>. Accessed: 2021-07-19.
- [6] L. Carroll, A. P. Au, L. Detwiler, T.-c. Fu, I. Painter, and N. Abernethy. Visualization and analytics tools for infectious disease epidemiology: A systematic review. *J. Biomed. Informatics*, 2014. doi: 10.1016/j.jbi.2014.04.006
- [7] D. Cay, T. Nagel, and A. E. Yantac. Understanding User Experience of COVID-19 Maps through Remote Elicitation Interviews. In *2020 IEEE Workshop on Evaluation and Beyond - Methodological Approaches to Visualization (BELIV)*, pp. 65–73. IEEE Computer Society, 2020. doi: 10.1109/BELIV51497.2020.00015
- [8] H. Chen, D. Zeng, and P. Yan. Data Visualization, Information Dissemination, and Alerting. *Infectious Disease Informatics*, 2009. doi: 10.1007/978-1-4419-1278-7\_5
- [9] J. Comba. Data Visualization for the Understanding of COVID-19. *Computing in Science & Engineering*, 2020. doi: 10.1109/MCSE.2020.3019834
- [10] R. Hafen. Introducing geofacet and a discussion of other geographic visualization techniques. <https://ryanhafen.com/blog/geofacet/>. Accessed: 2021-07-19.
- [11] R. D. Howe. Understanding Pandemic Outbreaks through Data Visualisation-An Assessment of Current Tools and Techniques. 2014.
- [12] Y. Lan, M. Desjardins, A. Hohl, and E. Delmelle. Geovisualization of COVID-19: State of the Art and Opportunities. *Cartogr. Int. J. Geogr. Inf. Geovisualization*, 2021. doi: 10.3138/cart-2020-0027
- [13] B. Preim and K. Lawonn. A Survey of Visual Analytics for Public Health. *Comput. Graph. Forum*, 2020. doi: 10.1111/cgf.13891
- [14] Y. Zhang, Y. Sun, L. Padilla, S. Barua, E. Bertini, and A. G. Parker. Mapping the Landscape of COVID-19 Crisis Visualizations. In *Proceedings of the 2021 CHI Conference on Human Factors in Computing Systems*, number 608, pp. 1–23. Association for Computing Machinery, New York, NY, USA, May 2021.

## A VISUALIZATIONS

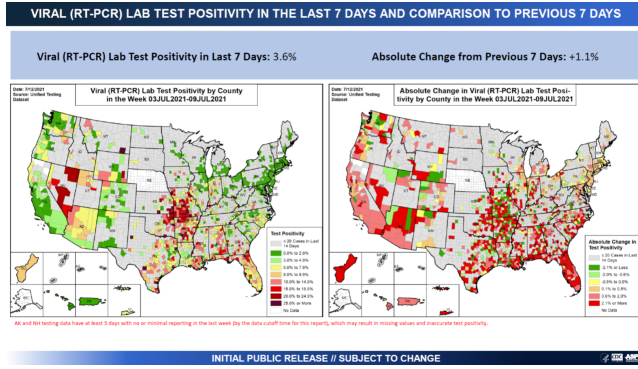


Figure 4: Dual geospatial visualizations showing test positivity by county along with the change since last week. The banner at the top shows the national average for each metric.

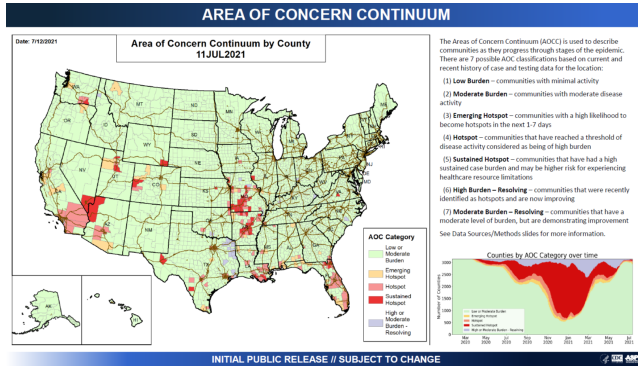


Figure 5: Choropleth geospatial visualization and accompanying sand chart showing changes in "Area of Concern" category by county and over time.

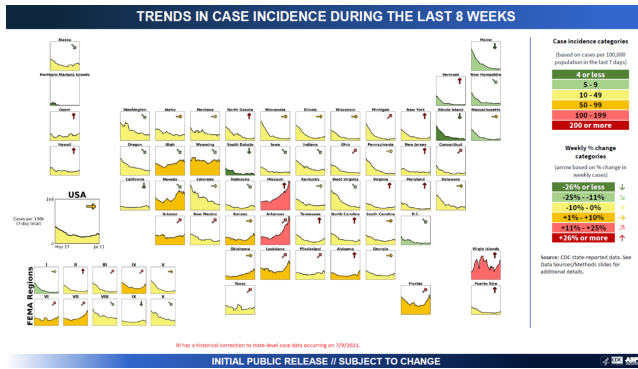


Figure 6: Geofacet visualization showing differences in case incidence for varying states and regions, with accompanying indicators to help users quickly identify disease trajectory and burden.

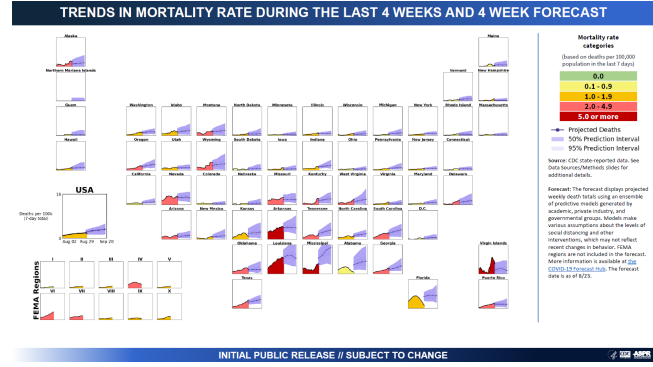


Figure 7: Geofacet visualization showing differences in mortality rate for varying states and regions, with additional visualization of confidence intervals for mortality forecasts.

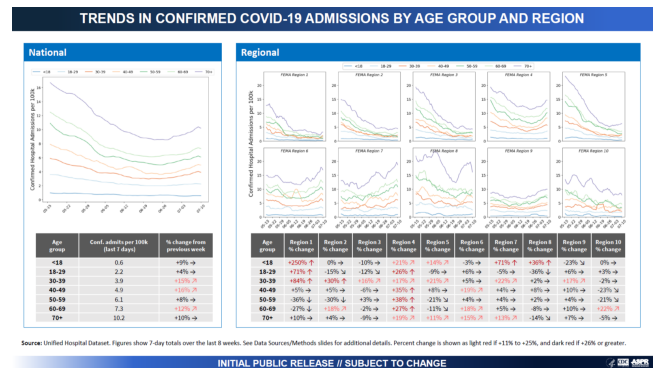


Figure 8: Small multiples visualization of COVID hospital admissions by age and HHS/FEMA Region. Colored indicators of percentage change for each age/region were a critical tool to monitor shifting demographics of hospital admissions in Spring 2021.

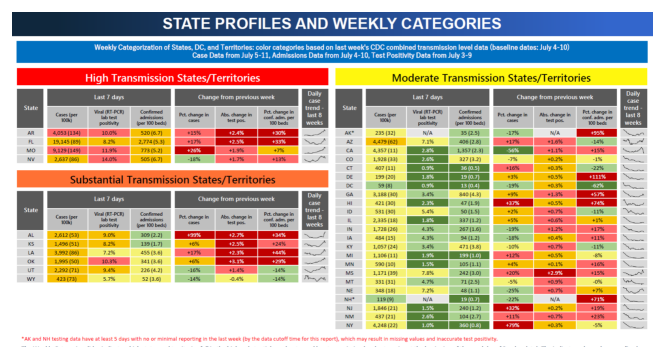


Figure 9: Table visualization of states, grouped by CDC's Community Transmission Level categories, along with six key indicators. In the report containing these, a second page shows the remaining Moderate Transmission states and the Low Transmission states.

# COVID-19 EnsembleVis: Visual Analysis of County-level Ensemble Forecast Models

Sanjana Srabanti\*

University of Illinois at Chicago

G. Elisabeta Marai†

University of Illinois at Chicago

Fabio Miranda‡

University of Illinois at Chicago

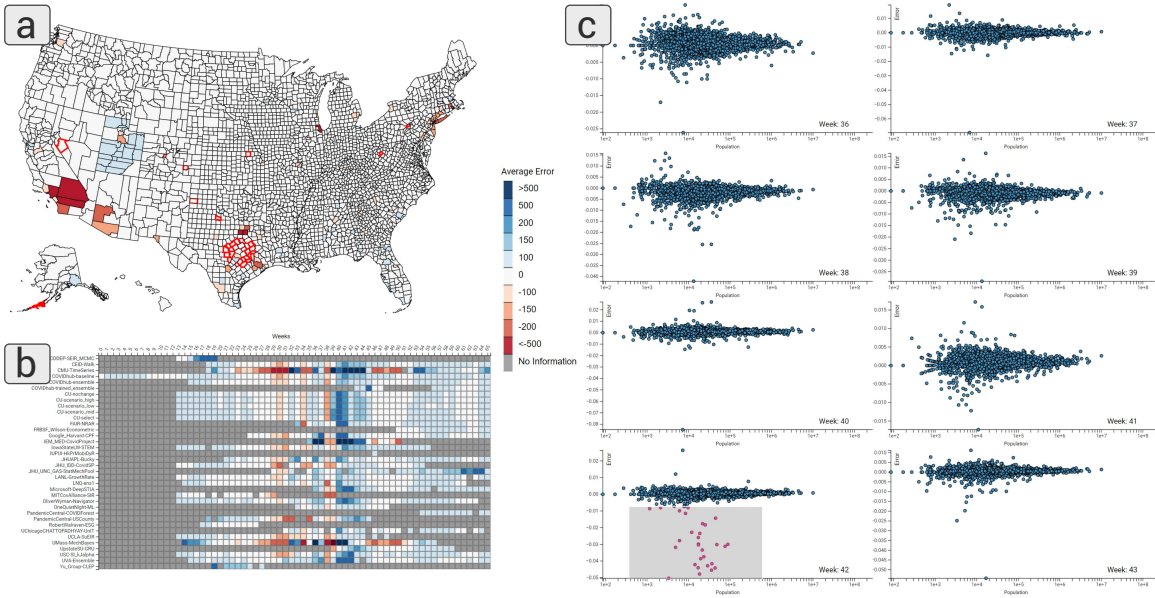


Figure 1: Enabling the visual analysis of COVID-19 ensemble forecast models with *COVID-19 EnsembleVis*. (a) We visualize the average error of the ensemble model at the county level. (b) Temporal distribution of the error of individual models, aggregated over all counties. (c) Distribution of errors over county population. Using the interface, we can notice that, in Week 42, the majority of the outlier counties are located in Texas (highlighted points in (c) and highlighted counties in (a)).

## ABSTRACT

The spread of the SARS-CoV-2 virus and its contagious disease COVID-19 has impacted countries to an extent not seen since the 1918 flu pandemic. In the absence of an effective vaccine and as cases surge worldwide, governments were forced to adopt measures to inhibit the spread of the disease. To reduce its impact and to guide policy planning and resource allocation, researchers have been developing models to forecast the infectious disease. Ensemble models, by aggregating forecasts from multiple individual models, have been shown to be a useful forecasting method. However, these models can still provide less-than-adequate forecasts at higher spatial resolutions. In this paper, we built *COVID-19 EnsembleVis*, a web-based interactive visual interface that allows the assessment of the errors of ensembles and individual models by enabling users to effortlessly navigate through and compare the outputs of models considering their space and time dimensions. *COVID-19 EnsembleVis* enables a more detailed understanding of uncertainty and the range of forecasts generated by individual models.

**Index Terms:** Human-centered computing—Visualization—Visualization application domains—Visual analytics;

## 1 INTRODUCTION

The COVID-19 pandemic has upended the world over the past year, in a health crisis not seen since the 1918 flu pandemic. As of July 2021, the disease has caused the death of more than 4 million people worldwide, 600,000 in the US alone. While waiting for an effective vaccine amidst the surging cases worldwide, governments adopted measures to inhibit the spread of the disease. Despite these efforts, waves of COVID-19 infection with varying characteristics, continued to ravage communities [24], highlighting the necessity to understand the spatio-temporal complexity of the problem [25]. Forecast models are among the tools available to public health experts and policymakers to predict likely pandemic outcomes (i.e., number of cases, deaths) and prepare for different scenarios. In the past year, several models have been proposed by a myriad of experts, and using vastly different assumptions, methodologies, parameters and data sources. As a result, models produce a range of sometimes radically different forecasts, especially at higher spatial resolutions, limiting their use by decision makers and the public in general. In order to address this problem, more recently, ensemble models have been proposed for COVID-19 forecasts, with promising results [35, 44].

Ensemble models are usually created by combining different individual models (i.e., members), either through simple weighted averages or more sophisticated approaches, such as multiple linear regression and principal component regression [27]. Rather than relying on individual models, a set of forecasts in an ensemble indicates a larger range of possible future scenarios. Because of their high prediction accuracy, ensemble approaches are widely used in

\*e-mail: ssraba2@uic.edu

†e-mail: gmarai@uic.edu

‡e-mail: fabiom@uic.edu

Table 1: Overview of the individual models considered by our tool.

Model name	Team	Data sources
CEID-Walk [11]	U. of Georgia	JHU case and death counts
CMU-TimeSeries [10]	CMU	JHU case and death counts
CU-Select [20]	Columbia U.	JHU case and death counts, hospitalizations and ICU admissions, mobility
FAIR-NRAR [8]	Facebook	NY Times case counts, weather, mobility
IEM_MED-CovidProject [9]	IEM MED	JHU case counts
IowaStateLW-STEM [3]	Iowa State	NY Times, Health department, county-level infected and death cases
JHUAPL-Bucky [14]	JHU	JHU, hospitalizations, mobility
JHU_IDD-CovidSP [19]	JHU	JHU, US Census (population, mobility)
JHU_UNC_GAS-StatMechPool [13]	JHU	Demographic parameters, weather, mobility
LANL-GrowthRate [16]	Los Alamos	HHU, population
LNQ-ens1 [17]	SAS	JHU
OneQuietNight-ML [4]	-	JHU, mobility
PandemicCentral-USCounty [18]	Pandemic Central	JHU case and death cases, US Census, CCVI, mobility
UCLA-SuEIR [21]	UCLA	JHU case and death cases, hospitalizations
UMass-MechBayes [1]	UMass-Amherst	JHU
UpstateSU-GRU [6]	SUNY	JHU, US Census, health surveys, behavioral risk factors
UVA-Ensemble [2]	U. of Virginia	Mobility

different domains, such as weather and climate [36], economy [47], and more recently in forecasting infectious diseases [35, 38]. Given the increasing importance of ensembles for COVID-19 forecasting, it is important to evaluate and compare ensemble members through space and time, as well as identifying potential limitations and guiding the improvement of both ensemble and individual models.

In this paper, we propose *COVID-19 EnsembleVis*, an open-source<sup>1</sup> web-based interface to enable the visual analysis of the county-level differences between forecast and ground truth data of ensemble models and their members. We focus on fine geographic level data since it can reveal staggering disparities among different locations that were missed at coarser aggregation levels [22, 33], which signifies the need for even more precise predictions. By enabling effortless navigation through ensemble members and allowing the evaluation and comparison of multiple models, our proposed approach can be used to obtain a more detailed understanding of uncertainty and the range of forecasts generated by individual models, and highlight limitations of the models at the county level. This last point is a particularly important one, given the impact of the pandemic on different communities at different levels throughout the past year. Since COVID-19 ensemble models have only recently been shown to be effective [44], our work offers the first steps in eliciting some of the particular challenges related to the visualization and analysis of ensemble models of COVID-19 forecasts. We focus our efforts on the visualization of the *outputs* of ensembles and individual models. While our approach addresses some of these challenges, we believe that our work goes toward creating the necessary connections between ensemble visualization (a popular topic, especially in the weather domain) and pandemic ensemble models.

## 2 RELATED WORK

In this section, we briefly survey existing literature related to COVID-19 forecasting, a topic that has received significant attention recently due to the different ways the pandemic has impacted the world. Given how widely used ensemble models are in other domains, we also survey ensemble visualization techniques and systems.

**COVID-19 forecasting.** Over the past year, different research groups from academia and industry have been developing models to forecast COVID-19 cases and deaths. In the US alone, over 50 teams have made their forecasts publicly available, according to the COVID-19 Forecast Hub [5]. The majority of these models forecast both cases and deaths at a state level, while a smaller number forecasts cases at the county level, (and one recent model also providing county-level fatalities [39]).

The vast majority of the models rely on the Johns Hopkins Coronavirus Resource Center confirmed case and death data [15], while a subset uses mobility [2, 4, 8, 13, 14, 18–20], weather [8, 13], US census [6, 18, 19], or hospitalization data [16, 20, 21]. Table 1 presents an overview of individual models. In April 2020, an initiative led by the Reich Lab at the University of Massachusetts started to collect and combine forecasts for US spatial units (states and counties), making the resulting ensemble data publicly available each week. This initiative was in close collaboration with the US Center for Disease Control and Prevention (CDC), who also release weekly ensemble forecasts as a *real-time tool to help guide policy and planning* [7].

Several interfaces and dashboards have also been made available with the goal of visualizing ensemble members [3, 9, 16, 18, 21], but they are restricted to individual members or lower spatial resolutions. *COVID-19 EnsembleVis* is the first visual interface that allows users to compare and analyze ensembles and individual members at the county level.

**Ensemble visualization.** Ensemble data is common in several domains, such as biomedical images [34], network security [32], climate simulations [40], machine learning [46], and due to the complexity of the data, ensemble visualization faces a variety of research challenges, such as scalability, extraction of trends, differences and commonalities [42]. Previous work has focused on proposing frameworks to support visual analysis of ensemble data through a combination of statistical visualization techniques and user interaction [43], visual glyphs, such as radar plots [37], ribbons and spaghetti plots [45], clustering [30, 31] and probabilistic [28, 29] and trend analysis [41]. A complete survey of visualization and visual analysis of ensemble data can be found at Wang et al. [48]; the survey focuses on more common ensemble data, such as weather and climate simulations, and lists a series of six common ensemble visualization tasks: overview, comparison, clustering, temporal trend analysis, feature extraction, and parameter analysis. In our work, we use a subset of these tasks to visualize COVID-19 forecast ensemble models, with the goal of indicating and starting to lay down bridges between ensemble visualization research and pandemic predictions.

## 3 COVID-19 FORECASTS AND ENSEMBLES

An initiative led by the University of Massachusetts has created a central repository, called COVID-19 Forecast Hub, that collects and organizes submissions with COVID-19 forecasts in the US, both at the state level and at the county level. These submissions are developed independently and shared publicly. Submissions can include week-ahead forecasts of COVID-19 deaths and/or cases following the CDC’s epidemiological weeks. For example, during epidemiological week 1 (EW1), a team can submit a forecast for the

<sup>1</sup><https://github.com/uic-evl/covid-19-ensemblevis>

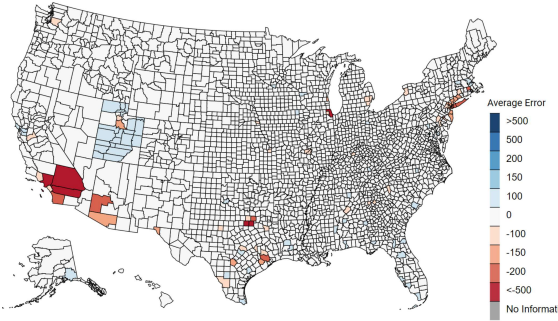


Figure 2: Spatial view: visualizing the spatial distribution of the ensemble model’s error (aggregated by counties).

subsequent weeks ( $\geq$ EW2). At the beginning of each week, an ensemble forecast will be created using the most recent *valid* forecasts from each team; the ensemble is composed of the median prediction across all eligible models at each quantile level. Both individual forecasts, as well as ensemble forecasts, are made available as CSV files with a weekly temporal resolution and state and county spatial resolutions. Ground truth data is also collected by the Forecast Hub, allowing the straightforward computation of error metrics. To be more precise, the error of a model can be calculated as the difference  $e_{c,t} = y'_{c,t} - y_{c,t}$ , where  $y'_{c,t}$  is the model’s predicted value for county  $c$  at week  $t$ , and  $y_{c,t}$  is the ground truth for county  $c$  at week  $t$ . In this paper, positive differences (i.e., predicted value greater than ground truth) are represented by shades of blue, and negative differences by shades of red.

On top of the individual forecast CSV files, the central repository also hosts a weight CSV file and an eligibility CSV file. For each week and geographical unit, the first file lists the models’ weights used in the computation of the ensemble forecast, and the second file informs whether or not a given model is eligible for inclusion in the ensemble forecast. Both files are updated weekly.

It is important to note that UMass’ center interprets forecasts as *unconditional* predictions about the future. In other words, predictions should consider uncertainty across a wide range of future scenarios (e.g., new social distancing mandates), and it is up to the team to select and submit one or a combination of predictions across the most likely scenarios. In this work, we make use of UMass’ COVID-19 Forecast Hub ensemble model, which combines the individual models highlighted in Table 1. We focus our attention on the visualization of 2-week-ahead predictions.

#### 4 REQUIREMENTS

The CDC recently highlighted how important it is *to bring forecasts together to help understand how they compare with each other and how much uncertainty there is about what may happen in the future* [7]. Considering that, we identified three main tasks that can be facilitated by a visual interface: 1) provide an overview summary of the errors of the models to assess uncertainty; 2) identify spatiotemporal trends, i.e., how a group of members changes over space and time; and 3) visually identify differences between two or more ensemble members. In order to accomplish these tasks, we identified the following requirements for our visual interface:

[R1] **Support the identification of spatiotemporal patterns.** Explore the spatial and temporal patterns of one or more ensemble members to identify regions or periods with above average forecast error and uncertainty.

[R2] **Support the comparison of ensemble members.** Compare predictions of different ensemble members to evaluate the spatiotemporal performance of different models.

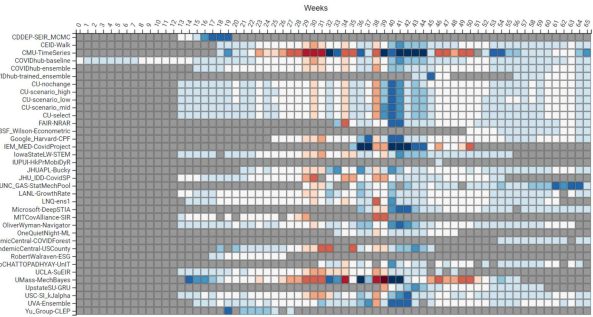


Figure 3: Temporal view: visualizing the temporal distribution of individual ensemble models (aggregated by weeks). Cells show positive (shades of blue) and negative (shades of red) prediction errors for each model (row). Cells without prediction information are shown in grey.

[R3] **Support the analysis of the relationship between model performance and sociodemographic features.** Explore the relationship between sociodemographic variables and model performance to identify regions not adequately represented in the model.

#### 5 COVID-19 ENSEMBLEVIS

In order to satisfy the previously detailed requirements, we built *COVID-19 EnsembleVis*, a web-based interface to facilitate the visual exploration of COVID-19 forecast ensembles. The interface is composed of three main views: spatial view, temporal view, and distribution view. These three views are all linked, such that a selection in one view will highlight the appropriate data in other views. In this work, we consider weekly predictions between April 6, 2020 and July 5, 2021.

**Spatial view.** This component is composed of a map with US counties (Figure 2) and enables the identification of spatial patterns (R1). Each county is painted according to the average ensemble’s forecast error over all weeks (i.e.,  $\sum_{t \in \text{weeks}} \frac{e_{c,t}}{\text{weeks}}$ , for each county  $c$ ). A divergent color scale is used to indicate negative and positive forecast errors. In order to enable detailed analysis, the user can select an individual county, and the temporal view will update accordingly.

**Temporal view.** This view uses a matrix heatmap to display the weekly average error for *each* ensemble member (Figure 3). Each cell is painted according to the average ensemble member’s forecast error over all counties (i.e.,  $\sum_{c \in \text{counties}} \frac{e_{c,t}}{\text{counties}}$ , for each week  $t$ ). The temporal view allows the visualization of forecast errors over time (R1) and the comparison of individual ensemble members (R2) that can help in the identification of weeks with bad predictions (e.g., predictions with high errors) from ensemble members. The temporal view is linked with the spatial view. If a single county is selected, the weekly average error for each model of that particular county will be shown (Figure 6). Furthermore, the temporal view enables the user to add temporal constraints by selecting specific weeks of interest, which will update the other views. The same divergent color scale from the previous component is also used in the temporal view. Missing predictions are displayed in light gray.

**Distribution view.** This view incorporates a 2D scatterplot that shows, for each week, the distribution of per-county ensemble prediction errors (normalized by population) by the log of the total county population. Each data point then represents the ensemble prediction error for a given county at a given week. Users can use the scroll wheel to view different weeks or select specific weeks from the temporal view. In this version of the interface, we only consider the population information, partially meeting R3. The main

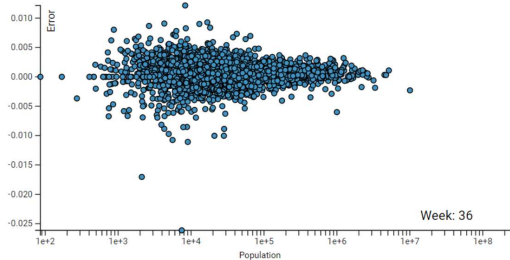


Figure 4: Distribution view: visualizing the distribution of ensemble prediction errors. Each data point represents the ensemble prediction error for a given county at a given week.

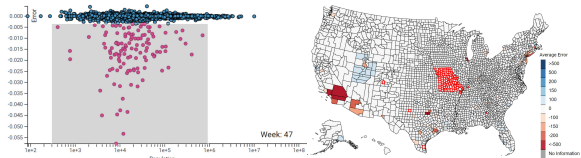


Figure 5: Spatial distribution of predictions with large error values. By selecting outlier points in Week 47 (left), we notice that they are mostly located in the state of Missouri.

purpose of the scatterplot is to assess any possible relationship between prediction error and demographic variables. The distribution view also allows the user to brush the scatterplot and select data points of interest; this will then update the other views, enabling the assessment of the spatiotemporal distribution of the errors.

**Implementation.** The *COVID-19 EnsembleVis* interface was implemented using Angular, D3 and TopoJSON so that it could be easily accessed through a web browser. We collected the predictions from UMass’ COVID-19 Forecast Hub and pre-processed them using Python and Jupyter Notebook. The EpiWeeks Python library was used to compute epidemiological weeks (following CDC’s standard). The pre-processing step is responsible for aggregating the data over counties and epidemiological weeks. The pre-processed data is then stored as a single JSON file and accessed by the front end. The source code and data pre-processing stages are available at <https://github.com/uic-evl/covid-19-ensemblevis>.

## 6 EXPLORING ENSEMBLE PREDICTIONS

In this section, we illustrate an initial case on how our tool can be used in the visual analysis of ensemble models, with a focus on understanding how prediction errors are spatially distributed over different counties. We begin the exploration by visualizing the distribution of ensemble prediction errors by county population using the distribution view (Figure 1(right)). We notice a particular week (Week 42) where certain counties present a larger prediction error. We select these data points in the scatterplot and notice that most of them are counties in Texas. While it is not possible to precisely say *why* this happened, such visualization can foment discussions on the shortcomings of current modeling practices, such as data availability, parametrization for those counties, etc.

We also used *COVID-19 EnsembleVis* to explore the spatial distribution of errors in Week 47, which showed another unusual pattern (Figure 5). After selecting a set of points in the scatterplot (left side of the figure), we noticed that these points are from counties in Missouri (right side). Unlike the previous example, however, we were able to pinpoint the source of such an unusual pattern: on March 8, 2021, the Missouri Department of Health and Senior Services updated the number of daily cases to show 81,206 previously unreported infections.

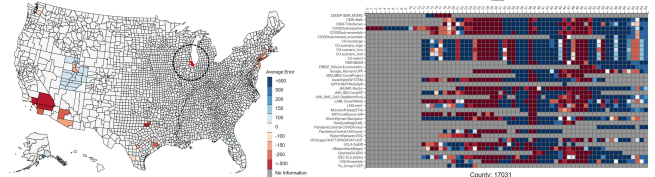


Figure 6: Temporal distribution of average error of an individual county. After selecting Cook County (left), we observe that there are large differences in average error over the weeks (right).

Our ongoing collaboration with public health experts interested in the impact of COVID-19 on underrepresented communities in Chicago enabled us to use *COVID-19 EnsembleVis* to better understand the prediction errors in Cook County. The data revealed significant differences in the average error over the weeks (Figure 6). In the initial weeks, the average error for each ensemble member was mostly negative, and with time the error increased to positive values. One possible hypothesis is that models were not able to capture the significant loss of life in Long-term Care Facilities, an ongoing problem due to inaccurate public health indicators [26]. Understanding the poor local accuracy of prediction models can create opportunities to investigate new sources of data or parametrizations for specific counties and communities.

## 7 CONCLUSION AND FUTURE WORK

*COVID-19 EnsembleVis* is a visual interface built specifically for the analysis of COVID-19 forecast ensemble models. By using three different visualization components, we enable the investigation of both the ensemble and individual models, from both spatial and temporal perspectives. *COVID-19 EnsembleVis* takes the first steps toward the visualization of county-level forecast ensemble models. Although only presenting a collage of known visualization metaphors, this work creates a foundation that will enable researchers to apply ensemble visualization techniques to efforts related to the recent pandemic. We hope this can help foment a discussion that builds bridges between ensemble visualization researchers (mostly focused on weather and climate data) and modeling and public health experts. Additionally, we believe there are several interesting challenges that could certainly benefit from collaboration between these fields. For instance, while we focus our efforts on the visualization of the output of the models, certain research teams do make their code publicly available, opening doors to have a more vivid picture of their computational mechanisms. Therefore, understanding the impact of different parametrizations through visual analytics tools is a path that can not only increase performance and accuracy but also increase public trust in these models.

We also believe that there is an opportunity to use metaphors that were previously introduced by visual analytics tools to visualize weather and climate ensemble data. Given the potential impact of COVID-19 predictions, in future work we will also investigate how predictions can better inform policymakers and their decisions from a visual analytics perspective [23]. Furthermore, we will explore the relationship between models and data sources. As shown in Table 1, models use different data sets, and this can heavily impact the predictive power of both individual members and ensembles. Given that, we believe it would be interesting to understand the relationship between data sets, model performance, and social demographic variables. Moreover, given the number of possible data slices, it would be important to guide the user in the exploratory process and highlight potentially interesting data features. We will also extend *COVID-19 EnsembleVis* to enable the visualization and exploration of COVID-19 forecasts from other regions of the world, including Europe [12].

## REFERENCES

- [1] Bayesian modeling of COVID-19. Available: <https://github.com/dsheldon/covid>. Accessed on: July 18, 2021.
- [2] Biocomplexity Institute. Available: <https://biocomplexity.virginia.edu/>. Accessed on: July 18, 2021.
- [3] COVID-19 Dashboard. Available: <https://covid19.stat.iastate.edu>. Accessed on: July 18, 2021.
- [4] COVID-19-forecast. Available: <https://github.com/One-Quiet-Night/>. Accessed on: July 18, 2021.
- [5] COVID-19 Forecast. Available: <https://covid19forecasthub.org/>. Accessed on: July 18, 2021.
- [6] COVID-19 Forecast from SUNY and Syracuse University Team. Available: <https://github.com/ylzhang29/UpstateSU-GRU-Covid>. Accessed on: July 18, 2021.
- [7] COVID-19 Forecasting. Available: <https://www.cdc.gov/coronavirus/2019-ncov/science/forecasting/forecasting.html>. Accessed on: July 18, 2021.
- [8] COVID-19 Forecasts - Facebook Data for Good. Available: <https://dataforgood.fb.com/tools/covid-19-forecasts/>. Accessed on: July 18, 2021.
- [9] COVID-19 Projection Dashboard. Available: <https://iem-modeling.com/>. Accessed on: July 18, 2021.
- [10] DELPHI. Available: <https://delphi.cmu.edu>. Accessed on: July 18, 2021.
- [11] e3bo/random-walks. Available: <https://github.com/e3bo/random-walks>. Accessed on: July 18, 2021.
- [12] European Covid-19 Forecast Hub. Available: <https://covid19forecasthub.eu/>. Accessed on: July 18, 2021.
- [13] Exploring methods for merging mechanistic and models to forecast epidemics. Available: <https://github.com/HopkinsIDD/EpiForecastStatMech>. Accessed on: July 18, 2021.
- [14] JHUAPL-Bucky COVID-19 model. Available: <https://github.com/mattkinsey/bucky>. Accessed on: July 18, 2021.
- [15] John Hopkins Coronavirus Resource Center. Available: <https://coronavirus.jhu.edu>. Accessed on: July 18, 2021.
- [16] LANL COVID-19 Cases and Deaths Forecasts. Available: <https://covid-19.bsvgateway.org/>. Accessed on: July 18, 2021.
- [17] locknquay — Kaggle. Available: <https://www.kaggle.com/sasrdw/locknquay>. Accessed on: July 18, 2021.
- [18] Pandemic Central. Available: <https://itsonit.com>. Accessed on: July 18, 2021.
- [19] Public shared code for doing scenario forecasting and creating reports. Available: <https://github.com/HopkinsIDD/COVIDScenarioPipeline>. Accessed on: July 18, 2021.
- [20] Shaman Group. Available: <https://blogs.cuit.columbia.edu/jls106/>. Accessed on: July 18, 2021.
- [21] UCLAML Combating COVID-19. Available: <https://covid19.uclaml.org/>. Accessed on: July 18, 2021.
- [22] Historical insights on coronavirus disease 2019 (covid-19), the 1918 influenza pandemic, and racial disparities: Illuminating a path forward. *Annals of Internal Medicine*, 173(6):474–481, 2020.
- [23] S. Afzal, S. Ghani, H. C. Jenkins-Smith, D. S. Ebert, M. Hadwiger, and I. Hoteit. A visual analytics based decision making environment for covid-19 modeling and visualization. In *2020 IEEE Visualization Conference (VIS)*, pp. 86–90, 2020.
- [24] G. Arling, M. Blaser, M. Cailas, J. R. Canar, B. Cooper, P. Geraci, K. M. Osiecki, and A. Sambanis. A second wave of covid-19 in cook county: What lessons can be applied? *Online journal of public health informatics*, 12:e15, 2020.
- [25] M. Blaser, M. Cailas, J. Canar, B. Cooper, P. Geraci, K. M. Osiecki, and A. Sambanis. Analyzing covid-19 mortality within the chicagoland area, Dec 2020.
- [26] M. Blaser, M. D. Cailas, J. Canar, B. Cooper, P. Geraci, K. OSIECKI, and A. SAMBANIS. Analyzing covid-19 mortality within the chicagoland area: Data limitations and solutions. *Research Brief*, (117), 2020.
- [27] L. Breuer, J. Huisman, P. Willems, H. Bormann, A. Bronstert, B. Croke, H.-G. Frede, T. Gräff, L. Hubrechts, A. Jakeman, G. Kite, J. Lanini, G. Leavesley, D. Lettenmaier, G. Lindström, J. Seibert, M. Sivapalan, and N. Viney. Assessing the impact of land use change on hydrology by ensemble modeling (luchem). i: Model intercomparison with current land use. *Advances in Water Resources*, 32(2):129–146, 2009.
- [28] A. Diehl, L. Pelorosso, C. Delrieux, K. Matković, J. Ruiz, M. E. Gröller, and S. Bruckner. Albero: A visual analytics approach for probabilistic weather forecasting. *Comput. Graph. Forum*, 36(7):135–144, 2017.
- [29] A. Diehl, L. Pelorosso, C. Delrieux, C. Saulo, J. Ruiz, M. E. Gröller, and S. Bruckner. Visual analysis of spatio-temporal data: Applications in weather forecasting. *Comput. Graph. Forum*, 34(3):381–390, 2015.
- [30] F. Ferstl, K. Bürger, and R. Westermann. Streamline variability plots for characterizing the uncertainty in vector field ensembles. *IEEE Trans. Vis. & Comp. Graph.*, 22(1):767–776, 2016.
- [31] F. Ferstl, M. Kanzler, M. Rautenhaus, and R. Westermann. Time-hierarchical clustering and visualization of weather forecast ensembles. *IEEE Trans. Vis. & Comp. Graph.*, 23(1):831–840, January 2017.
- [32] L. Hao, C. G. Healey, and S. E. Hutchinson. Ensemble visualization for cyber situation awareness of network security data. In *2015 IEEE Symposium on Visualization for Cyber Security (VizSec)*, pp. 1–8, 2015.
- [33] E. Hatef, H.-Y. Chang, C. Kitchen, J. Weiner, and H. Kharrazi. Assessing the impact of neighborhood socioeconomic characteristics on covid-19 prevalence across seven states in the united states. *Frontiers in Public Health*, 8:554, 2020.
- [34] M. Hermann, A. C. Schunke, T. Schultz, and R. Klein. Accurate interactive visualization of large deformations and variability in biomedical image ensembles. *IEEE Trans. Vis. & Comp. Graph.*, 22(1):708–717, 2016.
- [35] J.-S. Kim, H. Kavak, A. Züflie, and T. Anderson. Covid-19 ensemble models using representative clustering. *SIGSPATIAL Special*, 12(2):33–41, 2020.
- [36] T. N. Krishnamurti, V. Kumar, A. Simon, A. Bhardwaj, T. Ghosh, and R. Ross. A review of multimodel superensemble forecasting for weather, seasonal climate, and hurricanes. *Reviews of Geophysics*, 54(2):336–377, 2016.
- [37] T. Luciani, A. Burks, C. Sugiyama, J. Komperda, and G. E. Marai. Details-first, show context, overview last: supporting exploration of viscous fingers in large-scale ensemble simulations. *IEEE Trans. Vis. & Comp. Graph.*, 25(1):1225–1235, 2018.
- [38] P. Melin, J. C. Monica, D. Sanchez, and O. Castillo. Multiple ensemble neural network models with fuzzy response aggregation for predicting covid-19 time series: The case of mexico. *Healthcare*, 8(2), 2020.
- [39] K. Mueller and E. Papenhausen. Using demographic pattern analysis to predict covid-19 fatalities on the us county level. *Digit. Gov.: Res. Pract.*, 2(1), Dec. 2020.
- [40] T. Nocke, M. Flechsig, and U. Bohm. Visual exploration and evaluation of climate-related simulation data. In *2007 Winter Simulation Conference*, pp. 703–711, 2007.
- [41] H. Obermaier, K. Bensema, and K. I. Joy. Visual trends analysis in time-varying ensembles. *IEEE Trans. Vis. & Comp. Graph.*, 22(10):2331–2342, 2016.
- [42] H. Obermaier and K. I. Joy. Future challenges for ensemble visualization. *IEEE Comp. Graph. & Applications*, 34(3):8–11, 2014.
- [43] K. Potter, A. Wilson, P.-T. Bremer, D. Williams, C. Doutriaux, V. Pasucci, and C. R. Johnson. Ensemble-vis: A framework for the statistical visualization of ensemble data. In *2009 IEEE International Conference on Data Mining Workshops*, pp. 233–240. IEEE, 2009.
- [44] E. Ray, N. Wattanachit, J. Niemi, others, and on behalf of the COVID-19 Forecast Hub Consortium. Ensemble forecasts of coronavirus disease 2019 (covid-19) in the u.s. *medRxiv*, 2020.
- [45] J. Sanyal, S. Zhang, J. Dyer, A. Mercer, P. Amburn, and R. Moorhead. Noodles: A tool for visualization of numerical weather model ensemble uncertainty. *IEEE Trans. Vis. & Comp. Graph.*, 16(6):1421–1430, 2010.
- [46] B. Schneider, D. Jäckle, F. Stoffel, A. Diehl, J. Fuchs, and D. Keim. Integrating data and model space in ensemble learning by visual analytics. *IEEE Trans. on Big Data*, 7(3):483–496, 2021.
- [47] B. Soybilgen and E. Yazgan. Nowcasting us gdp using tree-based ensemble models and dynamic factors. *Computational Economics*, 57(1):387–417, 2021.
- [48] J. Wang, S. Hazarika, C. Li, and H.-W. Shen. Visualization and visual analysis of ensemble data: A survey. *IEEE Trans. Vis. & Comp. Graph.*, 25(9):2853–2872, 2019.

# Communicating Area-level Social Determinants of Health Information: The Ohio Children's Opportunity Index Dashboards

Pallavi Jonnalagadda,<sup>1</sup> Christine Swoboda,<sup>1</sup> Priti Singh,<sup>1</sup> Harish Gureddygari,<sup>1</sup> Seth Scarborough,<sup>1</sup> Ian Dunn,  
<sup>2</sup>Nathan J. Doogan,<sup>2</sup> Naleef Fareed<sup>\* 1,3</sup>

<sup>1</sup>CATALYST, Center for the Advancement of Team Science, Analytics, and Systems Thinking in Health Services and Implementation Science Research, College of Medicine, The Ohio State University, Columbus, Ohio, USA

<sup>2</sup>The Ohio Colleges of Medicine Government Resource Center, Columbus, OH

<sup>3</sup>Biomedical Informatics, The Ohio State University, Columbus, Ohio, USA

## ABSTRACT

Social determinants of health (SDoH) can be measured at the geographic level to convey information about neighborhood deprivation. The Ohio Children's Opportunity Index (OCOI) is a multi-dimensional area-level opportunity index comprised of eight health dimensions. Our research team has documented the design, development, and use cases of dashboard solutions to visualize OCOI. The OCOI is a multi-dimensional index spanning the following eight domains or dimensions: family stability, infant health, children's health, access, education, housing, environment, and criminal justice. Information on these eight domains is derived from the American Community Survey and other administrative datasets maintained by the state of Ohio. Our team used the Tableau Desktop visualization software and applied a user-centered design approach to developing the two OCOI dashboards— main OCOI dashboard and OCOI-race dashboard. We also performed convergence analysis to visualize the census tracts, where different health indicators simultaneously exist at their worst levels. The OCOI dashboards have multiple, interactive components: a choropleth map of Ohio displaying OCOI scores for a specific census tract, graphs presenting OCOI or domain scores to compare relative positions for tracts, and a sortable table to visualize scores for specific county and census tracts. Stakeholders provided iterative feedback on dashboard design in regard to functionality, content, and aesthetics. A case study using the two dashboards for convergence analysis revealed census tracts in neighborhoods with low infant health scores and a high proportion of minority population. The OCOI dashboards could assist end-users in making decisions that tailor health care delivery and policy decision-making regarding children's health particularly in areas where multiple health indicators exist at their worst levels.

**Keywords:** Data visualization, social determinants of health, geographical information system, area level deprivation, opportunity index

**Index Terms:** Visualization techniques; Visualization systems and tools; Public Health Informatics; Health Equity

## 1 INTRODUCTION

An abundance of research acknowledges the relationship between social determinants of health (SDoH) and health outcomes.[1] Individual-level factors alone have been deemed insufficient for explaining population disease patterns, thereby raising the importance of the spatial context.[2, 3] Neighborhoods have emerged as relevant contexts as they possess physical and social attributes that could affect health.[4] The impact of neighborhood deprivation has been well established by the Whitehall-II study that showed effects of neighborhood factors on health varied by socioeconomic position.[5] Neighborhood deprivation can be communicated using area-level measures of SDoH, which are composite, and often weighted, scores of measures representing different dimensions of deprivation. Across the world, multidimensional measures of deprivation have been computed at the level of census-based geographic units,[6-10] to be used as guides for resource allocation, community advocacy, and research.[11]

The impact of neighborhood is especially pertinent for children growing up in deprived neighborhoods.[12-14] Evidence links neighborhood deprivation with health outcomes such as behavioral problems and verbal ability.[15, 16] The Moving to Opportunity Experiment underscored the role of neighborhood in children's lives by showing that moving to more affluent neighborhoods in childhood had positive impacts on college attendance and earnings.[17] Other research indicates that risk factors tend to cluster within individuals, families and communities exacerbating the inverse relationship[18] that already exists between those who need healthcare and those who have access to it.[19]

### 1.1 Significance

Ohio ranks 31<sup>st</sup> in children's health nationally. Nearly 2.6 million of the 11.5 million population in Ohio are children aged zero to 17. Of these, about 20% live in poverty, 16% are chronically absent from school, over 0.7% are homeless, and 14 – 15% have disabilities. Thirty-one percent of children and teens have been classified as overweight or obese, and nearly half (46%) the teens and children report not exercising regularly. Further, a considerable health disparity exists in self-reported health between White and Black or African American children,[20] as well as in infant mortality rates between infants born to White and Black mothers.[21] Together, these statistics indicate room for improvement in children's health across Ohio.

With the objective of improving birth outcomes in Ohio, the project sponsor collaborated with researchers at a mid-Western academic medical center (AMC) to develop area-level measures of deprivation. The high rate of and wide race disparities in infant mortality in Ohio, [21, 22] prompted the creation of the Ohio Opportunity Index (OOI) and the Ohio Children's Opportunity

---

\* Naleef.Fareed@osumc.edu

Index (OCOI). Researchers at the AMC have already successfully visualized the OOI using a dashboard solution.[23] Dashboards are powerful tools supporting public health and clinical efforts.[24, 25] They offer several advantages over traditional methods of disseminating data, such as the ability to customize data presentations per the user's interest, to more effectively convey information on trends, to facilitate evaluation of the impact of interventions on communities and subpopulations, and to provide easy access to data with an internet connection.[26] Visualizing the OCOI using dashboards can assist policymakers, public health officials, and health care leaders in making decisions for better health care delivery to improve children's health. To this end, we developed two functional and interactive dashboards with training material in the form of instructional videos and user guides to analyze the distribution of the OCOI.

## 1.2 Objective

First, we describe the creation of the main OCOI dashboard bearing in mind two use cases: the project sponsor and community-based organizations using the dashboard to plan or deliver interventions and health care programs. Second, we describe the creation of another OCOI dashboard, that displays the race/ethnic distribution in census tracts across Ohio. Lastly, we provide a case study of how the two OCOI dashboards can be used to perform convergence analysis to visualize factors associated with children's health outcomes in combination with data on infant mortality rates in Ohio from the Ohio Department of Health.

## 2 METHODS

Our approach to developing and deploying the OCOI dashboard followed the principles of user-centered design, which involved constant engagement with subject matter experts and stakeholders represented by end-users from the project sponsors. This project is an extension of the Infant Mortality Research Project that was set up to improve birth outcomes in Ohio. Researchers at the AMC compiled the pertinent data and constructed the OCOI first by standardizing the measures, calculating domain scores, and finally calculating an index score. [27] The OCOI is constructed at the census tract level. Higher opportunity scores indicate relatively higher opportunity or lower deprivation. Similarly, lower opportunity scores indicate relatively lower opportunity or higher deprivation. The OCOI dashboards in their current form are intended for project-affiliated researchers and sponsors, and are therefore password protected on an online server. The stakeholders intend to release public versions in the future.

### 2.1 Data Sources

Census tracts were chosen as the geographical unit for data collection because they are uniform in terms of geography and socioeconomic characteristics, thus serving as proxies for neighborhood and individual-level SDoH measures. Of the 2952 census tracts in Ohio, 12 had zero population. Therefore, study data pertaining to the 2940 census tracts were collected from various sources including, but not limited to, the U.S. census based-American Community Survey (ACS) data set, which is a freely available resource, and other state level agency administrative data sets (e.g., Medicaid claims and Department of Education school report card data). Information was compiled from these sources based on census tracts for the creation of the OCOI. Finally, datasets corresponding to two different time periods, Period I (2010 – 2014) and Period II (2013 – 2017), were collated for developing OCOIs for each time period. [27] We used ACS data aggregated over two five-year periods 2010 – 2014 and 2013 – 2017 to obtain the race/ethnic distribution across census tracts in the state of Ohio. Our study visualized the percentage of White individuals, the

percentage of Black or African American individuals, the percentage of Hispanic individuals, and the percentage of minority individuals in the state of Ohio.

## 2.2 Domains and Measures

Outcomes related to the well-being of children depend on the economic, material, and psychosocial conditions in which they grow. These socioeconomic conditions relate to their parents or caregivers, housing units and the neighborhood in which they live.[28] Guided by these findings, the study team, with the help of subject matter experts outlined domains to develop the OCOI. Several iterations later, a set of eight domains were finalized for use: *family stability, infant health, children's health, access (to health care and food), education, housing, environment, and criminal justice.* [27] These domains are consistent with the SDoH attributes the Centers for Disease Control and Prevention has identified, such as food supply, housing, transportation, education, and health care, thus substantiating their use in our study.[29, 30] The OCOI is composed of eight equally-weighted domains. Each of the eight domains was measured by multiple variables also referred to as constituent measures. A total of 53 variables were proposed for use, however information on only 37 variables was available for Period I. As a result, for the purpose of comparison, the Period II dataset was treated in two ways; Period II (Reduced) comprising the same 37 variables as in Period I (Reduced) and Period II (Complete) with all 53 variables. Consequently, three datasets: Period I (Reduced), Period II (Reduced), and Period II (Complete) were used for study analyses. Additionally, a fourth dataset captured the differences between Period I (Reduced) and Period II (Reduced) measures, referred to as the "Change" dataset to illustrate shifts in area-level SDoH over time. Appendix table 1 presents a summary of the domains, associated variables, description of variables, data sources, and availability by time period. Of the 53 variables, the family stability domain comprised five, infant health comprised seven, children's health comprised eight, access domain seven, education comprised eight, housing comprised seven, environment comprised six, and the criminal justice domain comprised five. Some responses were reverse coded to maintain a consistent direction with respect to what higher (deprivation) versus lower (opportunity) values meant. [27] Seminal studies [31, 32] informed the stepwise, co-creation approach used to construct the OCOI. The details of constructing the OCOI are available elsewhere. [27] We tested the OCOI for association with health-related outcomes including death rate and life expectancy, which have been linked to area-level deprivation. [30] Results indicated that tracts with high OCOI have significantly lower ( $p < 0.001$ ) death rates and significantly higher ( $p < 0.001$ ) life expectancy compared to tracts with low OCOI, suggesting that the OCOI is a valid measure of area-level SDoH. [27]

## 2.3 Dashboard Structure

Our team previously developed a dashboard solution that visualized OOI information and its domains across all census tracts in the state of Ohio, displayed score plots allowing for comparison of constituent measure scores across tracts, included a sortable table to display OOI scores, and had interactive features so they would be updated whenever a user selected certain parameters.<sup>23</sup> The project sponsors requisitioned a similar dashboard for the OCOI with three additional requirements: first, visualization of change in OCOI based on data aggregated between 2010 – 2014 and 2013 – 2017; second, grouping of census tracts into ZIP codes, neighborhoods, and cities as end users tend to be more familiar with places in these terms rather than census tract numbers; and third, the creation of an additional dashboard to visualize OCOI and the race/ethnic distribution of the Ohio population.

Leveraging prior end user feedback for the OOI dashboard, the five components of the OCOI dashboard were: 1. Choropleth map of Ohio with OCOI scores for specific census tracts; 2. Plots of OCOI and/or individual domain scores to compare relative positions for census tracts; 3. A sortable table to view OCOI or individual domain scores for specific census tracts; 4. Information available from four data sources for users to select: the reduced data compiled over two different time periods 2010 – 2014 and 2013 – 2017, complete data compiled from 2013 – 2017, change in OCOI and the individual domain scores between 2010 – 2014 and 2013 – 2017 based on the reduced dataset; 5. A neighborhood filter so end users can filter census tracts corresponding to familiar geographies like cities, neighborhoods or ZIP codes.

To permit visualization of the OCOI and area-level race/ethnic distribution in Ohio, we created the OCOI-Race dashboard retaining the choropleth map of Ohio, choice of data sources, and the neighborhood filter from the main OCOI dashboard. New additions included a menu with options to visualize the race /ethnic distribution; a scatter plot with OCOI and domain scores on the X-axis and the frequency of the race/ethnic distribution factor on the Y-axis; as well as the categorization of the OCOI score and the race/ethnic distribution into four discrete categories. This OCOI-race dashboard can be adapted in the future to display information about other area-level indicators.

Project sponsors required the use of Tableau for constructing the dashboard. The dashboard was subsequently deployed to a secure Tableau Server environment. Tableau offers notable strengths over commonly used statistical software packages such as SAS and STATA. Tableau uses VizQL, a visual query language that converts drag-and-drop actions into queries. The visualization team used Tableau Desktop to first connect to a data set (stored in files, warehouses, and the cloud), and then used a front-end interface to query the data and view it in different graphical forms (charts, graphs, maps). Independent worksheets containing specific visuals were compiled to create dashboards to communicate key insights. The visuals were further linked together by the creation of filters, parameters, and actions so the dashboard displayed information as directed by user actions. Another advantage of Tableau is its ability to automatically recognize various geographical fields, like state, county, and ZIP code, to generate the corresponding latitude and longitude coordinates. We imported shapefiles of Ohio that had vector data for the latitude and longitude for each census tract, county, and neighborhood in Ohio. The data file with information on the measures to construct the OCOI and the shapefiles were linked using the Federal Information Processing Standard code as the primary key.

### 3 RESULTS

Our team applied project sponsor feedback on the OOI dashboard pertaining to content, aesthetics, and function to the OCOI dashboard (Figure 1).[23] Briefly, in terms of content, the OCOI like the OOI is a score of opportunity and not deprivation for easier interpretation and a positive connotation. Second, the scores are visualized as septile groups on a choropleth map of Ohio to provide adequate contrast between OCOI scores. Third, we displayed the actual OCOI values on the Y-axis of the distribution plot to facilitate easier interpretation of the distribution of OCOI scores across census tracts. Further, we included a breakdown of the domain scores in the score plot as standard deviations from the mean for every census tract, which facilitates comparison between selected tracts. In regard to aesthetics, we retained the divergent color scheme for the heat map approved for the OOI dashboard. Similarly, the score plot is presented as a bar graph rather than a line plot to effectively communicate scores across domains or domain variables.

In terms of dashboard function, we displayed street and highway patterns to better orient the end users to the communities within a census tract. Further, users could select a county from a drop-down list to assess census tracts within a specific county. We also incorporated information icons by each component to aid the end user. To address one of the sponsor requirements, we visualized change in OCOI score based on aggregate data between 2010 – 2014 and 2013 – 2017. When users visualize change in OCOI, the distribution plot shows a distribution of income adjusted differences in OCOI and absolute differences for the domains. The score plot displays absolute changes for OCOI domains and Z-scores for constituent measures (Figure 2). In terms of aesthetics, we ensured that the size of the map was sufficiently large to facilitate zooming in on a specific county.

The project sponsor additionally requested for the visualization of OCOI and the area -level race/ethnic distribution of the Ohio population to examine disparities in health outcomes at the intersection of race and SDoH. To fulfill this second requirement, we again engaged in iterative feedback from the sponsors. Appendix table 2 summarizes the modifications we made in response to feedback on the initial prototype. Continuous improvements were made to the dashboard throughout this project, but there is still a learning curve for those unfamiliar with data visualization tools. Therefore, we created training videos and user guides to help users understand the basic functions of Tableau along with the displayed features of the OCOI.

#### 3.1 Case Study

We present a case study where a health program manager in Columbus, Ohio seeks to gain a better understanding of children's opportunity in the counties across Ohio that have high infant mortality and high disparity in infant mortality between infants born to White and Black mothers. The health program manager has to strategically allocate resources to the Columbus area and wants to optimize them by identifying areas that have the lowest infant health scores and highest infant mortality rates.

Using the main OCOI dashboard, the program manager selects Franklin County in Ohio and examines the Columbus area. They first examine the OCOI and its domains and note the 10 tracts with the lowest scores for all the domains (Figure 1a). Because this program is targeting infant health disparities, they then examine the infant health domain. After looking at the 10 worst tracts for infant health, it is noted that many census tracts scoring low for infant health do not have significantly lower infant mortality, but their scores are low because of neonatal abstinence syndrome, maternal morbidity, Neonatal Intensive Care Unit (NICU) stays, or other factors (Figure 1b). Finally, in the score plot, the official clicks to keep only infant mortality to find the worst scoring tracts for infant mortality (Figure 3a). They highlight the 25 worst ranked infant health scores in the table, and look at the score plot (Figure 3b). They find that the two worst tracts for infant mortality, 049001400, and 049007511, are both in the South Linden area (Figure 4a).

The program manager decides to further examine the two lowest-scoring tracts (049001400, and 049007511), which also score poorly for preterm birth, but not on the other sub-domains of infant health. Both tracts are in the lowest quantile of overall OCOI score, criminal justice, and education, and score poorly in regard to the sub-domains like food access, asthma, free lunch access, high school graduation rates, reading ability, amount of green area, air quality, tobacco exposure, paternal involvement, poverty, crowding, evictions, and percentage renting. The health program manager examines the race/ethnic makeup of the census tracts using the OCOI-Race dashboard. Both the census tracts have low opportunity scores and over 75% minority population (Figure 4b). The health program manager decides to direct infant mortality prevention resources towards community-based organizations and

public health programs in the South Linden area. Programs should be prepared to provide referrals for help in access to food, educational resources, social services, drug and tobacco cessation, and housing.

#### 4 DISCUSSION

The OCOI dashboard visually summarizes and communicates quantitative information about SDoH through 53 measures organized into eight domains, showing opportunity for infants and children in the state of Ohio. This representation of SDoH can help characterize individual census tracts throughout the state and help policy makers, practitioners, and researchers assess their level of need.

Other national geographic indices displaying child health or economic opportunity are available. The Opportunity Atlas shows the average outcomes in adulthood for people based on where they grew up with a greater focus on economic opportunity than health.[33] Another index, the Child Opportunity Index 2.0, comprises 29 indicators grouped into three domains (education, health and environment, social and economic), available for all US neighborhoods at the census tract level for the years 2010 and 2015.[34] Unlike the OCOI, the COI 2.0 has a national focus, the indicators used to construct the COI have varying weights, the environment domain includes toxic exposures like proximity to hazardous waste dump sites, and there is no separate criminal justice domain.

Potential limitations exist to using and sharing area-level SDoH measures like the OCOI. This dashboard reflects average neighborhood measures, but does not describe individuals within neighborhoods; researchers and policymakers should remain sensitive to people within these communities and avoid negative characterizations. In addition, because these are neighborhood averages, there are still individuals in high opportunity areas who may need assistance in certain domains. The intention of tools like the OCOI is to help communities in need, but there is risk of decisions being made that negatively affect communities, such as companies choosing to purposely relocate from low opportunity areas to serve high opportunity areas. Finally, indices like the OCOI may impact rural and urban areas in different ways, [35] and policymakers should take the individual variables into account when developing interventions instead of attempting a one-size-fits-all approach for low domain scores.

Future use of the OCOI include monitoring change in neighborhood opportunity over time. Positive changes in opportunity in specific census tracts may point to improvements due to public health support, the actions of community programs, and movement of people and businesses to an area. Alternatively, decreases in opportunity due to crime, loss in property value, movement of residents, and closing of businesses, schools, and public buildings will also be reflected. Changes in SDoH may predict changes in health outcomes in an area. Researchers will be able to use the OCOI to study potential relationships between specific SDoH and infant and child health outcomes, further adding to public health knowledge about area-level predictors of health. Renewed focus on the “place” effect on health has shifted the conversation to innovation in health care delivery and collaboration between healthcare organizations, public health, and social services.

#### 5 CONCLUSION

The communication of OCOI through dashboard tools presents an opportunity to help increase awareness about pressing SDoH-related challenges faced by infants and children, with potential immediate and long-term implications for their development and health. The dashboards facilitate analysis of information from multiple perspectives. Users of the dashboards can make informed

decisions about allocating resources to individuals and their communities in order to ameliorate disparities in health care, with the goal of increasing health equity.

The OCOI may have applications in clinical practice by serving as a proxy for individual-level SDoH as is being increasingly advocated.[36, 37] Even though universal and comprehensive screening for SDoH during the clinical encounter is still debated [38], area-level measures of SDoH, like the OCOI, represent a rich resource of readily-available data that may be incorporated into electronic health records (EHR) and may be used to improve health care delivery. Compiling a more complete picture of patients’ neighborhood risk can help healthcare providers assist patients in a more tailored manner.

#### REFERENCES

- [1] P. Braveman, S. Egarter, and D. R. Williams, "The social determinants of health: coming of age," *Annu Rev Public Health*, vol. 32, pp. 381-398, 2011 2011, doi: 10.1146/annurevpublhealth-031210-101218.
- [2] A. V. Diez-Roux, "Bringing context back into epidemiology: variables and fallacies in multilevel analysis," *Am J Public Health*, vol. 88, no. 2, pp. 216-222, 1998/02/01 1998, doi: 10.2105/AJPH.88.2.216.
- [3] T. A. Blakely and A. J. Woodward, "Ecological effects in multi-level studies," (in eng), *Journal of epidemiology and community health*, vol. 54, no. 5, pp. 367-374, 2000, doi: 10.1136/jech.54.5.367.
- [4] A. V. Diez Roux, "Neighborhoods and health: where are we and were do we go from here?," *Rev Epidemiol Sante Publique*, vol. 55, no. 1, pp. 13-21, 2007/02// 2007, doi: 10.1016/j.respe.2006.12.003.
- [5] M. Stafford and M. Marmot, "Neighbourhood deprivation and health: does it affect us all equally?," *Int J Epidemiol*, vol. 32, no. 3, pp. 357-366, 2003/06// 2003, doi: 10.1093/ije/dyg084.
- [6] J. Atkinson, C. Salmond, and P. Crampton, "NZDep2013 index of deprivation," *Wellington: Department of Public Health, University of Otago*, 2014.
- [7] D. McLennan, S. Noble, M. Noble, E. Plunkett, G. Wright, and N. Gutacker, "The English Indices of Deprivation 2019: technical report," 2019.
- [8] G. K. Singh, "Area deprivation and widening inequalities in US mortality, 1969-1998," *Am J Public Health*, vol. 93, no. 7, pp. 1137-1143, 2003/07// 2003, doi: 10.2105/ajph.93.7.1137.
- [9] A. J. H. Kind and W. R. Buckingham, "Making Neighborhood-Disadvantage Metrics Accessible - The Neighborhood Atlas," *N Engl J Med*, vol. 378, no. 26, pp. 2456-2458, 2018/06/28/ 2018, doi: 10.1056/NEJMp1802313.
- [10] "Social Vulnerability Index." Centers for Disease Control and Prevention. <https://svi.cdc.gov/> (accessed).
- [11] R. L. Phillips *et al.*, "How Other Countries Use Deprivation Indices—And Why The United States Desperately Needs One," *Health Affairs*, vol. 35, no. 11, pp. 1991-1998, 2016, doi: 10.1377/hlthaff.2016.0709.
- [12] J. L. A. and, N. G. Bennett, D. C. Conley, and J. Li, "The Effects of Poverty on Child Health and Development," *Annual Review of Public Health*, vol. 18, no. 1, pp. 463-483, 1997, doi: 10.1146/annurev.publhealth.18.1.463.
- [13] J. Brooks-Gunn and G. J. Duncan, "The Effects of Poverty on Children," *The Future of Children*, vol. 7, no. 2, pp. 55-71, 1997, doi: 10.2307/1602387.
- [14] K. Larson and N. Halfon, "Family Income Gradients in the Health and Health Care Access of US Children," *Maternal and Child Health Journal*, vol. 14, no. 3, pp. 332-342, 2010/05/01 2010, doi: 10.1007/s10995-009-0477-y.
- [15] M. O. Caughy, S. M. Nettles, and P. J. O'Campo, "The effect of residential neighborhood on child behavior problems in first grade," (in eng), *Am J Community Psychol*, vol. 42, no. 1-2, pp. 39-50, Sep 2008, doi: 10.1007/s10464-008-9185-9.

- [16] R. J. Sampson, P. Sharkey, and S. W. Raudenbush, "Durable effects of concentrated disadvantage on verbal ability among African-American children," *Proceedings of the National Academy of Sciences*, vol. 105, no. 3, p. 845, 2008, doi: 10.1073/pnas.0710189104.
- [17] R. Chetty, N. Hendren, and L. F. Katz, "The Effects of Exposure to Better Neighborhoods on Children: New Evidence from the Moving to Opportunity Experiment," *American Economic Review*, vol. 106, no. 4, pp. 855-902, 2016, doi: 10.1257/aer.20150572.
- [18] J. Tudor Hart, "THE INVERSE CARE LAW," *The Lancet*, vol. 297, no. 7696, pp. 405-412, 1971/02/27/ 1971, doi: [https://doi.org/10.1016/S0140-6736\(71\)92410-X](https://doi.org/10.1016/S0140-6736(71)92410-X).
- [19] K. Fiscella and P. Shin, "The Inverse Care Law: Implications for Healthcare of Vulnerable Populations," *The Journal of Ambulatory Care Management*, vol. 28, no. 4, pp. 304-312, 2005. [Online]. Available: [https://journals.lww.com/ambulatorycaremanagement/Fulltext/2005/1000/The\\_Inverse\\_Care\\_Law\\_Implications\\_for\\_Healthcare.5.aspx](https://journals.lww.com/ambulatorycaremanagement/Fulltext/2005/1000/The_Inverse_Care_Law_Implications_for_Healthcare.5.aspx).
- [20] D. C. KIDS COUNT. Selected Indicators for Ohio [Online]. Available: <https://datacenter.kidscount.org/data/customreports/37/any>
- [21] Ohio Department of Health. "2017 Infant Mortality Report." <https://odh.ohio.gov/wps/wcm/connect/gov/5b43b42b-0733-42cd-8a01-063f831ec53f/2017+Ohio+Infant+Mortality+Report.pdf> (accessed).
- [22] Centers for Disease Control and Prevention. "Infant Mortality Rates by States." [https://www.cdc.gov/nchs/pressroom/sosmap/infant\\_mortality\\_rates/infant\\_mortality.htm](https://www.cdc.gov/nchs/pressroom/sosmap/infant_mortality_rates/infant_mortality.htm) (accessed).
- [23] N. Fareed, C. M. Swoboda, P. Jonnalagadda, T. Griesenbrock, H. R. Gureddygari, and A. Aldrich, "Visualizing Opportunity Index Data Using a Dashboard Application: A Tool to Communicate Infant Mortality based Area Deprivation Index Information.," *Applied Clinical Informatics*, 2020, doi: <https://doi.org/10.1055/s-0040-1714249>.
- [24] A. Joshi, C. Amadi, B. Katz, S. Kulkarni, and D. Nash, "A Human-Centered Platform for HIV Infection Reduction in New York: Development and Usage Analysis of the Ending the Epidemic (ETE) Dashboard," *JMIR Public Health Surveill*, vol. 3, no. 4, p. e95, 2017/12/11 2017, doi: 10.2196/publichealth.8312.
- [25] D. Dowding *et al.*, "Dashboards for improving patient care: Review of the literature," *International Journal of Medical Informatics*, vol. 84, no. 2, pp. 87-100, 2015/02/01/ 2015, doi: <https://doi.org/10.1016/j.ijimedinf.2014.10.001>.
- [26] D. Nash, "Designing and Disseminating Metrics to Support Jurisdictional Efforts to End the Public Health Threat Posed by HIV Epidemics," *Am J Public Health*, vol. 110, no. 1, pp. 53-57, 2020/01/01 2019, doi: 10.2105/AJPH.2019.305398.
- [27] N. Fareed, P. Singh, P. Jonnalagadda, C. M. Swoboda, C. Odden, and N. Doogan, "Construction and Validation of the Ohio Children's Opportunity Index," *medRxiv*, p. 2021.05.12.21257062, 2021, doi: 10.1101/2021.05.12.21257062.
- [28] A. Pearce, R. Dundas, M. Whitehead, and D. Taylor-Robinson, "Pathways to inequalities in child health," *Archives of Disease in Childhood*, vol. 104, no. 10, p. 998, 2019, doi: 10.1136/archdischild-2018-314808.
- [29] V. H. National Center for HIV/AIDS, STD, and TB Prevention. "Social Determinants of Health." CDC. <https://www.cdc.gov/nchstp/socialdeterminants/faq.html> (accessed).
- [30] R. Seaman, T. Riffe, A. H. Leyland, F. Popham, and A. van Raalte, "The increasing lifespan variation gradient by area-level deprivation: A decomposition analysis of Scotland 1981–2011," *Social Science & Medicine*, vol. 230, pp. 147-157, 2019/06/01/ 2019, doi: <https://doi.org/10.1016/j.socscimed.2019.04.008>.
- [31] M. Noble, G. Wright, G. Smith, and C. Dibben, "Measuring multiple deprivation at the small-area level," *Environ. Plann. A*, vol. 38, no. 1, pp. 169-185, 2006 2006, doi: 10.1068/a37168.
- [32] D. J. Exeter, J. Zhao, S. Crengle, A. Lee, and M. Browne, "The New Zealand Indices of Multiple Deprivation (IMD): A new suite of indicators for social and health research in Aotearoa, New Zealand," *PLOS ONE*, vol. 12, no. 8, p. e0181260, 2017, doi: 10.1371/journal.pone.0181260.
- [33] R. Chetty, J. Friedman, N. Hendren, M. R. Jones, and S. Porter, "The Opportunity Atlas: Mapping the Childhood Roots of Social Mobility," ed, 2018
- [34] C. Noelke *et al.*, "The Child Opportunity Index 2.0," 2019.
- [35] D. Fecht *et al.*, "Inequalities in rural communities: adapting national deprivation indices for rural settings," *Journal of Public Health*, vol. 40, no. 2, pp. 419-425, 2018, doi: 10.1093/pubmed/fdx048.
- [36] P. Jonnalagadda, C. M. Swoboda, and N. Fareed, "Using area-level measures of social determinants of health to deliver improved and effective health care," *Journal of Hospital Management and Health Policy*, vol. 4, 2020. [Online]. Available: <https://jhmhp.amegroups.com/article/view/6527>.
- [37] A. W. Bazemore *et al.*, "'Community vital signs': incorporating geocoded social determinants into electronic records to promote patient and population health," *Journal of the American Medical Informatics Association*, vol. 23, no. 2, pp. 407-412, 2015, doi: 10.1093/jamia/ocv088.
- [38] A. Garg, R. Boynton-Jarrett, and P. H. Dworkin, "Avoiding the Unintended Consequences of Screening for Social Determinants of Health," *JAMA*, vol. 316, no. 8, pp. 813-814, 2016, doi: 10.1001/jama.2016.9282.
- [39] N. J. Doogan, M. E. Roberts, M. E. Wewers, E. R. Tanenbaum, E. A. Mumford, and F. A. Stillman, "Validation of a new continuous geographic isolation scale: A tool for rural health disparities research," *Social Science & Medicine*, vol. 215, pp. 123-132, 2018/10/01/ 2018, doi: <https://doi.org/10.1016/j.socscimed.2018.09.005>.
- [40] M. L. Burgoon *et al.*, "Exposures to the tobacco retail environment among adolescent boys in urban and rural environments," (in eng), *Am J Drug Alcohol Abuse*, vol. 45, no. 2, pp. 217-226, 2019, doi: 10.1080/00952990.2018.1549562.

**APPENDIX**
**Table 1 Description of domain and variables used in OCOI construction**

<b>Domain</b>	<b>Measure Descriptions</b>	<b>Data Source</b>	<b>Time Period(s)</b>
Family Stability	1) Proportion of parents enrolled in Medicaid with a primary SMI diagnosis	Medicaid Admin	Both
	2) Proportion of children living in a household with below-poverty income	ACS	Both
	3) Proportion of births that include no father's first/middle/last name	VS births	Both
	4) Proportion of families with a parent served by Medicaid who has an SUD diagnosis	Medicaid Admin	Both
	5) Labor Market Engagement Index (HUD)(reversed)	HUD	2013 – 2017
Infant Health	1) Proportion of births that resulted in an infant mortality	VS Births, Deaths	Both
	2) Proportion of Medicaid infants who had an injury or poisoning in the first year of life	Medicaid Admin	Both
	3) Medicaid-enrolled infants with neonatal abstinence syndrome	Medicaid Admin	Both
	4) Medicaid-enrolled infants with NICU stay	Medicaid Admin	Both
	5) Proportion of infants born preterm	VS Births	Both
	6) Medicaid children with six or more well-child visits in first 15 months of life (reversed)	Medicaid Admin	Both
	7) Proportion of infants born to Medicaid-enrolled women with severe maternal morbidity	Medicaid Admin	Both
Children's Health (non-infant)	1) Proportion of Medicaid-enrolled children ages 1-5 with a diagnosis of developmental delay including sight and hearing impairment	Medicaid Admin	Both
	2) Proportion of Medicaid children age 3-6 meeting continuous enrollment criteria with one or more well-child visits with a PCP (reversed)	Medicaid Admin	Both
	3) Proportion of Medicaid-enrolled children ages 6-17 with a diagnosis of asthma	Medicaid Admin	Both
	4) Proportion of Medicaid-enrolled children ages 6-17 with a diagnosis of mental illness	Medicaid Admin	Both
	5) Proportion of Medicaid enrolled children ages 6-17 with a diagnosis of a developmental disability	Medicaid Admin	Both
	6) Proportion of Medicaid enrolled children ages 6-17 with a diagnosis of diabetes	Medicaid Admin	Both
	7) Proportion of Medicaid enrolled children ages 6-17 who received psychotropic BH medication	Medicaid Admin	Both
	8) Proportion of Medicaid-enrolled children ages 6-17 with a diagnosis of obesity	Medicaid Admin	2013 – 2017
Access	1) Proportion of Medicaid behavioral health visits for children that meet the access standards of CMS (reversed)	Medicaid Admin	Both
	2) Proportion of primary care visits for children that meet the access standards (driving time, driving distance) of CMS (reversed)	Medicaid Admin	Both
	3) Geographic isolation (rurality) of the Census tract	Doogan et al.,2018 [39]	Both
	4) Low Transportation Cost Index	HUD	2013 – 2017
	5) Percent occupied housing units in tract without a vehicle	ACS	2013 – 2017
	6) Percent tract population within a distance from the supermarket	USDA-ERS	2013 - 2017
	7) Distance to nearest elementary school	CURA	2013 – 2017
Education	1) Percent youth who have dropped out	ACS	Both
	2) Percent of adults in the tract with more than high school education	ACS	Both
	3) Percent of youth (age 5-17) not enrolled in school	ACS	Both
	4) Proportion of children not meeting third grade reading standards	ACS	2013 – 2017
	5) Free lunch distribution (reversed)	ACS	2013 – 2017
	6) Graduation rate (reversed)	ACS	2013 – 2017

	7) School performance index (reversed)	ODE	2013 – 2017
	8) School's value-added score (reversed)	ODE	2013 – 2017
Housing	1) Percentage putting 50 percent of income towards mortgage	ACS	Both
	2) Percentage of households with less than one person per room	ACS	Both
	3) Percentage putting 50 percent of income towards rent	ACS	Both
	4) Percent housing identified as vacant	ACS	Both
	5) Percent renting	ACS	2013 – 2017
	6) Percentage living in same housing unit for less than one year	ACS	2013 – 2017
	7) Rate of evictions among renters	Eviction lab	Both
Environment	1) Tract land area <i>not</i> covered by vegetation	NHGIS	Both
	2) Tract land area covered by open development (e.g., pavement, parking)	NHGIS	Both
	3) Percent of housing units constructed prior to 1980	ACS	2013 – 2017
	4) Annual average of daily pm25 measurements	EPA	Both
	5) Count of tobacco retail outlets within a 3/4 <sup>th</sup> mile buffered tract boundary	Burgoon et al., 2019 [40]	2013 – 2017
	6) Environmental Health Hazard Index (air quality)	HUD	2013 – 2017
Criminal Justice	1) Average number of homicide, assault, and sexual assault incidents per person reported to police each year during the period 2017-2018	OIBRS	Both
	2) The average number of robbery incidents per person reported to police each year during the period 2017-2018	OIBRS	Both
	3) The average number of burglary, larceny-theft, and motor-vehicle theft incidents per person reported to police each year during the period 2017-2018	OIBRS	Both
	4) The average number of drunkenness and driving under the influence incidents per person reported to police each year during the period 2017-2018	OIBRS	Both
	5) The average number of drug crime incidents per person reported to police each year during the period 2017-2018	OIBRS	Both

Note: SMI=Severe Mental Illness; ACS=American Community Survey; VS= Vital statistics; SUD= Substance use disorder; HUD= Housing and Urban Development; NICU=Neonatal intensive care unit; PCP=Primary care physician; BH=Behavioral Health; USDA\_ERS= U.S Department of Agriculture-Economic Research Service; CMS=Center for Medicare and Medicaid services; CURA=Center for Urban and Regional Analysis; ODE=Ohio Department of Education; EPA= Environmental Protection Agency; NHIGS= National Historical Geographic Information System; OIBRS= Ohio Incident Based Reporting System.

**Table 2** Modifications to OCOI dashboard based on sponsor feedback

Modification	Rationale
<b>Content</b>	
Creation of four categories for each race/ethnic group. These were 0% to 25%, 25 – 50%, 50 – 75%, and > 75%.	Using quantiles to create categories for race/ethnic group gave rise to very skewed categories. Therefore, the categories requested by the sponsor were created.
Switch from septile to quartile groups of the OOI score to use in the state-level heat map.	Using septile groups gave rise to too many categories and was visually busy. It was therefore decided that the quartile distribution was easier for interpretation.
Scatterplot of OCOI and its domain scores with the X-axis showing the OCOI scores and the Y-axis showing the frequency of the SDoh factor	The scatterplot allows the end users to see the scores for all census tracts at a glance. Each census tract is represented as a circle, which when selected highlights the census tract on the map
Discrete categories represented as tiles showing 16 combinations of the four COI categories and the four SDoh factors and the number of census tracts with each combination	End users can at a glance see how many tracts have low opportunity and how many have high opportunity based on the race/ethnic distribution of the census tract.
<b>Function</b>	

Selection of county results by filtering dashboard content to only the census tracts within that county.	This helped the end users specifically assess the census tracts within a county of interest.
Selection of neighborhood results by filtering dashboard content to census tracts within a city, neighborhood, or township	This helped end users find census tracts by specifying geographies that were more familiar to them such as the neighborhood, city, township, or zip codes
Provide an information icon by each component to help the end user understand it.	Provide end users with a conveniently located icon to quickly understand what the information a specific component can provide them, such as the source of the data.
Display street and highway patterns.	Allow end users to get a better sense of the communities present within a census tract by locating them using streets and highways.
<b>Aesthetics</b>	
Use a divergent color scheme for the heat map.	Attempts to preserve the color scheme used on the main dashboard proved inefficient because the original dashboard used three colors and the need was for four colors in the OCOI dashboard with other area-level indicators. We used shades of blue, orange, purple, and green. We avoided using certain shades of red and green to minimize the probability that end users would have trouble perceiving the colors.
Linking the color-coded tiles and the circles on the scatter plot	End users can select any combination of OCOI and area-level indicator of interest. This selection unselects all other census tracts from the scatter plot and at the same time highlights the census tracts in that particular category on the map. Alternatively, users can select any circle on the scatterplot and the selected tract is highlighted on the map and the color-coded tile that it corresponds to is highlighted as well.

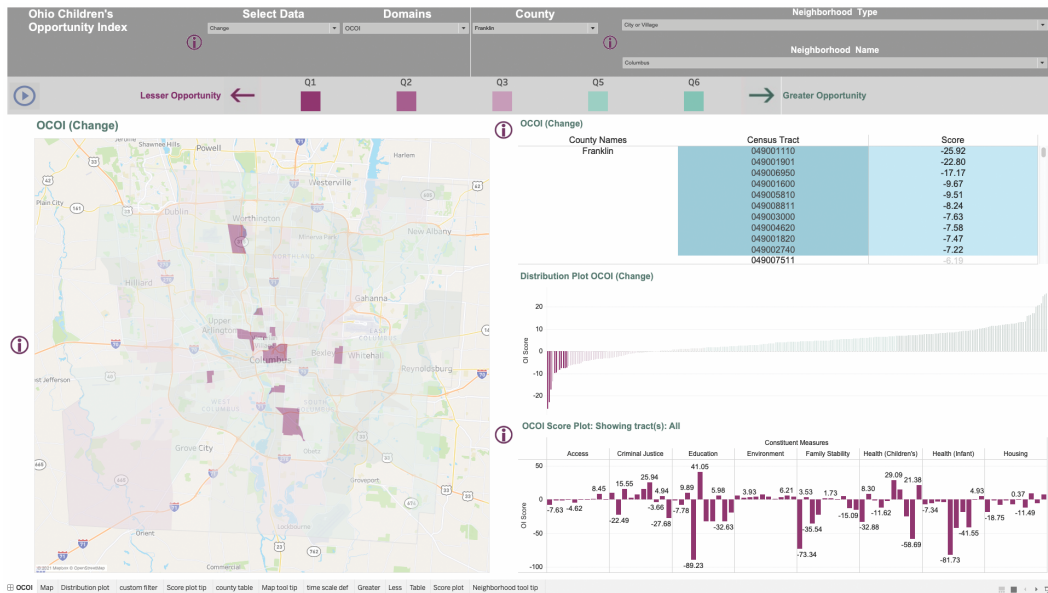


**Figure 1** Ten lowest ranked census tracts in terms of OCOI and Infant Health in Columbus, Ohio. Panel A shows the ten lowest ranked census tracts in terms of OCOI in Columbus, Ohio. Panel B shows the ten census tracts with lowest OCOI in Columbus, Ohio in terms of the Infant Health domain and subdomains of Infant Health

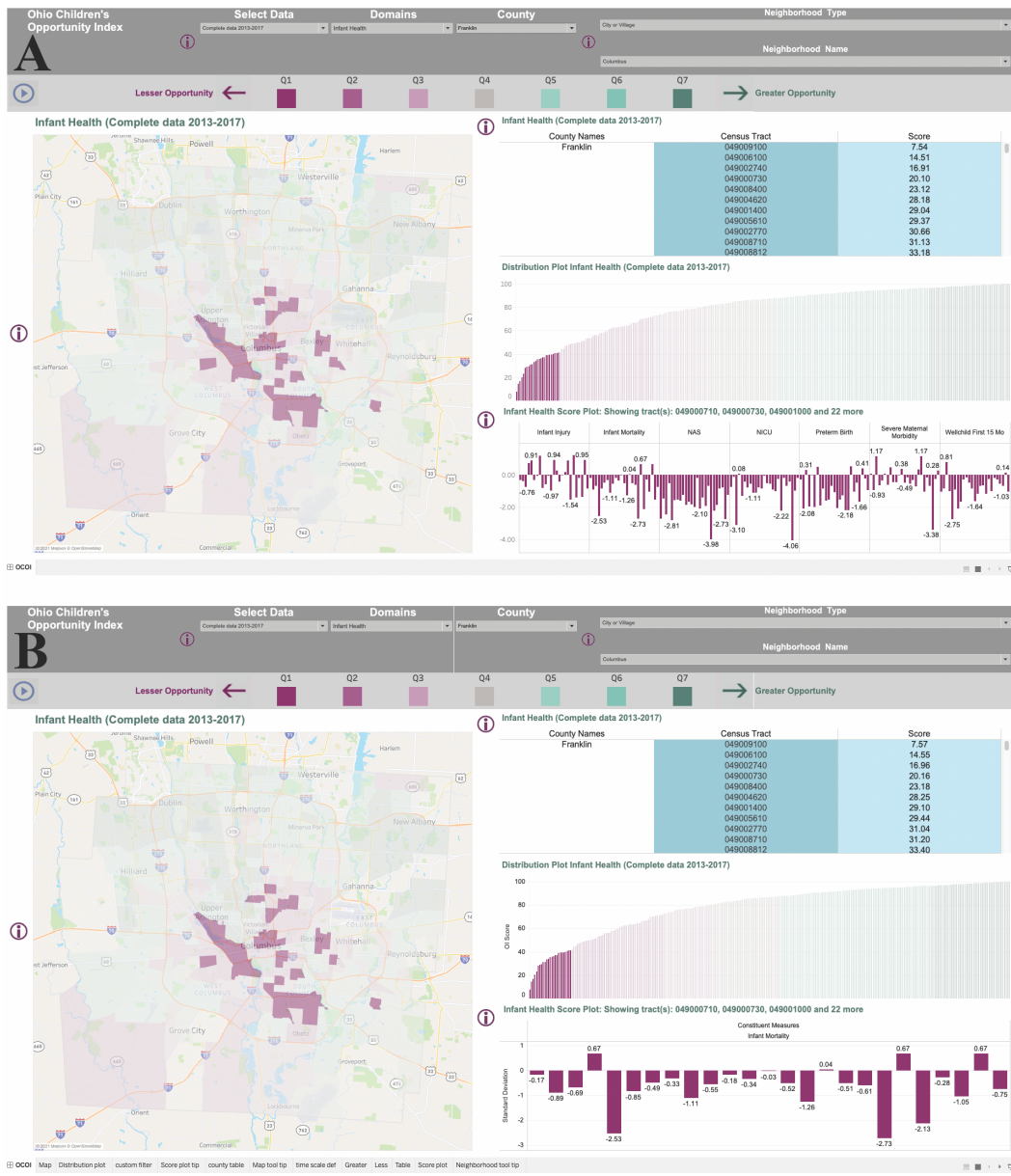


**Figure 2** Ten census tracts in Columbus, OH with the most negative change in OCOI

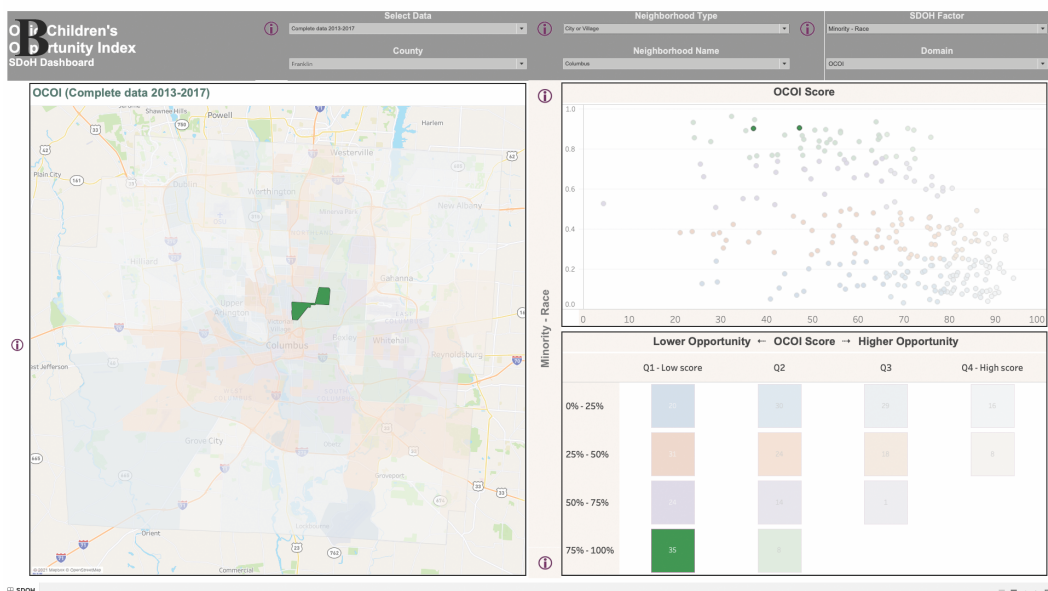
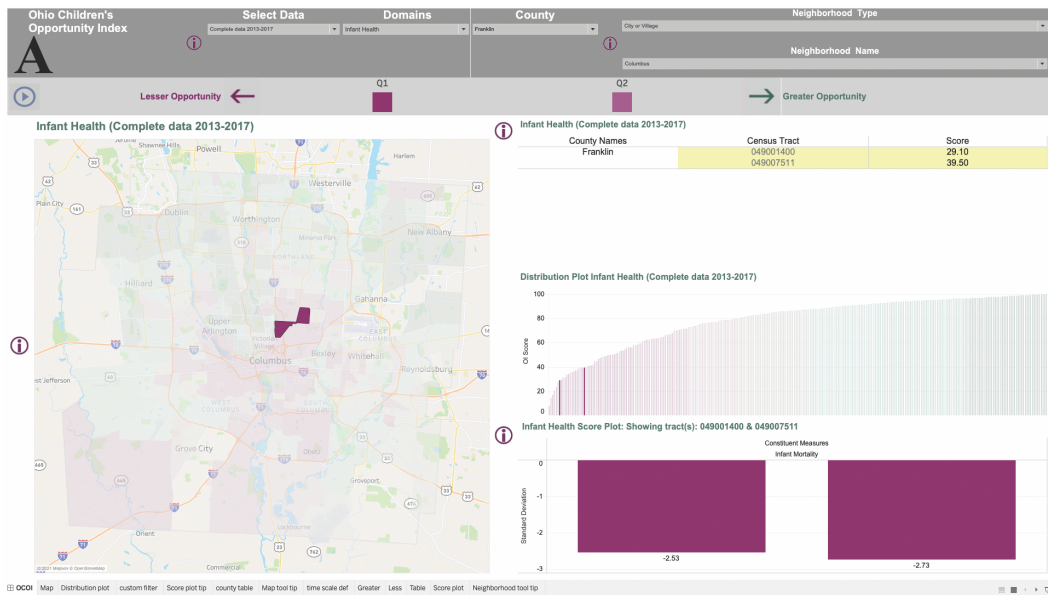


**Figure 3** 25 tracts with the lowest scores for Infant Health in Columbus, OH. Panel A shows 25 of the lowest-scoring census tracts in terms of Infant Health in Columbus, OH. Panel B shows 25 census tracts with the lowest scores for the Infant Mortality subdomain of the Infant Health domain of the OCOI.

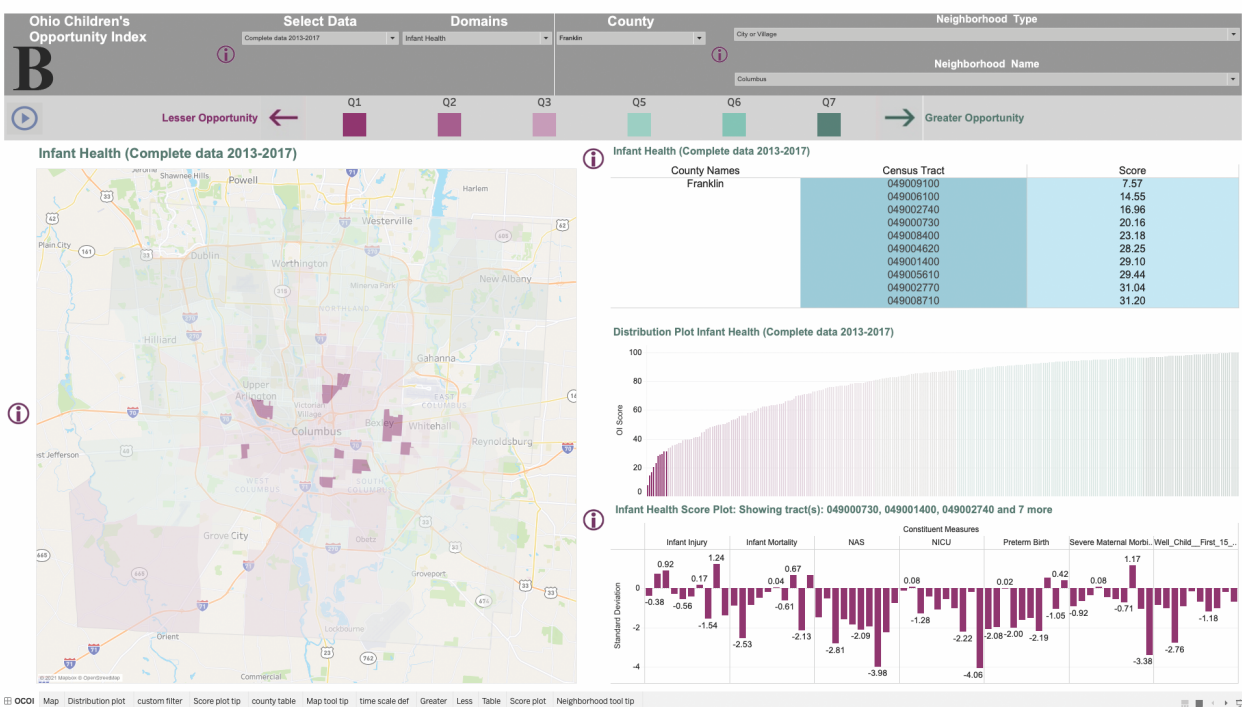
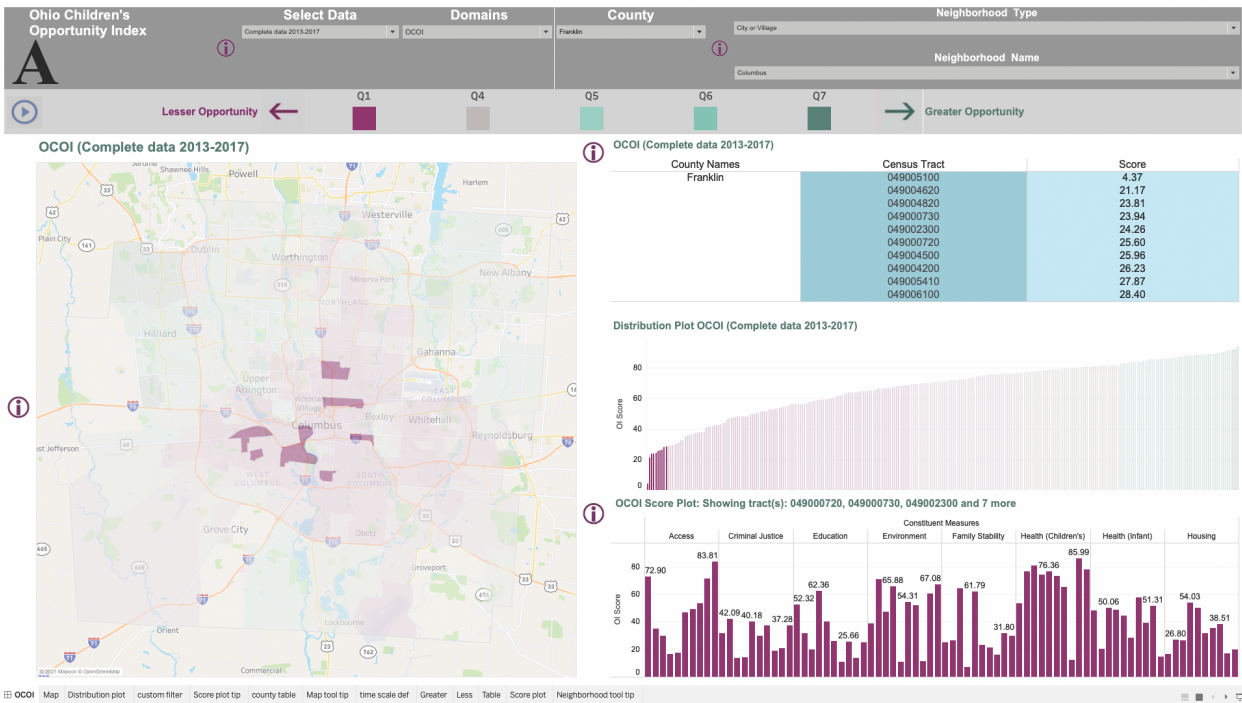


**Figure 4** Two lowest-ranked census tracts in terms of Infant Mortality in Columbus, OH. Panel A shows the two census tracts ranked the lowest in terms of Infant Mortality in Columbus, OH. Panel B shows the race distribution for the two lowest-scoring census tracts in terms of Infant Mortality in Columbus, OH in the South Linden neighborhood.